MONASH University

Deregulated IL-6/gp130 signalling in lung cancer development

Gavin Brooks

School of Medicine, Nursing and Health Sciences

This thesis submitted for the degree of
Doctor of Philosophy at Monash University 2016

Hudson Institute of Medical Research

Copyright notice

Abstract

Lung cancer is the most common and lethal form of cancer in Australia and worldwide, with lung adenocarcinoma (LAC) being the most common phenotype of lung cancer. LAC is strongly associated with chronic lung inflammation triggered by cigarette smoking, and one of the most established disease-associated consequences of the genotoxic effects of cigarette-derived carcinogens is activating mutations in the *Kras* proto-oncogene. The identification of activating mutations in a minority of LAC patients, mainly comprising never smokers, has paved the way for targeted therapies with substantial benefit. However, effective therapies for LAC with a more typical mutation profiles, especially those associated with smoking, are yet to be identified, thus highlighting the need for a better understanding of the molecular and genetic alterations involved in the initiation and progression of LAC. In this regard, components of the IL-6 cytokine family which signal through the shared gp130 signal-transducing receptor subunit, are commonly up-regulated in human lung cancer, and represents a promising target in anti-cancer therapy. Despite this, the molecular mechanisms associated with deregulated gp130 signalling in lung cancer has not been fully elucidated, largely due to the paucity of genetically defined pre-clinical mouse models that allow for identification of gp130 signalling pathway-related diseases.

This thesis addresses the question whether gp130 signalling contributes to the initiation and maintenance of the malignant phenotype of LAC by enhancing the oncogenic effects of mutated *Kras*. We utilised our novel *gp130*$^{F/F}$ mouse model for upregulated endogenous IL-6 production and associated spontaneous pulmonary inflammation as a result of a “knock-in” substitution within the IL-6 family co-receptor gp130. These mice display augmented activation of the latent transcription factor Stat3 in the absence of gp130-driven

PI3K/Akt and Mapk/Erk signalling. Importantly, Stat3, PI3K/Akt and Mapk/Erk have been implicated in lung cancer development.

We used *gp130*$^{F/F}$ mice generated onto the lung cancer susceptible genetic background *Kras(G12D*) (*gp130*$^{F/F}$:*Kras*^{G12D} mice) and elucidated for the first time that gp130 signalling driven cell proliferation augmented *Kras*-induced lung carcinogenesis. Importantly, we discovered a causal role for IL-6 via its pathogenic mode IL-6 trans signalling, as well as identify a potential therapeutic strategy to target discrete modes of IL-6 signalling in *Kras*-induced LAC. We also identified Stat3 as the downstream mediator of IL-6/gp130 driven inflammation associated with *Kras*-induced LAC. Furthermore, we validated above findings in clinical setting using lung cancer biopsies.

These results will therefore provide a significant and original contribution to our fundamental understanding of the mechanisms involved in lung cancer that will potentially strengthen the translational impact of early detection and treatment of the disease in the clinic.

Declaration

This thesis contains no material which has been accepted for the award of any other degree or diploma at any university or equivalent institution and that, to the best of my knowledge and belief, this thesis contains no material previously published or written by another person, except where due reference is made in the text of the thesis.

Signature: 

Print Name: Gavin Brooks

Date: 1st November 2016

Publications during enrolment

Brooks, G.D., McLeod, L., Alhayyani, S., Miller, A., Russell, P.A., Ferlin, W., Rose-John, S., Ruwanpura, S., and Jenkins, B.J. (2016). Interleukin-6 trans-signalling Promotes KRAS-Driven Lung carcinogenesis. Cancer Research 76, 866-876.

Miller, A., **Brooks, G.D**., McLeod, L., Ruwanpura, S., and Jenkins, B.J. (2015). Differential involvement of gp130 signalling pathways in modulating tobacco carcinogen-induced lung tumourigenesis. Oncogene *34*, 1510-1519.

Ruwanpura, S.M., McLeod, L., **Brooks, G.D**., Bozinovski, S., Vlahos, R., Longano, A., Bardin, P.G., Anderson, G.P., and Jenkins, B.J. (2014). IL-6/Stat3-driven pulmonary inflammation, but not emphysema, is dependent on interleukin-17A in mice. Respirology *19*, 419-427.

Ruwanpura, S.M., McLeod, L., Lilja, A.R., **Brooks, G**., Dousha, L.F., Seow, H.J., Bozinovski, S., Vlahos, R., Hertzog, P.J., Anderson, G.P., *et al.* (2013). Non-essential role for TLR2 and its signaling adaptor Mal/TIRAP in preserving normal lung architecture in mice. PloS one *8*, e78095.

Ruwanpura, S. M., McLeod, L., Dousha, L. F., Seow, H. J., Alhayyani, S., Tate, M. D., Deswaerte, V., **Brooks, G. D**., Bozinovski, S., MacDonald, M., Garbers, C., King, P. T., Bardin, P. G., Vlahos, R., Rose-John, S., Anderson, G. P., Jenkins, B. J. (2016). Therapeutic Targeting of the IL-6 Trans-signalling/mTORC1 Axis in Pulmonary Emphysema. AJRCCM

Acknowledgements

I would like to extend my sincere appreciation to the following people whose guidance, patience and direction throughout my PhD have been invaluable.

To my supervisors, Professor Brendan Jenkins and Doctor Saleela Ruwanpura. I appreciate the guidance and mentorship you have offered me during this arduous PhD, the experiences I have gained during my PhD will assist me in the future and aid in driving my career in science. Good luck to you both your future research.

To the staff and students of the Cancer and Immune signalling laboratory, both past and present. Thank each and every one of you for your support during this time of my life, all of you have impacted me and helped in my development as both a scientist and a colleague. A special mention to Louise who has been a constant rock throughout my PhD, someone who always (usually) had an ear to listen with and a shoulder to lean on. I respect and admire your professionalism and friendship, you are a pleasure to work with and a friend.

To all the members of the Centre for Innate Immunity & Infectious diseases, both past and present. You are by far the best centre within the Hudson Institute and the friendships and collaborations that will develop within this group will be strong and rewarding. Good luck to Paul Hertzog and the rest of the centre.

A special thanks to the generational crew, Alec and Jesse, whose lasting friendship and comradery were a godsend at times. Our continual gatherings are a welcome reprieve to the rigours of life and I look forward to these for a while to come.

Finally, to my loving family and Kirsten for all the support you have given me during this time of my life. Your guidance is always appreciated and will perpetually help me develop into a better man.

.

Table of content

CHAPTER 2

CHAPTER 7

REFERENCES

APPENDIX I

APPENDIX II

APPENDIX III

APPENDIX IV

(i) List of figures

Chapter 1

Chapter 3

Chapter 4

(ii) List of Tables

(iii) Abbreviations

AAH	Atypical adenomatous hyperplasia
ADAM	A disintegrin and metalloproteinase domain
AIS	Adenocarcinoma *in situ*
AKT	Protein kinase B
ALK	anaplastic lymphoma kinase
APS	Ammonium persulphate
BACS	Bronchoalveolar stem cells
BSA	*Bovine* serum albumin
CaCl2	Calcium Chloride
CD	Cluster of differentiation
CNTF	ciliary neurotrophic factor
COPD	Chronic Obstructive Pulmonary Disease
CSCLC	combined small cell lung carcinoma
CT	cardiotrophin
DAB	Diaminobenzidine cromogen
DDR	discoidin domain receptor tyrosine kinase
DepC	Diethylenepyrocarbonate
dNTP	Deoxynucleotide
DPBS	Dulbecco's Phosphate Buffered Saline
DTT	Dithiothreitol
EDTA	Ethylene diamine tetra acetic acid
EGFR	Epidermal growth factor receptor
ELM	echinoderm microtubule-associated protein-like
ERK	Extracellular signal regulator kinase
F/F	$gp130^{F/F}$
FCS	Fetal calf serum
FGFR	fibroblast growth factor receptor
FHIT	Fragile Histidine Triad
gp	glycoprotein
H&E	Hematoxylin and Eosin
hIL-6	Human IL-6
IFN	Interferon
IL	Interleukin
JAK	Janus Kinase
Kras	V-Ki-Ras2, Kirsten rat sarcoma viral
LAC	Lung adenocarcinoma
LC	Lung cancer
LCNEC	large cell neuroendocrine carcinoma
LIF	leukemia-inhibitory factor
MAPK	Mitogen-activated protein kinase
MEM	Modified Eagle's Medium
MgCL	Magnesium Chloride
MIMR	Monash Institute of Medical Research
MMP	matrix metalloproteinase

NaCl	Sodium Chloride
NaF	Sodium fluoride
NaV	Sodium orthovanadate
NFE2L2	Nuclear factor (erythroid-derived 2)-like 2
NNK	Nicotine-derived nitrosamine ketone
NS	Not significant
NSCLC	Non-small cell lung carcinoma
OBB	Odyssey blocking buffer
OSM	oncoStatin-M
PAH	polycyclic aromatic hydrocarbons
PBS	Phosphate Buffered Saline
PBST	Phosphate Buffered Saline + Tween 20
PCNA	Proliferating Cell Nuclear Antigen
pfu	Plaque-forming units
PI3K	Phosphatidylinositol 3-kinase
PVDF	Polyvinylidene fluoride
qPCR	Reverse Transcription - Polymerase chain reaction
RB	retinoblastoma
ROS	reactive oxygen species
RPMI	Roswell Park Memorial Institute
RT	Room temperature
SCLC	Small cell lung carcinoma
SDS-PAGE	Sodium dodecyl sulphate - Polyacrylamide gel electrophoresis
SEM	Standard error of the Mean
sgp130	Soluble gp130
sgp130Fc	Soluble gp130 Fc-Fusion protein
SHP	src-homology phosphotase
sIL-6R	soluable IL-6 receptor
SOCS	Suppressor of cytokine signalling
STAT	Signal transducer and activator of transcription
TEMED	N, N, N', N'-Tetramethylethylenediamine
TKI	tyrosine kinase inhibitor
TNF	tumour necrosis factor
TTF	Thyroid Transcription Factor
TUNEL	Terminal deoxynucleotidyl transferase dUTP end labelling
VEGF	vascular endothelial growth factor
Y	Tyrosine

Chapter 1
Literature review

1.1 Lung Cancer

1.1.1 - *Epidemiology*

Lung cancer (LC) is the most common and lethal form of cancer worldwide and accounts globally for approximately 1.5 million deaths[1] and in Australia accounts for 7,000 deaths[2]. However in recent years there has been a significant drop in the prevalence of young people taking up smoking and fewer adults smoking daily[3]. Proportionally, fewer women smoke than men with 21% of men and 17% of women being daily smokers. Interestingly daily smoking is more common in men aged 25-34 but in women it is more common during their forties[2]. Globally however this drop in the prevalence of young smokers is limited to western countries, with an increase seen in countries in Asia, South America and Africa[4], with about 80% of the worlds' smokers now living in low to middle income countries, primarily due to poor tobacco controls and laws[5].

Lung cancer is broadly divided into two types; small cell lung carcinoma (SCLC) and non-small cell lung carcinoma (NSCLC). SCLC is an aggressive tumour of neuro-endocrine origin that is very closely linked to cigarette smoking with malignant epithelial tumour consisting of small cells with little cytoplasm, ill-defined cell borders, finely granulated nuclear chromatin and inconspicuous nucleoli[6]. In addition the cells are irregular in shape, display prominent nuclear moulding, and consist of extensive necrosis. NSCLC accounts for approximately 85% of all lung cancer diagnoses and is further subtyped into adenocarcinoma (the most common), squamous cell carcinoma and large cell carcinoma based on similarities

in diagnosis, staging, prognosis, and treatment. NSCLC is defined as malignant epithelial tumour with glandular differentiation or mucin production, showing acinar, papillary, bronchioalveolar or solid carcinoma with mucin growth patterns, or a mixture of these patterns[6]. NSCLC, and more particularly adenocarcinoma, is the focus of this thesis as it is the most common form of lung cancer, the most frequent in non-smokers, and the most significant advances in therapy have been attained in sub-classes of adenocarcinoma[7].

The heterogeneity of lung cancer is such that most tumours can contain two or more elements of both SCLC and NSCLC which, since the new WHO classifications that were published in 2004, are classified as combined-SCLC (CSCLC). Unless, it has neuroendocrine carcinoma, then it is classified as large cell neuroendocrine carcinoma (LCNEC)[6]. From a clinical perspective, this makes it difficult to diagnose and subsequently treat as staging for SCLCs and NSCLCs are different, and as such, so are the prognosis and treatment options[8]. More recently, it has become clinical practice to test for genetic mutations as a number of somatic mutations have been identified that complicate the, rather descriptive, nomenclature of lung cancer classification[9]. While the greatest risk factor for lung cancer is cigarette smoking, only 10-15% of smokers develop lung cancer suggesting there are other genetic, epigenetic or environmental factors that predispose an individual to lung cancer in the following section these specific risk factors for lung cancer will be discussed.

1.1.2 - *Risk factors for lung cancer*

Chemical risk factors

(i) Cigarette smoke

It has been shown that the risk of developing lung cancer is closely linked to the duration of smoking rather than the intensity or "packs per year"[10], as such the age at which an individual and the duration they have been smoking for are far more important than the number of cigarettes per

day[11]. Cigarette smoke accounts for almost 90% of Lung Cancer (LC) in men and 70% to 80% in women[12,13] and compared to non-smokers, smoker have an almost 30-fold increased risk of developing lung cancer[14,15]. However, only around one in six smokers will develop lung cancer[16] suggesting there are other environmental and/or genetic factors at play.

Cigarette smoke contains over 70 known carcinogenic compounds including 1,3-butadiene, cadmium, radioactive compound polonium, polycyclic aromatic hydrocarbons, and nicotine-derived nitrosamine ketone (NNK)[17], with the latter being intimately studied in a number of animal studies[18-21]. NNK-induced lung carcinogenesis is an established and widely used model to examine the molecular and cellular events that promote the initiation and progression of lung adenocarcinoma, especially since cigarette smoke induces pronounced lung inflammation in mice rather than lung cancer[22]. NNK-induced lung cancer occurs independent of the route of administration[23] and is characterised by the reproducible and sequential development of focal proliferation of alveolar type II epithelial cells (i.e. airway epithelial hyperplasia) that progresses to adenocarcinomas. In addition, DNA damage has been linked to the generation of point mutations and chromosomal alterations affecting proto-oncogenes (i.e Kirsten rat sarcoma (*Kras*)) and tumour suppressors (i.e. Tumour protein (T*p)53*)[24,25]. NNK also activates specific signalling pathways leading to deregulation of cell survival and cell proliferation[24,26] in bronchial epithelial cells.

In addition to the above carcinogens, cigarette smoke also contains and induces a high concentration of oxidants generating reactive oxygen species (ROS)[27] and induces airway inflammation in all smokers[28,29]. The induction of ROS is an essential component of the acute inflammatory response[30] and, if unresolved, this oxidative stress contributes to chronic inflammation and, amongst other problems, an increased risk of cancer[31]. Persistent high levels of ROS leads to DNA damage that outstrips DNA repair mechanisms[32]. In support of the pathogenic role of ROS in lung cancer, is the association between increasing levels of oxidative stress and reduced anti-oxidant levels with advancing lung cancer stage[33].

Cigarette smoke-induced inflammation is associated with the induction of a cascade of cytokines, growth factors, and deregulation of normal cell function, and thus has a detrimental effect on the lung microenvironment. However, the importance of specific pathways associated with cigarette smoke leading to lung cancer development is poorly understood and highlights the need for a better understanding of the molecular and genetic alterations that promote the initiation and progression of lung adenocarcinoma.

(ii) Radon

The first occupational characterisation of lung cancer was described in 1879 by Friedrich Hugo Härting and Walther Hesse through an account of the health and working conditions of miners in the Schneeberg mines[34,35]. While the original paper in 1879 failed to find the causal agent for disease they did determine it was primarily lung cancer. It was later determined that radon gas, a naturally occurring radioactive gas, was the source of disease[35]. Radon gas has since been associated with lung cancer development and is considered the second most common cause of lung cancer behind cigarette smoke[36].

Radon, along with its progenies, damage tissues by emitting alpha particles[37] and while this can be easily protected against, if particles are inhaled, either as free particles or attached to airborne particulates these ionising radioactive particles can lodge in the respiratory epithelium. Lung cancer ensures and while the mechanisms by which alpha particles cause lung cancer are yet to be elucidated, it is conceivable that this is via gene mutations, generation of ROS, dysregulation of cytokines and disruption of proteins associated with cell-cycle regulation[36,37].

(iii) Asbestos

Asbestos, another naturally occurring mined resource and widely used in industry, accounts for 4% of lung cancer development in the US[38]. Asbestos related lung disease is generally considered a disease of occupation as the highest risks have been observed in chronic, heavy exposure to the friable asbestos materials[39]. Although many countries in the western world have taken steps to limit and restrict exposure to asbestos[39], past exposure and continued production and use in other parts of the world increase incidence worldwide[38].

Similar to Radon associated lung cancer, the molecular mechanisms involved in asbestos related lung disease development are yet to be elucidated, however studies have shown that asbestos fibres are able to induce, gene mutations, DNA damage, and cause chromosome aberrations[40]. Importantly, asbestos related lung disease appears to have a synergistic effect with cigarette smoking since patients with occupational exposure to asbestos and who are smokers have an increased risk of developing lung cancer[38,39,41]. These patients also displayed mutations in the *Tp53* and *Kras* genes, consistent with observation in cigarette smokers[39].

While there are a plethora of chemical risk factors for lung cancer, the causes and specific impact of these carcinogens on the lungs is poorly understood. A number of genetic mutations have been identified such as; *Kras*[42], *Tp*53 [43], Liver kinase (*LK*)*B1/* Serine/threonine (*STK*)*11*[44], and more recently epidermal growth factor receptor (*EGFR*)[45] and phosphatidylinositol-4,5-bisphosphate 3-kinase (*PI3K*)[46]. However the heterogeneity of lung cancer and the preferential trend for carcinogens to be specific to a histological type of lung cancer suggest the genetic risk factors may be of more importance than the avoidable chemical risk factors.

Genetic risk factors for lung cancer

Despite the association between smoke exposure and lung cancer, only 10-15% of smokers develop lung cancer. In addition, there is an increasing incidence in lung cancer cases independent of smoking (especially in Asia[47]), which collectively suggest the presence of other ill-defined genetic, epigenetic factors which predispose certain individuals to lung cancer. To address this shortcoming in our understanding of the molecular pathogenesis of lung cancer, gene expression profiling has identified a complex array of genes of diverse molecular function, including inflammation, oxidant stress and glutathione metabolism, as well as oncogenes and tumour suppressors, in human airway epithelial cells whose expression is altered by cigarette smoking[48]. More recently, an expression signature of approximately 80 genes implicated in inflammation, cell cycle progression, antioxidant defence, ubiquitination and DNA repair has been assigned as a putative biomarker for smoke-induced lung cancer susceptibility[49]. More recently, extensively annotated somatic mutations present in human lung adenocarcinoma were identified in paired tumour and normal tissue samples using both whole genome and whole exome sequencing[50]. While mutational frequencies in some of the most commonly mutated genes were similar to previously studies, the larger sample size coupled with advances in technology allowed for a clarification of the roles of previously reported genes and identification of new putative driver mutations. Thus, while such studies have started to unravel the complex genetic and epigenetic processes which contribute to the initiation and progression of lung cancer, they also highlight that many genes involved in lung carcinogenesis remain to be discovered.

(i) *Kras*

One of the most extensively studied genes implicated in LC is the proto-oncogene *Kras*. *Kras,* belonging to the ras family, is a membrane GTPase signalling protein that regulates cell

proliferation, differentiation and survival[51]. Activating *Kras* mutations are found in approximately 10% to 50% of LC, both smokers and never smokers, with the predominant histological subtype affected being lung adenocarcinoma[12,52]. *Kras* is strongly associated with cigarette smoke, is especially activated by cigarette carcinogens[53] and has been reported to promote an intense inflammatory infiltrate, although this latter finding is somewhat controversial[54]. In addition, an exacerbation of lung tumour development in mice with an activating *Kras* mutation and co-existing pulmonary inflammation showed that these mice developed epithelial hyperplasia of the bronchioles, adenoma, and adenocarcinoma[55], and a 3.2-fold increase in lung surface tumour numbers[55]. Despite the overwhelming evidence implicating *Kras* signalling in lung cancer pathogenesis, its role in the development of lung inflammation is controversial, with conflicting reports as to whether or not *Kras* activation in the lung promotes an inflammatory response[51,56,57]. However, these conflicting results are mainly associated with *Kras* activation in different cell types within different mouse models. For instance, *Kras* activation in the bronchiolar epithelium was associated with a robust inflammatory response characterized by an abundant infiltration of alveolar macrophages and neutrophils[57], whereas within the alveolar compartment, oncogenic *Kras* activation promoted lung adenocarcinoma driven by intralesional vascularity and neutrophil infiltrates[58].

The most common mutation of *Kras* is a point mutation in codon 12 changing a glycine to an aspartic acid[59] , thus referred to as *Kras(*G12D). These point mutations result in a conformational change leading to constitutive transduction of a growth promoting signal[60]. An activating mutation in *Kras* has been shown to be an early initiating event in murine models of lung cancer[56] and is frequently present in up to 80% of spontaneous and all experimentally-induced murine lung cancers[61]. A definitive role for *Kras* in the initiation and progression of lung cancer is evidenced by the spontaneous development of lung adenocarcinoma in mouse models genetically engineered to express the oncogenic *Kras*^{G12D} allele conditionally, somatically, or inducibly in the lungs of mice[12,51,56,57,62].

Although the downstream mediators of Kras-induced lung adenocarcinoma are yet to be formally identified, likely candidates include the extracellular signal regulating kinase/Mitogenic-activated protein kinase (Erk/Mapk) and Phosphatidylinosiotol-4,5-bisphosphate 3-kinase (PI3K)/Akt pathways and more recently the Signal transducer and activator of transcription (Stat)3 latent transcription factor[42,46,63]. This has been demonstrated by inhibition of elements of these pathways resulting in rescued or reduced tumour formation in mouse models expressing the *Kras* mutation[64-66].

(ii) Epidermal growth factor receptor

EGFR (also known as HER1 and ErbB1) is a transmembrane glycoprotein that belongs to the erbB family of tyrosine kinase receptors, activated by members of the EGF family including EGF, TGF-α, amphiregulin and epiregulin[67]. Ligand binding leads to homo-dimerisation, and, as the intra-cellular domain has intrinsic kinase activity[68], subsequent autophosphorylation of the cytoplasmic tyrosine kinase and subsequent activation of signal transduction pathways that are involved in regulating cellular proliferation, differentiation, and survival[69]. Down-stream mediators of EGFR activation include *Kras*, MAPK, PI3K/Akt, and Stat3[70]. Akca et al. (2006) showed that cells transfected with a mutant EGFR had prolonged survival in a serum free environment by increased activation of both Akt and Stat3[70].

EGFR is implicated in a number of cancers including bowel[71], squamous cell carcinoma of the head and neck[72], and importantly NSCLC[8]. EGFR displays activating mutations in NSCLC: between 10% and 40% in adenocarcinoma[73] but infrequently in other NSCLC or SCLC[74,75]. These mutations consist of amino acid substitutions and deletions largely located within the kinase domain in exons 18, 19 and 21[76] and are predicted to enhance activation of downstream signalling cascades. Interestingly, mutations of the EGFR appear to be mutually exclusive of mutations of Kras in lung adenocarcinoma. The identification of EGFR-activating mutations in 15% to 20% of lung adenocarcinoma patients, mainly females Asian non-

smokers, has paved the way for targeted therapy with tyrosine kinase inhibitors (TKIs)[77]. There are two first generation TKIs in use today being Gefitinib and Erlotinib, which selectively target intracellular tyrosine kinase domains of EGFR[8] and in 2010 a phase III trial showed treatment with Getfitinib, in conjunction with Chemotherapy, improved progression-free survival of patients compared to standard chemotherapy[78]. This lead to recommended testing for EGFR mutations in all patients with advanced NSCLC by the American Society of clinical Oncology. Recently it has shown that a number of third generation *EGFR* inhibitors approved for treatment in NSCLC, specifically Osimertinib, Rociletinib and PF-06747775[79]. However, patients receiving these inhibitors subsequently developed resistance due to the development of the *EGFR* C797S mutation[79].

(iii) PI3K/Akt

PI3K is involved in cellular functions such as cell growth, proliferation, differentiation, and survival and signals through the Akt/mTOR pathway which is implicated in both cancer[80] and metabolic disorders[80]. Specifically in NSCLC, mutations in the *PIK3CA* gene usually affect the helical binding domain (exon 9) or the catalytic subunit (exon 20)[81]. In lung carcinoma, copy number gains in the *PIK3CA* gene were found to be exclusively in *PIK3CA* gene mutations and as such were thought to exhibit oncogenic potential in the lung[82]. However, in contrast to other oncogenic mutations, PI3K mutations in adenocarcinoma were found to be mutually inclusive and occurred in other aberrations such as *EGFR*, *BRAF*, *ALK*, and most frequently *Kras*[83] and as such synergy between PI3K and Kras mutations is evident[81].

(iv) *TP53*

TP53, also known as p53 (human) and TRP53 (mice) prevents cancer formation in multicellular organisms and is classified as a tumour suppressor gene[84]. Studies have shown

that inactivation of *TRP53* in combination with activated *Kras*^{G12D} mutations in mouse models results in aggressive tumour formation and metastasis[85], this was attributed to genomic instability and increased malignant progression. The p53 deficiency above was also found to augment NFκB signalling[85] and was corroborated by an NFκB inhibitor, bortezomib; a small molecule inhibitor of nuclear NFκB, that delayed tumourgenesis progression in mouse models[86]. *TP53* was also shown to be dependent on c-Jun NH_2-terminal kinase (JNK) signalling as in *Kras*-dependent mouse models, a deficiency in *Jnk* ameliorated the exacerbated tumour development seen in *Trp*$^{-/-}$ mice[87].

(v) *Stat3*

Stat3 belongs to a family of 7 transcription factors[88], and the oncogenic potential of Stat3 was demonstrated over 15 years ago by Bromberg and colleagues Bromberg (1999), by engineering a constitutively dimerisable Stat3 that is capable of driving transcription and induces cell transformation[89]. Stat3 is persistently activated in many human primary tumours, including up to 50% of NSCLC, with the predominate subtype being LAC[90]. One of the key mechanisms attributed to the oncogenic activity of Stat3 is its ability to directly induce the transcription of many genes involved in cell cycle progression (e.g. c-myc, cyclinD1)[89,91,92], cell survival (e.g. bcl-xl)[91] and angiogenesis (e.g. vegf)[93] which are frequently overexpressed in human lung cancer[94-98], and Stat3 has been linked with mediating survival of human NSCLC cells[99]. The importance of Stat3 in lung cancer is suggested by the requirement of Stat3 for ras mediated oncogenesis[63], as evidenced by tumour regression in a *Kras* mouse lung adenocarcinoma model[42] after reduced Stat3 phosphorylation, although the specific mechanistic basis by which Stat3/Kras-driven lung carcinogenesis was not investigated. In that regard, increased Stat3 activity is a critical downstream regulator of tumour cell survival triggered by epidermal growth factor receptor (EGFR) mutants displaying enhanced tyrosine

kinase activity in a subset of lung adenocarcinomas[100]. More recently, in these tumours it has been proposed that increased Stat3 activation is mediated by up-regulated expression of IL-6[90], however this requires further investigation.

Stat3 itself and a subset of target genes are upregulated in human lung cancer tissue irrespective of patient smoking history[101]. In support of a direct role for Stat3 in lung cancer pathogenesis, overexpression of an artificial, constitutively-active (dimer) Stat3-C variant in the pulmonary epithelium of mice causes spontaneous lung inflammation and adenocarcinoma[102]. The former observation is consistent with the potent proinflammatory activities of Stat3 which are linked to the initiation and progression of various inflammation-associated tumours[103-105]. However, these studies fail to identify the upstream factors that induce Stat3 hyperactivity in lung disease. Accordingly, there is an urgent need for new lung cancer models in which the proinflammatory and oncogenic activities of endogenous Stat3 are modulated by defined genetic alterations to upstream activators of Stat3. Using an MMP-12 over-expression model, Qu et al. showed that both IL-6 levels in BALF and activation of Stat3 in epithelial cells led to adenocarcinoma in the presence of significant pulmonary inflammation[106], thereby strengthening the link between IL-6/Stat3 signalling, inflammation and lung adenocarcinoma.

1.2 The Interleukin 6 family of cytokines and gp130 signalling

The IL-6 cytokine family plays a crucial role in regulating cellular responses including cell survival/apoptosis, proliferation and functional maturation in most physiological systems, and is linked strongly to the immune system and inflammation[107]. IL-6 family of cytokines includes IL-11, Leukaemia Inhibitory Factor (LIF), OncoStatin-M (OSM), IL-31[108], Ciliary Neurotrophic Factor (CNTF), Karyopherin Subunit α1 (NPI), Cardiotrophin-1 (CT-1)[109] and

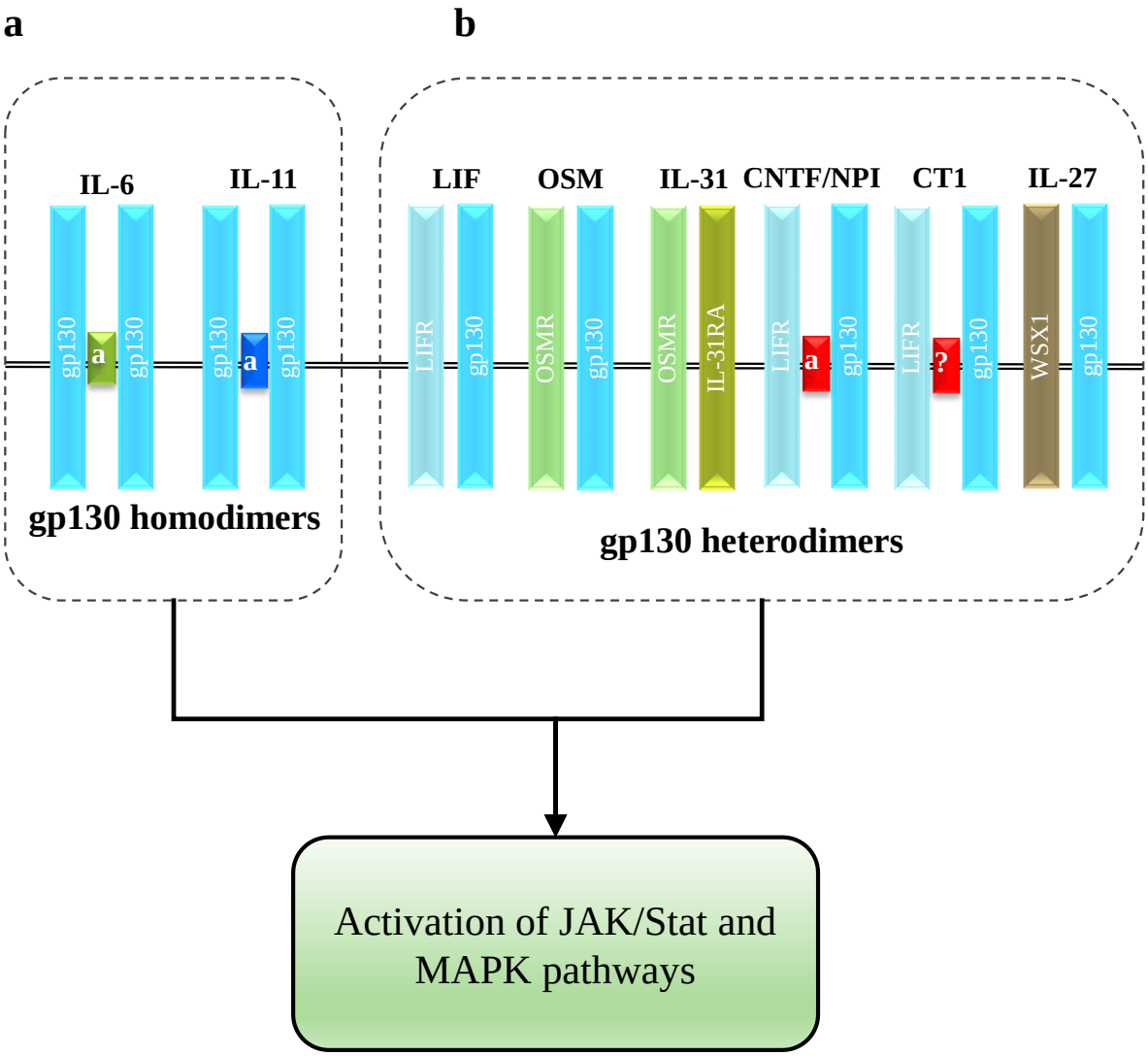

Figure 1.1. Schematic illustration of IL-6 cytokine family members

Schematic illustration of IL-6 cytokine family members. (a) gp130 homodimers with corresponding membrane bound α–receptors for IL-6 and IL-11. (b) gp130 heterodimers with corresponding membrane bound receptors for LIF, OSM, IL-31, CNTF/NP1, CT1, and IL-27. Activation of these receptors causes phosphorylation of downstream JAK/Stat and MAPK pathways.

IL-27[110], that share structural, signalling and functional properties (Figure 1.1). IL-6 family of cytokines are specifically characterised by four anti-parallel long-α-helix structures[111] which are either straight (for IL-6 and IL-11) or kinked, and signal through the common receptor sub unit gp130[111-113] (as described below).

Gp130 is a 130kD trans-membrane glycoprotein that is ubiquitously expressed on cells[114]. Being a classical type I cytokine receptor it consists of 6 extra-cellular modules[115], a trans-membrane domain and a cytoplasmic domain, the latter lacking any intrinsic kinase activity[112]. The N-terminal component is an Immunoglobulin (Ig)-like domain, with modules 2 and 3 making up the Cytokine Binding Domain (CBD) followed by three further fibronectin type-III modules[116]. Module 2 contains four conserved cysteine residues and module 3 a tryptophan-serine-X-tryptophan-serine (WSXWS) motif[115]. Notably, the intracellular module does not have any intrinsic kinase activity[109] but is constitutively associated with membrane proximal Janus Kinases (JAKs)[115]. Crucially, the cytoplasmic domain also contains 5 tyrosine residues that are essential for intracellular signal transduction.

Signal transduction of IL-6 cytokine family via gp130 includes two distinct types of cellular receptors; a ligand specific α subunit (such as IL-6 receptor (IL-6Rα) and IL-11 receptor (IL-11Rα)), and a common ubiquitously-expressed gp130 signal-transducing β subunit[109]. IL-6 and IL-11 signal through gp130 homodimers (Figure 1.1a) while all the other members of the gp130 cytokine family signal through heterodimers with gp130 and either LIFR (LIF, CT1, CNTF, CLC), OSMR (OSM), or WSX1 (IL-27) (Figure 1.1b). Following formation of this complex, gp130 binds to and activates JAK family tyrosine kinases such as JAK1, JAK2 and TYK2 (Tyrosine Kinase 2)[107,109,112] (Figure 1.2a and b). Following activation, the JAKs dimerise and phosphorylate and then subsequently phosphorylate tyrosine residues within the cytoplasmic domain of gp130, allowing signalling intermediates

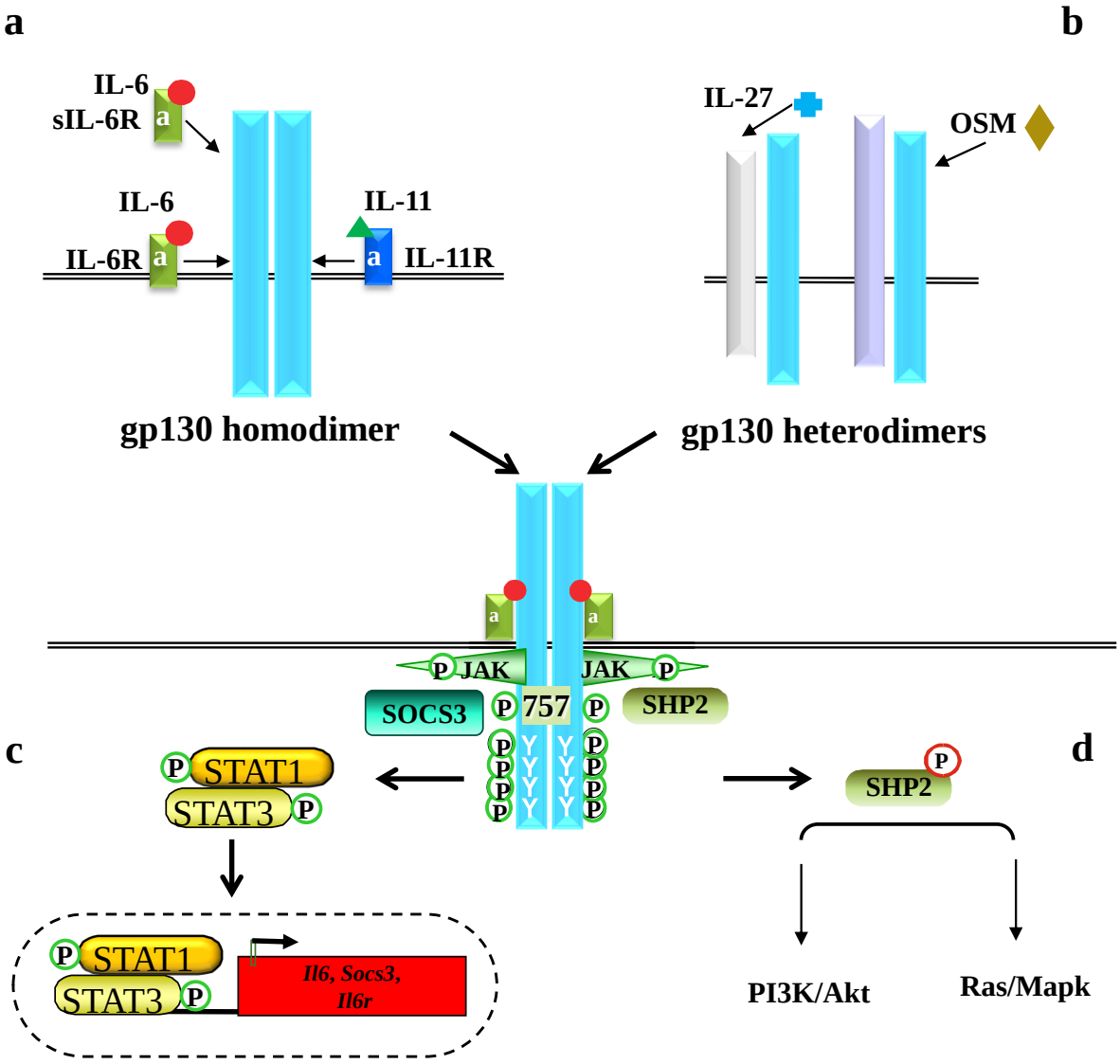

Figure 1.2. Schematic illustration of IL-6 cytokine family member signalling

Schematic illustration of IL-6 cytokine family members signalling through the common gp130 receptor. (a) gp130 homodimers with corresponding α–receptors for IL-6 and IL-11. (b) gp130 heterodimers with corresponding receptors for IL-27 and OSMI. (c) Tyrosine mediated STAT signalling. (d) pY757-mediated SHP2 signalling.

factors Stat1 and Stat3, which bind to the C-terminal tyrosine residues, are phosphorylated, then form either homo- or heterodimers before translocation to the nucleus where they with

SHP2 domains to bind[109,112,113,117]. Amongst these factors are the ubiquitously expressed latent transcription regulate gene transcription[112] (Figure 1.2c). In addition to recruitment of the Stats, tyrosine phosphorylation of the cytoplasmic tyrosine residues on gp130 leads to activation of the Src Homology tyrosine Phosphatase (SHP2). In this case it is the membrane proximal pY757 (in mice, pY759 in humans) which recruits SHP2[118,119] leading to activation of the PI3K/Akt and RAS/MAPK pathways (Figure 1.2d)[109,112].

1.3 Interleukin 6 signalling

IL-6 is produced by T cells, monocytes/macrophages, fibroblasts and endothelial cells[120]. IL-6 gene expression is stimulated by a number of stimuli such as IL1β, TNF-α and the type-I IFN cytokines[121], and is also produced by pattern-recognition receptors such as Toll like receptors (TLRs) by microbial and endogenous ligands[121]. IL-6 transduces signals to regulate many cellular functions (e.g. survival, apoptosis, proliferation, differentiation) on a vast array of immune and non-immune (e.g. endothelial, epithelial) cells in many organ systems[122] via two distinct types of cellular receptors; a ligand-binding IL-6 receptor alpha subunit (IL-6R), and gp130 signal-transducing beta subunit (gp130)[114]. As discussed above, the IL-6/IL-6R complexes associate with gp130 to activate Stat3 (and Stat1), SHP2/ERK MAPK and SHP2/PI3K/AKT and suppressor of cytokine signalling (SOCS)3 signalling pathways[116]. Despite the common usage of these pathways, IL-6 signals via two distinct modes, “classical” and “trans” signalling (TS) (Figure 1.3a and b).

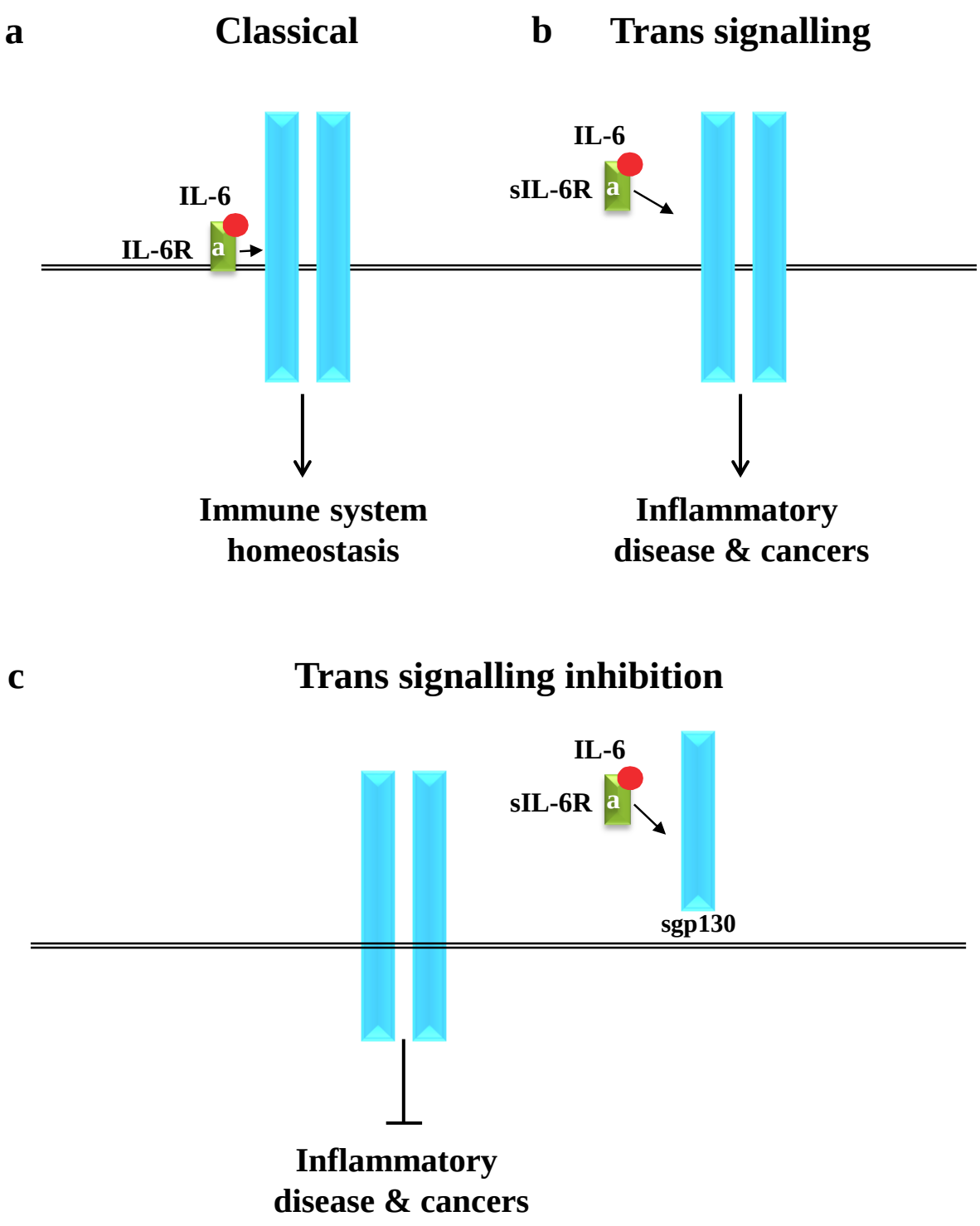

Figure 1.3. Schematic illustration of IL-6 modes of signalling

Schematic illustration of IL-6 modes of signalling through the common gp130 receptor. (a) classical IL-6 signalling through the membrane bound α–receptor subunit. (b) Trans IL-6 signalling through a soluble form of the α–receptor subunit. (c) IL-6 trans signalling inhibition mediated by a soluble form of gp130.

(i) Classical IL-6 signalling

In classical signalling, IL-6 binds to mIL-6R that is expressed on the surface of a limited number of target cells, predominately confined to sub-types of leukocytes, hepatocytes, and intestinal epithelial cells[114,123] (Figure 1.3a). Classical IL-6 signalling appears to dramatically influence the early immune responses by regulating the expression of diverse acute phase response proteins such as C-reactive protein, and the stimulation of B-cells to produce antibodies against invading pathogens, as such is considered to be anti-inflammatory[114]. To investigate the role of classical IL-6 signalling in vivo, researchers have traditionally employed IL-6 deficient mice, often leading to the assignment of an anti-inflammatory role for this mode of signalling. For instance, IL-6 deficient mice treated with dextran sodium sulfate showed a higher inflammatory score than wild type mice in colitis-associated colo-rectal cancer, most likely explained by the defect in IL-6 signalling on intestinal cell proliferation and inhibition of cell apoptosis[124]. Additional studies using IL-6 deficient mice have also shown that IL-6 signalling protects against mucosa against ulcerations from bacterial pathogens, such as *Citrobacter rodentium* infection[125]. Therefore, these studies highlight how, under certain situations, blocking (classical) IL-6 signalling may have detrimental consequences. Furthermore, they also imply that another mode of IL-6 signalling promotes chronic inflammatory responses associated with disease pathogenesis.

(ii) IL-6 trans signalling

Cells including stem cells, haemopoietic progenitor cells, T-cells and endothelial cells which lack mIL-6R are still capable of responding to IL-6 via a soluble form of the extra-cellular portion of the receptor (sIL-6R) which forms an IL-6/sIL-6R complex[113] (Figure 1.3b). The sIL-6R receptor can be generated in two ways, either through alternate splicing of the *IL-6r* gene[126] or the proteolytic cleavage of mIL-6Rα by A disintegrin and metalloproteinase

domain-containing protein (ADAM)10 and ADAM17[127] which leads to shedding of the receptor from the cell surface[128]. This shedding is inducible in response to inflammatory stimuli, including TNF-α, IL1β and elevated C-reactive protein (CRP)[129,130]. Shedding from apoptosing cells, particularly neutrophils, may act to augment the inflammatory process by allowing IL-6 to act on epithelial cells, leading to the release of more pro-inflammatory chemokines and cytokines[131,132]. IL-6 trans signalling has been implicated as the pathogenic mode of IL-6 signalling in many inflammatory conditions such as arthritis, diabetes mellitus, Crohn's disease, septic shock and Alzheimer's[133 134,135]. Although the underlying pro-inflammatory mechanisms still remain unresolved, IL-6 trans signalling appears to affect the nature of the inflammatory response by modulating the switch from innate to adaptive immune responses via regulation of chemokines[136]. In addition, IL-6 trans signalling has been implicated in numerous cancers, such as those of the colon[137,138], pancreas[139] and ovary[111], and while the downstream oncogenic molecular and cellular processes driven by IL-6 trans signalling remain ill-defined, it is presumed that IL-6 trans signalling promotes cell proliferation and survival by activating Stat3[138,140].

A naturally-occurring antagonist exists for the sIL-6R in the form of soluble (s)gp130[141] (Figure 1.3c). The sgp130 specifically binds to sIL-6R/IL-6 complex and thus antagonizes signalling from the IL-6/sIL-6R complex without interfering with classical signalling[142] under physiological conditions. Although the IL-6/sIL-6R complex has equal affinity for both sgp130 and gp130, a molar excess of sgp130 leads to competitive inhibition of IL-6 trans signalling[143]. Garbers et al. (2011) have shown that contrary to previous findings, sgp130 may inhibit classical signalling as well as trans-signalling[128]. These authors proposed that this is dependent on the concentration of sgp130 and the ratio of IL-6 to sIL-6R, suggesting that sgp130 was able to hold IL-6 in IL-6/sIL-6R complexes thereby diminishing the amount of IL-6 available for classical signalling. Alternate splicing of gp130 mRNA results in a stop codon prior to the trans-membrane coding region, leading to the production of sgp130[144]. It has been detected at

substantial levels in human serum[141], as well as in pleural fluid[145]. It has been proposed that sIL-6R and sgp130 work cooperatively to modulate the action of IL-6[112].

The importance of such negative regulatory mechanisms for IL-6 cytokine family signalling (especially IL-6) and their downstream signalling pathways is highlighted by studies, including in our own laboratory, showing that gp130/Stat3 hyper-activation promotes cancers such as gastric and colorectal inflammation-associated tumours in mice[146,147] and human inflammatory hepatocellular cancers[148]. Furthermore, molecular factors associated with IL-6 cytokine family/gp130 signalling are found to be altered in lung diseases, especially in lung cancer.

1.4 IL-6 signalling in lung cancer

An impressive body of preclinical and clinical evidence has documented the increased production of IL-6 in a variety of chronic inflammatory diseases including rheumatoid arthritis (RA), and inflammatory bowel disease[114,149], as well as numerous cancer phenotypes, including lung, colon, liver, ovarian and pancreatic[139,150,151]. In regard to lung cancer, elevated levels of IL-6 and CRP (an acute phase protein induced by IL-6) have been shown to be increased in lung cancer patients[152,153]. In addition, IL-6 is elevated in BALF, serum and tumour tissue from patients with NSCLC[90,154] and higher serum IL-6 levels in patients with advanced NSCLC correlate with worse prognosis[155]. IL-6 is produced in human lung epithelial cells in response to cigarette smoke and protects against apoptosis triggered by smoke-induced DNA damage in a Stat3-dependent manner[156].

A number of animal models of lung cancer have reinforced the clinical data showing the importance of IL-6 in lung cancer. In an inducible transgenic mouse model for lung epithelial-specific MMP12 over-expression, adenocarcinoma was associated with elevated

BALF IL-6 levels and epithelial cell STAT3 activity[106]. Similarly, in a triple knockout (IFN-γ, GM-CSF and IL-3) mouse model of spontaneous lung cancer development, IL-6 was elevated in BALF and serum, and was further elevated as tumours progressed[157]. Increased IL-6 levels were also demonstrated in an *LSL-Kras*^{G12D} model with pulmonary inflammation, which was associated with increased tumour load[55]. However, in this latter model it is unknown whether IL-6 contributed to cancer development or was merely a consequence of the inflammatory process. To help answer this question, Ochoa et al. genetically ablated IL-6 in a *LSL-Kras*^{G12D} mutant mouse, which led to attenuation of the tumour load both with and without the presence of COPD-like inflammation[150].

Notably, elevated levels of sIL-6R are a common observation in these chronic inflammatory diseases and cancers, and appear to correlate well with disease severity[114,127,134,158], suggesting a potential causal role for IL-6 trans signalling. Although the downstream signalling pathways which facilitate these IL-6-driven disease States remain to be fully elucidated, a recurring theme is the presence of hyper-activated Stat3, which has potent oncogenic and immuno-modulatory activities[146,159]. Indeed, during colon and pancreatic tumourigenesis, the IL-6/gp130/Stat3 trans signalling axis has been shown to stimulate the survival and proliferation of epithelial and endothelial cells, most likely via the Stat3-induced expression of genes important for cell cycle progression (e.g. cyclin D1, c-myc, PCNA) and anti-apoptosis (e.g. Bcl-X_L, Bcl-2, Mcl-1)[19,160-162].

1.5 Therapeutic approaches to targeting IL-6 signalling

In light of the above observational and experimental data, focus has also fallen on IL-6 as a therapeutic target in lung cancer. Antibodies and inhibitors against IL-6 and the IL-6R are used

clinically and have been investigated in a number of other cancers and chronic inflammatory conditions, including RA, Inflammatory Bowel Disease (IBD), and brain[163] and bowel cancer[164].

(i) Antibodies

The alleviation of disease in experimentally-induced mouse models for arthritis and IBD upon antibody-mediated neutralization of IL-6R or IL-6 itself[165,166] has led to the translation of this strategy into the clinic, the success of which is evidenced by the efficacy of the humanized anti-IL-6R monoclonal antibody (mAb) tocilizumab in phase II and III clinical trials in the management of Crohn's disease and RA[165,167,168]. Despite these observations, it should be noted that tocilizumab inhibits binding of IL-6 to the mIL-6R and sIL-6R comparably, thus primary targeting of "classical" over "trans signalling" cannot be determined, which may explain the observation that not all candidate patients with RA respond appropriately to tocilizumab therapy[168]. Furthermore, a common drawback associated with these anti-IL-6 therapeutics is the numerous adverse events, including infections, skin rashes and nausea[169], most likely a consequence of suppressing the "immuno-protective" classical IL-6 signalling pathway.

Therefore, we need to design superior anti-IL-6 therapies with a longer half-life to minimise the dose, and a preferential specificity to antagonise pathogenic IL-6 trans signalling compared to classical signalling, to prevent disease while minimising the occurrence of side effects. To address this our collaborator, Dr Walter Ferlin (NovImmune, Switzerland), has recently developed a novel series of mAbs which selectively target IL-6 trans signalling and/or classical signalling, and demonstrated their efficacy at suppressing inflammatory responses *in vivo* driven by either IL-6 classical signalling or IL-6 trans signalling[170]. While these studies were performed in mice with anti-mouse mAbs, they

nonetheless pave the way for humanised variants to be further developed for clinical applications.

With regard to the therapeutic targeting of IL-6 in cancer, although studies to date are very limited, one such agent is siltuximab, a chimeric mouse/human mAb that binds to and neutralizes human IL-6 with high affinity, thus blocking both IL-6 classical and trans signalling[171] . Siltuximab has displayed promise in preclinical xenograft models of NSCLC[172], where the inhibition of cancer cell growth *in vivo* aligned with reduced Stat3 activation in response to siltuximab treatment. While the clinical benefits of such an approach against LAC are yet unknown, an inherent issue that may arise again revolves around targeting "protective" IL-6 classical signalling. Accordingly, the search continues for superior anti-IL-6 therapies, for example, molecules with a longer half-life that will allow for less frequent dosing and/or administration of lower dose levels, together with a preferential specificity to antagonize pathogenic IL-6 trans signalling, to ameliorate disease while minimizing the occurrence of side effects.

(ii) sgp130Fc

The gp130 subunit also exists in a naturally-occurring soluble form (sgp130) which specifically binds to sIL-6R and thus antagonises signalling from the IL-6/sIL-6R complex without interfering with classical signalling [111]. To take advantage of this as a potential therapeutic, sgp130Fc was generated (by collaborator Professor Rose-John), which consists of recombinant sgp130 fused to the Fc region of human IgG1, and acts as a potent specific inhibitor of IL-6 trans signalling with more than 10-fold higher inhibitory potential compared to the naturally-occurring sgp130[111]. Importantly, sgp130Fc has been administered to mouse disease models with a high degree of therapeutic efficacy in alleviating arthritis, IBD, septic shock, and colon tumourigenesis[143,158,173]. In addition, transgenic mice over-expressing

sgp130Fc that were crossed with a pancreatic cancer model, the latter involving the targeted expression of the endogenous *Kras(G12D)* oncogene to the pancreas, were recently shown to develop significantly less pancreatic tumours which correlated with reduced STAT3 activation[139]. Therefore, sgp130Fc represents a novel therapeutic for potential clinical use against inflammatory diseases and cancers characterised by deregulated IL-6 trans signalling.

1.6 Mouse models for lung cancer

As previously mentioned LC exists as into two types, SCLC and NSCLC, with these specific cancer types having limited and mutually exclusive genetic mutations and is evidenced by particular tumours having distinct mutations in other disease types, such as, BCR mutations in chronic myeloid leukemia[174], *Kras* in pancreatic cancer[175] and DDR2 in SQ[77]. While in LC tumour formation is largely heterogeneous, the isolation of specific pathways associated with specific mutations is the key to therapeutic treatment, even if this will require a number of drugs to be administrated.

1.6.1 - *Mouse models for SCLC*

Small cell lung carcinoma is closely associated with cigarette smoke exposure and as such has a high mutation load due to chronic exposure to carcinogens and ROS linked to cigarette smoke. In spite of this only very few models for SCLC exist.

(i) Retinoblastoma and Tumour protein 53

In SCLC, the *Rb* and tp53 tumour suppressor genes have an extremely high degree of inactivation and the only model for SCLC makes use of the Cre/lox-based system for somatic mutation for both conditional alleles for *Rb*($Rb^{lox/lox}$) and *tp53*($p53^{lox/lox}$)[176]. Through

intrabronchial infection with adenoviral or lentiviral vectors expressing Cre recombinase, Rb and tp53 can be conditionally inactivated[177]. The invariable development of SCLC closely resembles human SCLC and metastasises to the same organs[178]. Interestingly, this mouse model displayed multiple foci of neuroendocrine hyperplasia (NE) development throughout the bronchi within three months of adenoviral administration[177]. This as I have discussed before would classify it now as large cell neuroendocrine carcinoma and not SCLC.

(ii) Human achaete-scute homolog 1

The proneural transcription factor Human achaete-scute homolog (hASH)1 is another highly present mutation in SCLC [179]. These mice with constitutive expression of hASH1 through the clara cell 10-kDa secretory protein (CC10) promoter resulted in bronchiolisation of alveoli and progressive airway epithelial hyperplasia near the bronchioloalveolar junctions[180]. However, when crossed with a transgene CC10-SV40 large T-antigen, the bi-transgenic CC10-hASH1:CC10-Tag mice developed progressive NE after 3 months and aggressive lung adenocarcinomas with both focal NE differentiation and CC10 expression[180,181]. Similar to the *Rb* and *tp53* mouse models mentioned before, the adenocarcinomas in these bi-transgenic mice did not resemble human SCLC but closer to NSCLC with NE differentiation and as such now would not be classified as a model for SCLC.

Mouse models for SCLC have yet to significantly contribute to the development of new intervention strategies, and this may be due to tumour heterogeneity in SCLC, poor classification of LC mouse models and the length of time it takes for SCLC to develop in a spontaneous tumour growth environment. Additionally, we have seen that the past classification of the models is currently not in line with the current World Health Organisation (WHO) classification for lung cancers.

1.6.2 - *Mouse models for NSCLC*

Unlike mouse models for SCLC, the number of mutations found in NSCLC is large and extensive studies worldwide have yielded a plethora of mouse models expressing these mutations. These mutations include *Kras* (25-40%), *Egfr* (10-15%), *Braf* (3%), *Alk* (4%), *Her2* (1.6-4%), *Lkb1, Rac1, NfκB* and *p53*; and a number of microRNAs[182]. However, I will focus on a specific few here, namely *Kras, Egrf* and *Braf/Al*k as these are the major genetic aberrations found in NSCLC specifically LAC.

(i) *Kras* models for LAC

Kras mutations are one of the most extensively studied genes in LC. Activating Kras mutations are found in approximately 15% of NSCLC cases (both smokers and never smokers), with the predominant histological subtype affected being adenocarcinoma[12,183], and correlate with poor survival prognosis[183]. There were number of earlier animal models of lung cancer which focused on Ras family mutations H- and N-ras genes[184]. However these models showed a high incidence of lung tumours and other solid organ tumours as early as one week of age[56,185]. Further to this other laboratories[51,177] were involved in development of additional *Kras* mutation mouse models with organ specific sporadic activation of oncogenic *Kras* using adenoviral based delivery of a Cre-recombinase (Figure 1.4). A definitive role for Kras in the initiation and progression of lung cancer is evidenced by the spontaneous development of lung adenocarcinoma in mouse models genetically engineered to express the oncogenic $Kras^{G12D}$ allele conditionally, somatically, or inducibly in the lungs of mice[51,56,57,62,186]. However, the majority of studies have been performed utilising the Lox-Stop-Lox conditional $Kras^{G12D}$ mutation engineered in the endogenous locus[51,187]. Introduction of Cre recombinase in cells of *LSL-*$Kras^{G12D}$ mice result in expression of the mutant allele at the endogenous level. The key benefit of this model for LAC is that the

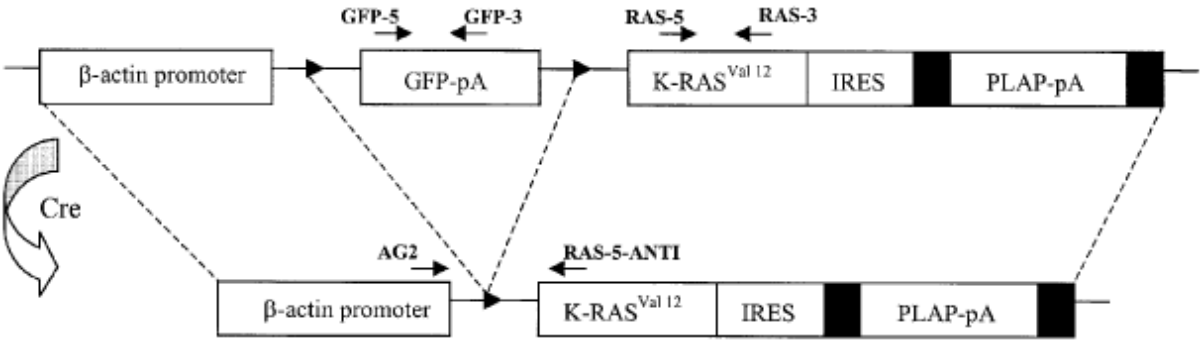

Figure 1.4. Schematic representation of the conditional *LSL-Kras*^{G12D} construct.

Schematic illustration of Kras construct, without Cre recombinase the GFP mRNA is expressed and Kras remains silent. With Cre recombination the β-actin controls Kras oncogene upregulation[51] (Adapted from Jackson E.L. *et al*, 2001).

conditional expression of this mutant allele later in life closely mimics the conditions for tumour initiation and development found in humans. As such, most models for Kras-dependent carcinogenesis utilise this *LSL-Kras*^{G12D} model rather than transgenic models[51,62,177].

(ii) Epidermal growth factor receptor

Somatic mutations encoding the tyrosine kinase domain of the *EGFR* gene are found in human LAC and are associated with increased sensitivity to Gefitinib and Erlotinib[188]. While in *Kras*^{G12D} models for LAC, deletion of the predominate *Egfr* mutation in *Egfr*^{L858R} mutant mice,

resulted in diffuse lung cancer that closely resembles bronchioalveolar carcinoma[189]. Additionally, mice that express an exon 19 deletion of Egfr (EGFR$^{\Delta L747\text{-}S752}$) displayed multifocal tumours embedding in normal lung parenchyma with a longer latency[188]. Both these models for LAC showed susceptibility to Gefitinib and Erlotinib with rapid tumour regression when treated with either therapeutic drug.

(iii) Braf and Alk

In addition to *Kras* and *EGFR*, *Braf* and *Alk* have been implicated in a number of cancer including; melanoma, colorectal, ovarian and NSCLC, albeit only 3-5%[190-192]. While these mutations are found in very few cases they are predominantly found in young patients and never smokers. In a model for Braf (Braf^{V600E})[193], utilising the *LSL-Kras*^{G12D} model, it was shown that in the lungs infection with adenovirus expressing cre recombinase developed lung tumours, albeit benign, that did not progress to adenocarcinoma[193]. These tumours were also shown to be initiated by oncogenic activation of a single cell that underwent gross cellular proliferation to develop adenoma. This is consistent with observations that *Braf*^{VE} mutations

induce melanocytic nevi and undergo multiple rounds of proliferation before senescence takes place. Similarly, transgenic mice expressing lung specific EML4-Alk fusion proteins develop multiple lung adenocarcinomas[194].

(iv) Stat3-C

As inappropriate and persistent activation of Stat3 occurs in at least 50% of human lung adenocarcinoma[195], a mouse model of persistent Stat3 activation was developed in an effort to better understand the pathways leading to tumourigenesis. Stat3-C, which contains a substitution of two cysteine residues within the SH2 domain, dimerises spontaneously and translocates to the nucleus leading to gene transcription, mimicking persistent activation[89]. Li et al. demonstrated that over-expression of Stat3-C within the pulmonary epithelium of mice led not only to marked pulmonary inflammation but also the development of lung adenocarcinoma[196]. While this model certainly supports the observation of increased Stat3 activation in human lung cancer, the artificial nature of the over-expression leaves room for a model displaying endogenous hyper-activation of Stat3.

There is a plethora of models for LC and increasing amounts of targets for personalised treatments are being identified often. Gefitinib, erlotinib, along with afatinib, brigatinib, and icotinib are EGFR inhibitors are currently used in the treatment of LAC[197]. Vemurafenib, a Braf inhibitor, is used in late stage melanoma and has shown promising results in NSCLC and crizotinib as a Alk inhibitor[192]. However, effective therapies for lung adenocarcinoma with more typical mutation profiles, namely those associated with cigarette smoking, which accounts for 80% to 90% of lung adenocarcinoma cases[13], remain to be identified, thus highlighting the need for a better understanding of the molecular and genetic alterations that promote the initiation and progression of lung adenocarcinoma.

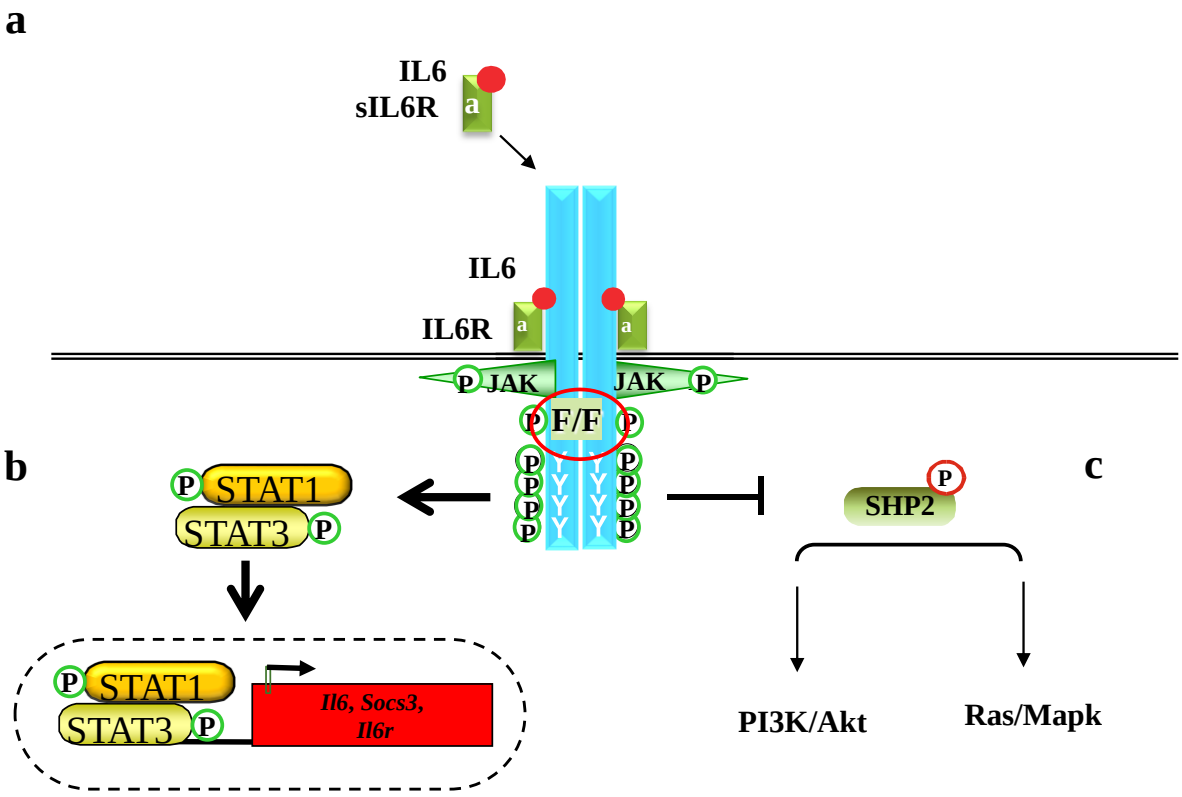

Figure 1.5. Schematic illustration of gp130$^{F/F}$ mouse model signalling

Schematic illustration of the gp130$^{F/F}$ model for deregulated IL-6/gp130 signalling. (a) Deregulated IL-6 signalling through the gp130 homodimer with corresponding α–receptors for IL-6. (b) Loss of binding of SOCS3 leads to hyperactivation of Stat3 homodimers and an upregulation of Stat target genes. (c) Loss of binding of SHP2 inhibits activation of the PI3K/Akt and Ras/Mapk pathways.

1.7 The gp130$^{F/F}$ mouse model

The pathological role of gp130 signalling in promoting lung cancer has not been investigated, largely due to the paucity of genetically-defined preclinical mouse models for pulmonary inflammation and LAC that allow for identification of disease-related gp130 signalling pathways *in vivo*. To address this we took advantage of our *gp130*$^{F/F}$ mouse model for pulmonary inflammation and associated deregulated gp130 signalling[146] (Figure 1.5).

(i) Genetics and signalling

At the molecular level, these gp130$^{F/F}$ (F/F) mice have been engineered to contain a phenylalanine (F) knock-in substitution of the cytoplasmic Y_{757} in gp130[146,198], leading to a hyperactivation of Stat3 signalling (Figure 1.5b) in the absence of signalling from the Ras/MAPK and PI3K/Akt pathways due to inhibition of binding of both SOCS3 and SHP2 (Figure 1.5c and d).

(ii) Phenotype

The gp130$^{F/F}$ mouse model was initially generated to determine whether deregulated gp130 signalling would have specific pathological consequences on the gp130 pathway, specifically gp130-dependent ERK/MAPK signalling, and the Stat3 pathway[199]. It was later found that compromising the ligand-bound gp130 receptor mediated exaggeration of Stat1 and Stat3 activation[133] and impaired activation of the ERK/MAPK pathway and associated target genes, specifically the tumour suppressor gene *Tff1*[146]. This group showed that hyperactivation of Stats, specifically Stat3, in *gp130*$^{F/F}$ mutant mice caused splenomegaly and gastric adenomatous hyperplasia, the latter by the induction of Smad7 and in turn antagonising the cytostatic activity of TGFβ[146]. Notably, our laboratory has also demonstrated that augmented

IL-6 trans signalling via Stat3 hyperactivation in *gp130*$^{F/F}$ mice promotes deregulated inflammatory responses leading to hypersensitivity to LPS-mediated septic shock[147], suggesting that *gp130*$^{F/F}$ mice provide an invaluable genetic tool to formally elucidate whether IL-6 trans signalling contributes to inflammatory-related diseases.

(iii) Lung disease

The mice develop enlarged airspaces by 6 months of age and are noted to have inflammatory infiltrates. Further examination confirms the airspace enlargement is consistent with emphysema[200] rather than hypoplasia. In addition, these mice display impaired expression of tumour suppressor genes in response to the chemical carcinogen NNK[21], this correlated with reduced surface tumour development in the lungs of these mice. These mice were also utilised to elucidate the role that IL-6 trans signalling plays on the pathogenesis of emphysema[173]. Specifically, it was shown that smoke-induced *gp130*$^{F/F}$ mice were characterised by excessive production of sIL-6R and that genetic blockade of IL-6 trans signalling ameliorated emphysema in these mice[173]. This data showed a prospect for the therapeutic targeting of IL-6 trans signalling in emphysema.

1.8 Hypothesis and Aims

Given all the evidence that involving IL-6 with lung cancer, we hypothesised:

1) gp130/Stat3-driven inflammation will interact with genetic (Kras) risk factors to facilitate LC initiation and progression in vivo.

2) IL-6 signalling via classical and/or trans signalling, is the upstream mechanism of gp130/Stat3-driven lung carcinogenesis.

3) The IL-6/gp130/Stat3 signalling axis in human airway epithelial cells cooperate with lung cancer risk factors to augment inflammatory and oncogenic cellular process in vitro. The overall aim is to investigate whether IL-6 trans signalling is a viable target for therapeutic diagnosis.

The specific aims of the project were:

(i) Identify whether deregulated gp130 signalling-driven lung inflammation exacerbates Kras-induced lung carcinogenesis *in vivo*.

(ii) Define IL-6 signalling via classical and/or trans-signalling as the key driver for Kras-induced lung carcinogenesis.

(iii) Investigate the role of Stat3 in IL-6 trans signalling-driven lung cancer in Kras associated development and progression of lung carcinogenesis.

(iv) Investigate the molecular and cellular consequences of cooperation between the gp130/Stat3 pathway and lung cancer risk factors in human airway epithelial cells in vitro.

This study will develop a significant and original understanding of the mechanisms involved in LC initiation and progression and exploration of the basic concepts of IL-6 trans signalling in LC. Accordingly, this work has the potential to strengthen the translational impact of IL-6 targeted therapeutics in the clinic.

Chapter 2
Materials and Methods

2.1 Animal procedures

2.1.1 – *Mouse generation*

The gp130$^{F/F}$ mice (C57BL/6 x Sv129 background) homozygous for the $Y_{757}F$ knock-in mutation (F/F), along with compound mutant mice homozygous for IL-6 knockout (IL-6$^{-/-}$), or heterozygous for Stat3 (Stat3$^{-/+}$) were generated to produce *gp130*$^{F/F}$:*IL-6*$^{-/-}$ (F/F:*IL-6*^{KO}) and *gp130*$^{F/F}$:*St3*$^{-/+}$ (F/F:*St3*$^{-/+}$) mice on a mixed background previously as described[119,146]. Accordingly, we cross bred F/F mutant and *gp130*$^{+/+}$ (WT) mice onto the lung cancer susceptible genetic background *Kras*^{G12D} [51] (available from Professor N Watkins' laboratory, Hudson Institute) carrying an activated oncogenic *Kras* mutation which is proceeded by a Lox-P stop codon to generate *gp130*$^{F/F}$:*Kras*^{G12D} (F/F:*Kras*^{G12D}), *gp130*$^{F/F}$: *Kras*^{G12D}:*IL-6*$^{-/-}$ (F/F:*Kras*^{G12D}: *IL-6*^{KO}) and *gp130*$^{F/F}$:*Kras*^{G12D}:*Stat3*$^{-/+}$ (F/F:*Kras*^{G12D}:*Stat3*$^{-/+}$) mice. In addition, the F/F:*Kras*^{G12D} and *gp130*$^{+/+}$:*Kras*^{G12D} (*Kras*^{G12D}) mice were crossed with the transgenic mouse model sgp130Fc[132] that blocks the endogenous IL-6 trans signalling by competitive binding of IL-6 and soluable (s) IL-6 receptor complex; to produce *gp130*$^{+/+}$:*Kras*^{G12D}:*sgp130Fc*$^{tg/tg}$ (*Kras*^{G12D}:sgp130Fc) and *gp130*$^{F/F}$:*Kras*^{G12D}:*sgp130Fc*$^{tg/tg}$ (F/F:*Kras*^{G12D}:sgp130Fc) mice. Mice were housed at the Monash Medical Centre Animal Facility (Clayton, VIC, Australia) under specific Pathogen Free (SPF) conditions at 18-24^{0}C with relative humidity of 40-70%, and *ad libitum* food and water. All experiments were fully endorsed by the Monash University Animal Ethics Committee (Monash Medical Centre "A", APP no: 2009-05, 2013-06).

2.1.2 - *Genotyping Polymerase Chain Reaction (PCR)*

Genotyping of mice for *gp130, Kras, IL-6* and *Stat3* was performed by amplifying specific regions of genomic DNA. DNA extraction and genotyping was performed by either myself or other members of the Cancer and Immune Signalling Laboratory (CIS, Hudson Institute) from tail cuttings. Tails cuttings were incubated overnight in tail buffer (Appendix I) and 1.3% Proteinase K (Roche, Mannheim, Germany) at 55°C. Next, 5M sodium chloride was added and the mix incubated at room temperature for 10 minutes and then centrifuged for 25 minutes at 13.5Krpm. The aqueous phase was removed to a new eppendorf tube and mixed with 100% isopropanol and centrifuged for 15 minutes at 13.5Krpm to pellet the DNA. The DNA pellet was washed in 70% ethanol and re-pelleted before drying at 37°C. The dried pellet was re-suspended in MilliQ water (Millipore, Bedford, MA, USA) overnight at 4°C. Additional purification was performed using a vacuum manifold utilising a Whatman UNIFILTER 800 plate (Sigma, Saint Louis, USA), PB binding buffer, and PE wash buffer (Qiagen, Hilden, Germany). DNA was finally eluted from the filter plate using 0.23% TE buffer (Appendix I).

PCR was conducted in a standardised manner optimised by members of the CIS Laboratory. PCRs were performed utilising the GoTaq Flexi or G2 GoTag Flexi DNA polymerase kit (Promega, WI, USA): 100ng of genomic DNA, 0.2mM deoxynucleotides (dNTPs), 1.5mM magnesium chloride (MgCl), 5% green buffer, 0.5U Taq enzyme, primers at 1µM (Sequences see Appendix II) and MQH_20 to a total of 25µl. PCR's were run on Veriti ® 96 well thermo cycler (Life Technologies, California, USA) using the condition outlined in appendix II.

PCR products were run on 2% agarose gels (Appendix I) and SYBRSafe ® (Invitrogen, Lohne, Germany) for DNA visualisation. A 1kb DNA ladder (NEB, Ipswich,

MA) was used to identify band size. Gels were run for 40 minutes at 90V in 1xTAE buffer (Appendix I) and visualised under UV light in a gel dock (SafeImage, Invitrogen).

2.1.3 – *Cre recombinase adenovirus inhalation*

Mice at 6 weeks of age were anesthetised with Avertin (Sigma, Saint Louis, USA) at a dose range of 0.4-0.75mg/g (0.5-0.7ml of working solution) via a single intraperitoneal injection. Following deep anaesthesia, mice were treated with either a single dose of $5x10^6$ plaque-forming units (pfu) per mouse of inhaled adenovirus expressing *Cre recombinase* (*Cre*, University of Iowa, Gene Transfer Vector Core, Iowa city, USA) as previously described (Dupage et al., 2009) or a vehicle control. A working solution of either *Cre* (125ul/per mouse) or vehicle (0.01M PBS, pH 7.4) was prepared by combining with Minimum Essential Medium Eagle (MEM, Sigma) and 2M calcium chloride ($CaCl_2$, Fluka, Steinheim, Germany), and then administered to mice via the tip of the nostrils.

2.1.4 - *Therapeutic treatment of mice*

Two anti-IL-6R monoclonal antibodies; 25F10, and 1F7, and an isotype control (kindly donated by Dr Walter Ferlin, NovImmune, Geneva, Switzerland) were administrated to mice via a single intraperitoneal injection at 10mg/kg injection twice a week for 6 weeks of observation, with the initial injection given the day after Cre inhalation.

2.1.5 – *Lung tissue collection and preparation*

Following 6 weeks post inhalation, mice were culled by an intraperitoneal injection of >100mg/kg Pentobarbitone sodium euthanasia (Ilium, Smithfield, NSW, Australia). Blood was collected via cannulation of the inferior vena following death, collected blood was placed into 1.5ml eppendorf tubes for serum preparation. Lungs were collected for histology, protein

and RNA extraction, if both perfused lung and frozen tissue was required, the left main lobe was first isolated by securing a suture around the hilum before the lobe was removed. For histology the lungs were perfused with 4% normal Buffered Formalin (Amber Scientific, Midvale, WA, Australia) at a pressure of 20cm H_2O for at least 5 min, before the trachea was tied off and the lungs and mediastinum removed *en bloc*. After 16 hours in formalin, tissues were transferred to 70% ethanol for long term storage. For molecular analyses, the lobe or the whole lungs were placed in 1.5ml eppendorf tubes, snap frozen in liquid nitrogen and stored at -80°C.

2.2 Histology

2.2.1 - *Sample embedding and sectioning*

The lungs were isolated from other mediastinal tissues and placed, whole, into a histology cassette and processed at the Hudson Institute Histology Facility using standardised procedures before embedded in low melting point paraffin (Paraplast Plus, Leica Microsystems, Peterborough, UK). Briefly, samples were processed through dehydration by a series of ethanol stages and xylene (Clearing) stages and finally infiltration and impregnation with Paraplast Plus paraffin (See Appendix III for specific process) using the Leica Automated processor (ASP300, Leica Microsystems). The paraffin-embedded lungs were then serial sectioned at 5µm andtwo tissue sections per slide were prepared.

2.2.2 - *Rehydration and Dehydration*

Prior to histological analyses, all slides containing tissues sections were dewaxed twice in 100%(v/v) Xylene (Merck, Kilsyth, Australia) and rehydrated in a series of ethanol; twice in 100% (v/v) and once in 70% (v/v) for 5 minutes in each steps. Stained slides followed the

reverse of this procedure to dehydrate the slides before cover slipping with DePeX (BDH, Nottingham, UK) for long term storage.

2.2.3 - *Haematoxylin and Eosin staining*

Following dewaxing and rehydration, slides were placed in Harris Haematoxylin (Amber Scientific) for 5-7 minutes and then rinsed three times in water. Differentiation was achieved with a single dip in acid alcohol (Appendix I) and 30 seconds in a basic solution (Scott's tap water, Appendix I). Slides were observed under microscope for intensity before staining with Eosin (Amber Scientific) for 4-6 minute. Excess stain was washed off before dehydration and cover slipping.

2.2.4 - *Immunohistochemistry*

Antigen detection for proteins of interest were performed on paraffin-embedded lung sections with specific antibodies for Thyroid Transcription Factor (TTF)-1 (Novis Biologicals, CO, USA), CD45 (BD biosciences, CA, USA), and Proliferating Cell Nuclear Antigen (PCNA, Cell signalling, MA, USA). Antigen retrieval was performed by boiling slides in Citrate buffer (Appendix I) for 2 minutes at a high heat and a further 4 minutes at a low heat then allowing to cool in a fume hood. The slides were then washed thoroughly in distilled water and endogenous peroxidises were quenched by incubating sections in 3% peroxidase (H_2O_2, Merck). All antibody incubations were carried out in a humidified chamber. Non-specific background staining was blocked using 10%(v/v) Normal Goat Serum (NGS, Vector Laboratories, CA, USA) for TTF1, CAS block (Invitrogen) for CD45, and MOM blocking reagent (Vector Laboratories) for PCNA. All primary antibodies were diluted in appropriate blocking buffer or Phosphate buffered saline (PBS) (Appendix I) and incubated either at room temperature (RT) for 1 hour (PCNA) or 4°C overnight (TTF-1, CD45) and then washed

thoroughly in PBS and Tween 20 (PBS/T) (Appendix I). Detection was performed by incubation in specific biotinylated secondary antibodies (Vector Laboratories) for 1 hour at RT and washed in PBS/T. The sections were then amplified using the Vector ABC Kit (Vector Laboratories, CA, USA) by incubation for 30 minutes at RT and thoroughly washed in PBS/T prior to signal development in Diaminobenzidine chromogen (DAB) (Dako, CA, USA). This reaction was stopped by rinsing the sections in distilled water. Finally, sections were counter-stained using Harris Haematoxylin (Amber Scientific) and blueing using Scott's tap water (Appendix I) for 1 minute before dehydration and cover slipping.

Apoptosis was determined by the terminal deoxynucleotidyl transferase (tdT)-mediated dUDP nick-end labeling (TUNEL) technique using an ApopTag Peroxidase *In Situ* Apoptosis Detection kit (Millipore, Billerica, MA) according to manufacturer's instructions.

2.2.5 – Immunohistochemical quantification

Quantitative enumeration of the above chromogen labelled antibodies on positively stained sections were performed by imaging 20 times in randomly chosen fields of view at 100x magnification. Positively stained cells in all images were counted using Fiji (ImageJ 1.49f). Biological replicates were averaged and Statistics (See section 2.5) of experimental replicates were determined using GraphPad Prism (version 6.0).

For quantitative enumeration of H&E stained sections, images of the whole slide was procured utilising Aperio digital imaging and percentage of the whole lung was determined using Fiji. Briefly, slides of H&E stained sections were imaged by the Victorian Cancer Biobank, Monash Medical Center, Clayton using the Aperio digital imaging system. Files of whole slide images were accessed using Apero Imagescope (version 12.1.0.5029) and region of interest was extracted into a TIF bio-format. Using Fiji (ImageJ 1.49f), the area of the

whole lung verses the percentage of damaged parenchyma was determined and Statistics (See section 2.5) determined using GraphPad Prism (version 6.0).

2.3 RNA preparation and analysis

2.3.1 - *RNA extraction from tissue*

Total RNA from frozen tissue samples was extracted using the phenol-based reagent TRISure (Bioline, Alexandria, NSW, Australia) containing a combination of denaturants and RNase inhibitors. Tissues (about 50mg) were homogenised in 1ml of TRISure (Bioline) in a flat bottomed tube and transferred to a 1.5ml eppendorph tube. Insoluble materials were then discarded by centrifugation at 3000rpm for 30 minutes at 4°C and the supernatants were collected. The supernatants were then mixed with 200µl of chloroform and incubated for 5 minutes at RT prior to centrifugation at 3,000rpm for 45 minutes at 4°C for separation (3 phases). The upper phase (aqueous layer containing RNA) was collected into a fresh 1.5ml eppendorf tube and the RNA was precipitated by incubating 10 minutes at room temperature with 500µl of 100% isopropanol and then centrifugation at 3,000rpm for 45 minutes at 4°C. The supernatant was discarded and the pellet washed in 75% (v/v) ethanol/Diethyl pyrocarbonate (DepC) water (Appendix I) and centrifuged at 3,000rpm for a further 15 minutes at 4°C. The supernatant was again discarded and the pellet air dried and re-suspended in 50µl DepC water. The RNA concentration was then determined by utilisation of a Nanodrop (Thermo Scientific, Wilmington, USA) by measuring the optical density (OD) at 230, 260 and 280nm.

2.3.2 – *DNase Treatment*

Extracted RNA was purified “on column” utilising the QIAGEN RNeasy(R) kit according to the manufacturer’s specifications. Briefly, 50µl DepC water was added to previously extracted RNA with 350µl 99% RLT buffer and 1% (v/v) β-Mercaptoethanol followed with the addition of 250ul of 100% ethanol. Then sample mixtures were transferred into an RNeasy column and centrifuged for 30 seconds at 8000rpm. The flow through was discarded and the column was washed with 350ul of RW1 buffer. For on column DNase treatment, 80µl of DNase incubation mix (Appendix I) was added directly to the RNeasy column membrane and incubated for 15 minutes at RT. The membrane was then washed with 350µl of RW1 buffer, followed by 2 washes of 500µl of RPE buffer with centrifugation for 30 seconds at 8000rpm. The flow through was discarded and the RNeasy column was place into a collection tube for RNA elution with 2x30µl aliquots of RNeasy-free H2O before the concentration determined by Nanodrop. RNA was then stored at -80°C for further analysis.

2.3.3 - *Reverse Transcription (RT) Reaction*

For the synthesis of cDNA, 1µg concentration of RNA was reverse transcribed in a final volume of 20µl using the Transcriptor High Fidelity cDNA synthesis kit (Roche) in accordance with manufacturers’ instructions. Briefly, 11.4µl of template-primer mix containing sample RNA and 60µM of random hexamers was firstly denatured for 10 minutes at 65°C. The sample was then chilled on ice before the addition of 8.6µl of Roche master mix containing 8mM of magnesium chloride ($MgCl_2$), 20U of protector RNase inhibitor, 1mM of Deoxynucleotide (dNTP), 5mM of Dithiothreitol (DTT) and 10U of High Fidelity Reverse Transcriptase. The absence of contaminating genomic DNA in RNA samples (-RT control) was confirmed using reactions in which Reverse Transcriptase enzyme was omitted. Samples were then incubated for 1 hour at 55°C and the enzyme was inactivated by heating for 5

minutes at 85°C. The cDNA was either stored at -20°C prior to quantitative-PCR (qPCR) analysis or used immediately.

2.3.4 – *Quantative Reverse Transcription – Polymerase chain reaction (qPCR)*

The qPCR was performed using the Applied Biosystems 7900HT Fast RT PCR system (Forster city, USA) and SYBR magic (Invitrogen). Specific oligonucleotide primer sequences were designed using Primer-BLAST (http://www.ncbi.nlm.nih.gov/tools/primer-blast/) or were obtained from published sources, all primer sequences are shown in appendix II. For qPCR analyses, a master mix with a final volume of 8ul was prepared consisting 5ul of SYBR magic mix, 0.2ul of forward and reverse primers (10uM, Appendix II), 2.6µl of DepC-treated water per well of 384 detection plate (Applied Biosystems). Once the master mix was added to each wells, 2ul of cDNA (refer to section 2.3.3) was added in the appropriate wells. For all qPCRs, the samples were performed in triplicates with conditions 50^{o}C for 2 minutes, 95^{o}C for 10 minutes followed by 40 cycles of 95^{o}C for 15 seconds and 60^{o}C for 1 minute. A melting curve analysis was included at the end of the 40cycles reaction to monitor PCR product purity (primer dimer formation). The delta-delta CT method (Based on relative comparative threshold) was used to determine the relative expression or fold-induction of specific genes and 18S was used as a house-keeping reference gene.

2.4 Protein expression analysis

2.4.1 – *Protein sample preparation from tissue and cells*

For the preparation of protein lysates from snap-frozen lung tissues, about 50mg of tissues were homogenised in 1ml of ice cold 1x protein lysis buffer (Appendix I) supplemented with 0.1mM sodium fluoride (Sigma), 16µM of sodium orthovanadate (Sigma) and 0.1% (v/v)

protease inhibitors (Roche, Mannheim, Germany). Homogenates were agitated for 60 minutes, and then centrifuged for 10 minutes at 14,000rpm at 4°C prior to the transfer of supernatants to fresh 1.5ml eppendorf tubes. The protein lysates were then pre-cleared of non-specific immunoglobulins with 2% (v/v) sepharose beads (GE Healthcare, Uppsala, Sweden) by agitating for 30 minutes at 4°C. The beads were pelleted by centrifugation at 3,000rpm for 3 minutes at 4°C before transferring the supernatants to fresh 1.5ml eppendorf tubes for storage at -80.

2.4.2 - *Lowry protein assay*

Protein concentrations were determined utilising the Lowry assay described by Oliver H Lowry, 1951 [201]. Briefly, 1mg/ml of *bovine* serum albumin (BSA, Sigma) was prepared in PBS as the standard for serial dilution in a flat-bottomed 96 well microtitre plate (Becton, Franklin lakes, USA) at concentration showed below (Table 2.1). Samples were diluted in PBS to 1:1 ratio. Both standards and samples were performed in duplicate for which 5µl was added to each well. Then 25µl of Lowry working reagent (20µl of reagent S per 1ml of reagent A) and 200µl of reagent B was added and incubated for 15 minutes at RT. Absorbance at 450nm was read using the FLUROstar Optima plate reader (BMG LABTECH, Ortenberg, Germany).

Table 2.1: Preparation of standards for Lowry Assay.

BSA Stock	-	1mg/ml	1mg/ml	5mg/ml	5mg/ml	10mg/ml	10mg/ml
Standard Conc.	**-**	**1µg**	**2µg**	**4µg**	**8µg**	**10µg**	**20µg**
Stock Volume.	0µl	1µl	2µl	4µl	1.6µl	1µl	2µl
dH2O volume.	5µl	4µl	3µl	1µl	3.4µl	4µl	3µl
Final Volume.	5µl	5µl	5µl	5µl	5µl	5µl	5µl

2.4.3 - *Sodium Dodecyl Sulphate – Polyacrylamide Gel Electrophoresis (SDS-PAGE)*

SDS-page was used to resolve proteins on 10%, 1.5mm thick gels. Polyacrylamide gels were prepared by using 30% (w/v) (29:1) acrylamide/bis mix (Bio-Rad, Hercules, USA), either with lower gel buffer (Appendix I; resolving gel pH 8.8) or upper gel buffer (Appendix I; stacking gel pH 6.8), 10% (w/v) ammonium persulphate (APS, Bio-Rad) and 0.001% N,N,N',N'-Tetramethylethylenediamine (TEMED, Bio-Rad), the latter of which were used to polymerise the acrylamide gels. Polyacrylamide gel mixtures were poured using Mini-PROTEAN Tetra Electrophoresis casting plates (Bio-Rad) for polymerisation. After polymerisation, the gels were transferred to a Mini-PROTEAN Tetra Electrophoresis System (Bio-Rad) filled with 1 x SDS-PAGE running buffer (Appendix I). An equal volume of 2 x sample buffer (Appendix I) was added to samples which were heated for 5 minutes at 95°C, centrifuged and loaded into wells alongside a benchmark molecular weight marker (New England Biolabs, Ipswich, USA) to estimate protein size/mobility. Gels were electrophoresed at 100V through the resolving gel until the leading band touched the bottom of the gel. Protein samples were transferred to a membrane for western blot analysis (Section 2.4.4).

2.4.4 – *Western blotting*

Fractionated proteins were transferred either onto nitrocellulose Hybond-C extra membranes (Amersham, Buckinghamshire, England) or polyvinylidene fluoride (PVDF) immobilon-P membranes (Millipore) using the wet transfer technique in a Mini Trans-Blot Electrophoretic Transfer Cell (Bio-Rad) apparatus. Two fiberpads, two filter papers and the membrane was soaked in transfer buffer (Appendix I) for 5 minutes, the resolving gel was soaked in transfer buffer for 10-20 minutes prior to transfer. Specifically, PVDF membranes were pre-treated with 100% Methanol (AR grade) followed by rinsing in Milli-Q H_2O. Proteins were transferred at 100V in transfer buffer for 90 minutes.

Membranes were then blocked in Odyssey blocking buffer (OBB, LI-COR, Lincoin, USA) supplemented with 0.2% (w/v) BSA (Sigma) and 0.01% Tween-20 (Sigma) for 1 hour at RT. Membranes were then probed with appropriate primary antibody (Appendix IV) diluted in the above blocking buffer for 1 hour at RT or overnight at 4°C. Subsequently, membranes were washed in PBS supplemented with 0.1% (v/v) Tween-20 (PBS/T) at 3 x 5 minutes per wash and further incubated for 1 hour at RT with the appropriate AlexaFluor 680 (Invitrogen) or IRDye800CW (LI-COR) fluorescent labelled secondary antibodies (2^{o} Ab) diluted at 1:3000 in appropriate blocking buffer. Membranes were then washed twice for 10 minutes in 1 x PBS/T and once for 10 minutes in 1 x PBS. Visualisation of target proteins on membranes was performed with the Odyssey fluorimager (LI-COR) infrared imaging system.

2.4.5 - *Western blot membrane stripping*

Membranes requiring additional antibody detection were stripped using membrane stripping buffer (Appendix I) for 5 minutes at 55°C. Membranes were washed in PBST solution 3 x 5 minutes and blocked for 30 minutes at RT in OBB. From this point on, antibody re-blotting followed the same procedure as outlined above (section 2.4.4).

2.4.6 - *Enzyme-Linked Immunosorbent Assay (ELISA)*

Human and mouse IL-6(BD Biosciences, Franklin lakes, NJ, USA), sIL-6R (R&D, Minneapolis, MN, USA) and sgp130 (R&D, Minneapolis, MN, USA) were quantified using commercial ELISA kits according to manufacturer's specifications. Briefly, flat-bottomed 96-well plates (Sigma) were coated with 100µl of diluted capture antibody in coating buffer (Appendix I) and incubated overnight at 4°C. The plate was then washed 3 times with 0.5% PBS/T before non-specific binding was blocked using 300µl of assay diluent for 1 hour at RT. The plate was washed again for 3 times with 0.5% PBS/T before serial dilutions of

standards was added and 100µl of samples was added in duplicate. A top standard of 10,000pg/ml and a bottom of 15.63pg/ml was used and diluted where necessary in assay diluent. Plate was incubated for 2 hours at RT and again washed as described above. For human and mouse IL-6 the detection antibody and streptavidin-HRP were added together (Working detection, Appendix I) and incubated for 2 hours at RT. For sgp130 and sIL-6R the detection antibody was added and incubated for 2 hours at RT before being washed and 100µl of the Streptavadin-HRP was added and incubated for 20 minutes at RT. Following a final three washes with 0.5% PBS/T 100µl of substrate solution was added and incubated for 20 minutes at RT. The reaction was terminated by application of 50µl of Stop wash buffer (Appendix I) and absorbance measured at 450nm on the FLUROstar Optima plate reader (BMG LABTECH, Ortenberg, Germany).

2.5 Statistical analyses

All Statistical analyses were performed using GraphPad Prism for Windows version 5.0. As all data were normally distributed, one-way ANOVA and student t-test were used to determine the differences between all genotypes with *Cre*/vehicle inhalation and between $gp130^{F/F}$:$Kras^{G12D}$ and control $gp130^{+/+}$:$Kras^{G12D}$ mice with *Cre* inhalation, respectively. Additionally, a $P < 0.05$ was considered Statistically significant. Data are expressed as the mean ± SEM.

Chapter 3
Elucidating the involvement of deregulated gp130 signalling in Kras induced lung carcinogenesis

3.1 Introduction

Human lung cancers are classified into 2 major histopathological types, NSCLC which represents the majority (~85%) of LC cases, and SCLC. NSCLC is further subtyped into lung adenocarcinoma (LAC, ~40%, the most common), squamous cell carcinoma and large cell carcinoma based on similarities in diagnosis, staging, prognosis, and treatment. LAC is strongly associated with chronic lung inflammation triggered by cigarette smoking[13], and one of the most established disease-associated consequences of the genotoxic effects of cigarette-derived carcinogens is activating mutations in the *Kras* proto-oncogene[202]. However, effective therapies for LAC with more typical mutation profiles such as *Kras* are yet to be identified, thus highlighting the need for a better understanding of the molecular and genetic alterations which promote the initiation and progression of LAC.

In this regard, activating *Kras* mutations are found in approximately 10%-40% of NSCLC cases (both smokers and never smokers), with nearly all mutations occurring in codon 12 and 13, with the predominant histological subtype affected being adenocarcinoma[203], and correlate with poor survival prognosis[12]. A definitive role for *Kras* in the initiation and progression of lung cancer is evidenced by the spontaneous development of lung adenocarcinoma in mouse models genetically engineered to express the oncogenic

†St Vincent's Hospital, 41 Victoria Parade, Fitzroy, Victoria 3065, Australia;
‡Department of Pathology, Melbourne Medical School, Melbourne University, Grattan Street, Parkville, Victoria 3010, Australia

Kras^{G12D} allele conditionally, somatically, or inducibly in the lungs of mice[62,204]. Despite the overwhelming evidence implicating *Kras* signalling in lung cancer pathogenesis, a signalling pathway or pathways which promote *Kras*-induced lung adenocarcinoma are yet to be formally identified. However, there is evidence to suggest that downstream mediators such as Erk, Mapk and PI3K/Akt are likely candidates, and more recently Stat3[42,46,63]. However, these studies failed to identify upstream signalling pathway leading to activation of latter downstream mediators.

Since the pleotropic effects of IL-6 family cytokines, for instance, cell survival and proliferation, angiogenesis and inflammation, are mediated via gp130, it is of interest that somatic constitutively-activating mutations in gp130 have been identified in human inflammatory hepatocellular adenomas[148], thus invoking the possibility of similar mutations in other inflammatory-related cancers (e.g. lung). In addition to IL-6 family cytokines, Ras proteins have been known for their capability to activate signalling pathways important for cell proliferation and cell migration. This is evidenced by Ras/Erk Mapk and PI3K/Akt signalling pathways being activated in *Kras*-induced lung carcinogenesis has been shown by the dependent nature of lung tumour development via the proto-oncogene serine/threonine-protein kinase C-raf but not the B-raf gene[205,206]. In contrast, *Kras*^{G12D} expression in the Ras-related C3 botulinum toxin substrate 1 (Rac1) null background mice had significantly impaired lung tumour development[207], indicating that Rac1 signalling is crucial for the oncogenic activity in mutant Kras.

In contrast, pY_{757} of gp130 plays a crucial role in attenuation of gp130 signalling by recruiting Socs3 to gp130[117], which regulates Stat activation. The importance of such a negative regulatory mechanism for gp130 signalling is highlighted by studies, including our own lab, showing gp130/Stat3 hyperactivation promotes gastric and colorectal inflammation-

†St Vincent's Hospital, 41 Victoria Parade, Fitzroy, Victoria 3065, Australia;
‡Department of Pathology, Melbourne Medical School, Melbourne University, Grattan Street, Parkville, Victoria 3010, Australia

associated tumours in mice[119,133,146]. The importance of Stat3 in lung cancer is suggested by the requirements of Stat3 for Ras-mediated oncogenesis[51], including in lung cancer cells[208,209], and that reduced Stat3 phosphorylation in associated with tumour regression in a Kras mouse LAC model[208]. Collectively despite above evidence, the causal role gp130 signalling in Kras induced lung cancer is not yet known.

Therefore, to elucidate whether gp130 signalling plays a role in Kras induced lung adenocarcinoma development, I utilised the *gp130*$^{F/F}$ (F/F) mouse model back-crossed onto the well-defined *Kras*^{G12D} background (as described above) for conditional lung cancer development[51] to produce an exacerbated inflammation-driven lung cancer susceptible mouse model. Therefore, unlike conventional transgenic and knock-out models, the *gp130*$^{F/F}$:*Kras*^{G12D} mouse model will provide an invaluable genetic tool to formally elucidate whether gp130-driven signalling in the lung contributes to this disease process.

3.2 Exacerbated adenocarcinoma *in situ* (AIS) in the lungs of *gp130*$^{F/F}$:*Kras*^{G12D} mice

As expected, no lesions were observed in the lungs of control *gp130*$^{F/F}$:*Kras*^{WT} and *Kras*^{WT} mice expressing wild-type *Kras* which were subjected to intranasal inhalation with PBS vehicle (Figure 3.1a and b). Classification of *gp130*$^{F/F}$:*Kras*^{G12D} lung pathology, following activation of oncogenic Kras^{G12D} specifically within the lung epithelium of 6 week old mice was initiated upon intranasal administration of adenoviral Cre recombinase. At 6 weeks post activation of oncogene *Kras*, a qualified anatomical pathologist of note in the field of lung cancer, Dr Prudence A. Russell[†‡], evaluated the pathological phenotype of *Kras*^{WT},

---

†St Vincent's Hospital, 41 Victoria Parade, Fitzroy, Victoria 3065, Australia;
‡Department of Pathology, Melbourne Medical School, Melbourne University, Grattan Street, Parkville, Victoria 3010, Australia

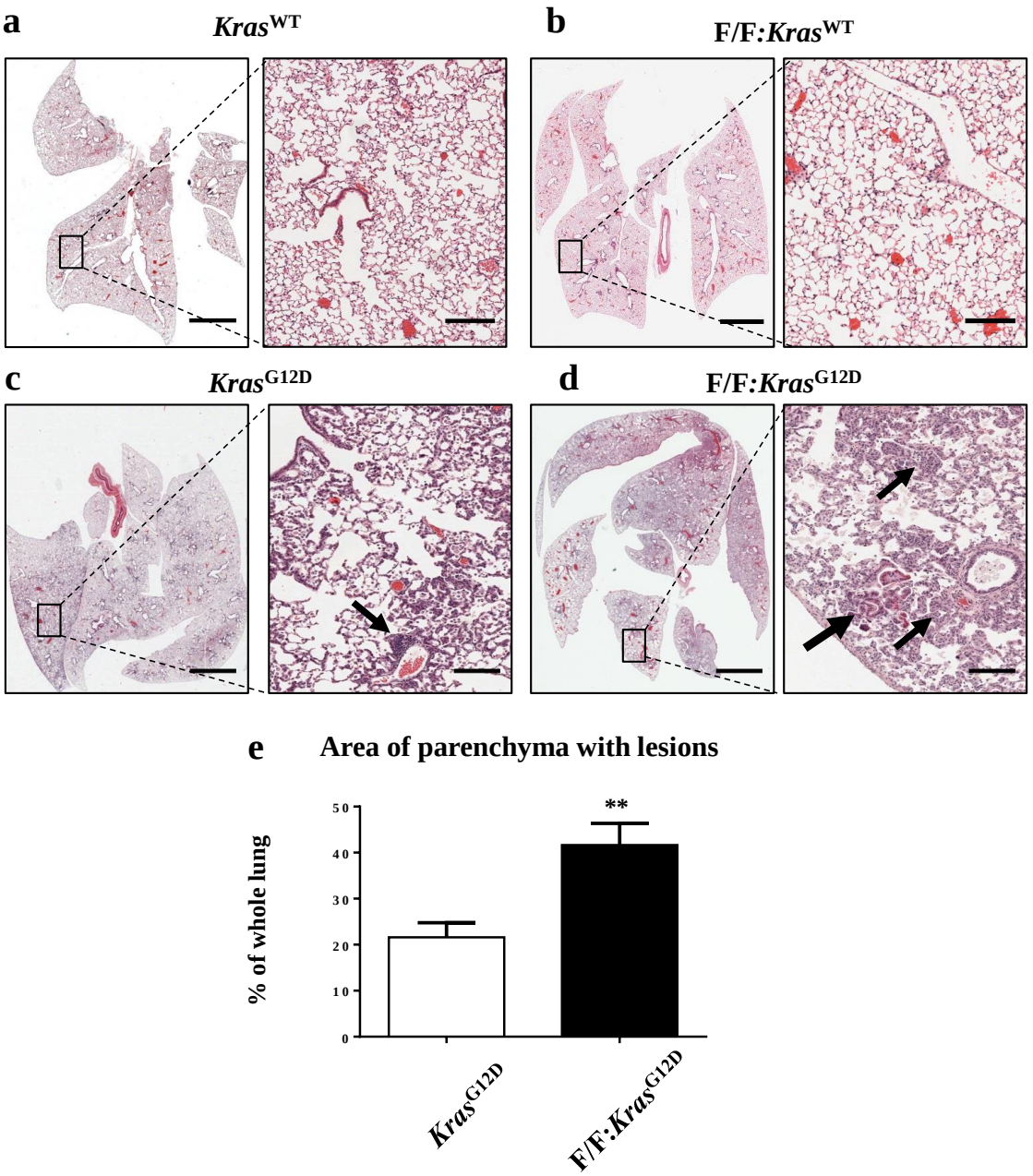

Figure 3.1. *gp130*$^{F/F}$:*Kras*^{G12D} mice show exacerbated *in situ* adenocarcinoma

Representative haemotoxylin and eosin-stained lung cross-sections from either *gp130*$^{+/+}$:*Kras*^{WT} (*Kras*^{WT}) (a) and *gp130*$^{F/F}$:*Kras*^{WT} (F/F:*Kras*^{WT}) (b) mice treated with vehicle control for 6 weeks or *gp130*$^{+/+}$:*Kras*^{G12D} (*Kras*^{G12D}) (a) and *gp130*$^{F/F}$:*Kras*^{G12D} (F/F:*Kras*^{G12D}) (d) mice treated with Cre-recombinase for 6 weeks. Small arrows, discrete AIS lesions. Large arrows, an invasive AIS lesion. Scale bar, 3mm left pane, 300µm right pane. (e) Quantification of lung parenchyma area occupied by AIS lesions for whole lung at 20X magnification. Data from 6 and 9 mice per genotype expressed as mean +/- s.e.m, ** $p<0.01$.

gp130$^{F/F}$:*Kras*^{WT}, *Kras*^{G12D} and *gp130*$^{F/F}$:*Kras*^{G12D} mice, in Haemotoxylin & Eosin (H&E) stained lung tissues sections.

The lungs of *Kras*^{G12D} mice revealed the presence of mild atypical adenomatous hyperplasia (AAH) in a peribronchial and peripheral lung location together with small, sporadicadenocarcinoma in situ (AIS) throughout the whole parenchyma. In addition, the cells were cuboidal with eosinophilic cytoplasm, have small uniform nuclei and some showed small basophilic nucleoli consistent with previous observations[51,208] (Figure 3.1c).

Comparatively, development of multiple large confluent foci of AIS was observed located peripherally, as well as in and around the small airways, and accompanied by large and diffuse foci throughout the parenchyma, in the lungs of *gp130*$^{F/F}$:*Kras*^{G12D} mice. In addition, larger tumour cells with clear cytoplasm, larger and more prominent nucleoli were noted. The *gp130*$^{F/F}$:*Kras*^{G12D} mouse lungs also developed invasive tumours with both solid and papillary architecture (Figure 3.1d, arrow). There was an overall significant, 2-fold, increase in the area of lung parenchyma affected by these lesions in *gp130*$^{F/F}$:*Kras*^{G12D} compared to *Kras*^{G12D} mice (Figure 3.1e). No such lesions were observed in the lungs of control *gp130*$^{F/F}$:*Kras*^{WT} and *Kras*^{WT} mice expressing wild-type *Kras* which were subjected to intranasal inhalation with PBS vehicle (Figure 3.1a and b). Collectively, the above data indicate that deregulated gp130 signalling augments tumour burden in *Kras*-induced lung cancer.

3.3 Exacerbated lung tumourgenesis in *gp130*$^{F/F}$:*Kras*^{G12D} mice correlated with an increase in Thyroid Transcription Factor (TTF)-1

To verify the exacerbated lung tumourigenesis phenotype in *gp130*$^{F/F}$:*Kras*^{G12D} mice, immunohistochemical evaluation with the alveolar epithelial type II cell marker TTF-1,

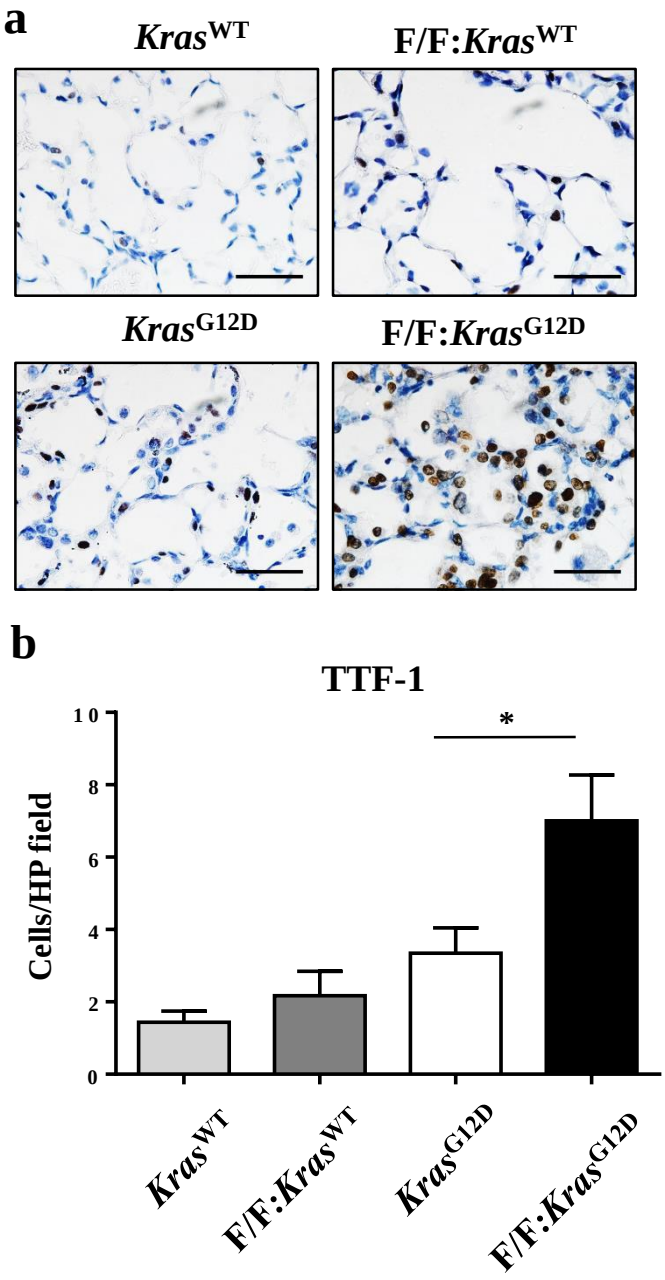

Figure 3.2. *gp130*$^{F/F}$:*Kras*^{G12D} mice show increased Thryoid transcription factor (TTF)-1
(a) Representative high-power photomicrographs of TTF-1-stained lung cross-sections from either *gp130*$^{+/+}$:*Kras*^{WT} (*Kras*^{WT}) and *gp130*$^{F/F}$:*Kras*^{WT} (F/F:*Kras*^{WT}) mice treated with vehicle control for 6 weeks or *gp130*$^{+/+}$:*Kras*^{G12D} (*Kras*^{G12D}) and *gp130*$^{F/F}$: *Kras*^{G12D} (*Kras*^{G12D}) mice treated with Cre-recombinase for 6 weeks. Scale bar, 300µm. (b) graph depicts quantitation of TTF-1 positive cells per high powered field (100x magnification) in the lungs of indicated mice. Data from 4 to 12 mice per genotype expressed as mean +/- s.e.m, * $p<0.05$.

which is used for the clinical diagnosis of LAC[203,209], was undertaken. The photomicrographs of TTF-1 immunostaining showed no changes in the lungs of control, vehicle treated, *gp130*$^{F/F}$:*Kras*^{WT} and *Kras*^{WT} mice expressing wild-type *Kras*, while a qualitative increase in TTF-1 positive cells in the lungs of *gp130*$^{F/F}$:*Kras*^{G12D} compared to *Kras*^{G12D} mice was observed (Figure 3.2a). Furthermore, quantitative stereological analysis indicated a significant, 2-fold, increase in the number of TTF1 positive cells in the lungs of *gp130*$^{F/F}$:*Kras*^{G12D} compared to *Kras*^{G12D} mice (Figure 3.2b). Thus, these data further demonstrate the exacerbated lung tumourgenic phenotype upon aberrant gp130-dependent signalling in *Kras*^{G12D} mice.

3.4 Pulmonary inflammation, cellular apoptosis and angiogenesis is not associated with exacerbated lung carcinogenesis in *gp130*$^{F/F}$:*Kras*^{G12D} mice

It has been well published that there is a definitive link between inflammation and cancer development[210]. With the recruitment of leukocytes to specific sites of damage over a chronic period of time, neoplasia-associated angiogenesis produces an array of cytokines and chemokines that change the tumour microenvironment and promote tumour growth[210-212]. In relation to this, inflammatory cell populations within the lung have been suggested to play a role in the pathogenesis of lung cancer[210,213]. It has been shown that therapeutic anti-inflammatory targeting using thymoquinone and sgp130Fc in human cell lines and mouse models respectively, ameliorates the progression of lung cancer development[214,215]. However, the role of inflammation in Kras-induced lung carcinogenesis remains unclear, with conflicting reports regarding the extent of pulmonary inflammation elicited upon oncogenic activation of *Kras*^{G12D} within the lung epithelium in mice[51,57,151].

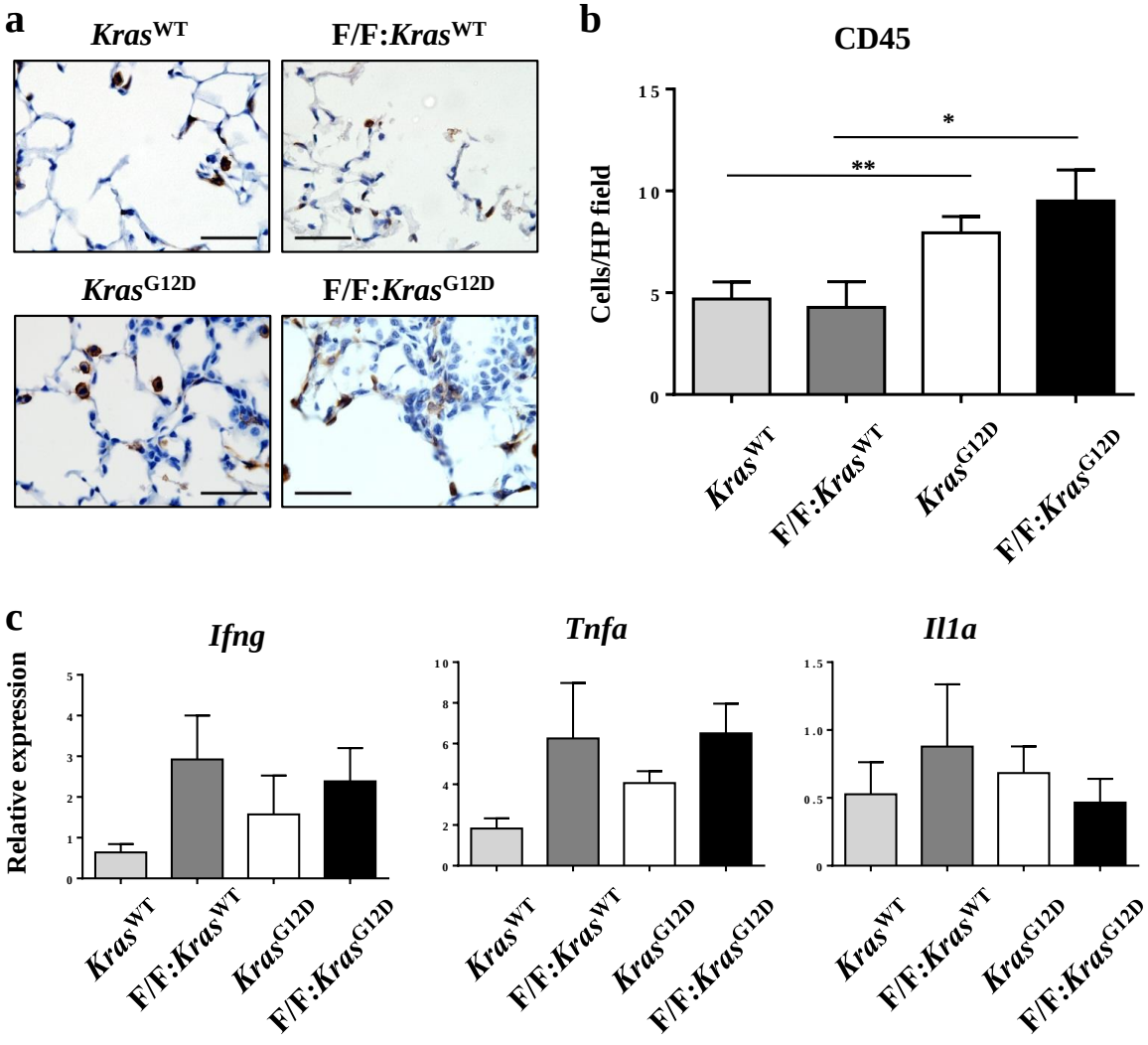

Figure 3.3. Augmented *Kras*-induced LAC in *gp130*$^{F/F}$:*Kras*^{G12D} mice is not associated with increased inflammation

(a) Representative photomicrographs of CD45-stained lung cross-sections from either *gp130*$^{+/+}$:*Kras*^{WT} (*Kras*^{WT}) and *gp130*$^{F/F}$:*Kras*^{WT} (F/F:*Kras*^{WT}) mice treated with vehicle control for 6 weeks or *gp130*$^{+/+}$:*Kras*^{G12D} (*Kras*^{G12D}) and *gp130*$^{F/F}$:*Kras*^{G12D} (F/F:*Kras*^{G12D}) mice treated with Cre-recombinase for 6 weeks. Scale bars = 50μm (b) Graph depicts quantitative enumeration of CD45 positive cells per high powered field (x100 magnification). Data from 4 to 12 mice per genotype expressed as mean +/- s.e.m, * $p<0.05$, ** $p<0.01$.

At 6 weeks post activation of *Kras*, we observed a comparable increase in the number of $CD45^+$ immune cells in the lungs of both *gp130*$^{F/F}$:*Kras*^{G12D} and *Kras*^{G12D} mice compared to control tumour-free *gp130*$^{F/F}$:*Kras*^{WT} and *Kras*^{WT} mice, respectively (Figure 3.3a and 3.3b). Despite this increase, the gene expression of the pro-inflammatory cytokines IFNγ, TNFα and IL1α were unchanged upon oncogenic activation of *Kras* (Figure 3.3c). Therefore, while these data suggest that oncogenic activation of *Kras* within the lung epithelium can elicit pulmonary inflammation, this is however not associated with the exacerbated lung tumourigenesis observed in *gp130*$^{F/F}$:*Kras*^{G12D} mice.

Avoidance of apoptosis is considered one of the hallmarks of cancer[93] and while the role for apoptosis in pulmonary disease is well documented[200,216,217], our knowledge of apoptosis in lung cancer development is relatively poor. In mouse models for LAC harbouring a *Kras* mutation, apoptosis levels were generally unchanged regardless of genetic ablation of other signalling factors[151,186,208].

As with previous observations for the *Kras*^{G12D} LAC model[151,208], the numbers of apoptotic TUNEL positive cells in the lungs of either *gp130*$^{F/F}$:*Kras*^{G12D} or *Kras*^{G12D} mice compared to their *Kras* wild-type controls were unchanged (Figure 3.4). In this regard, we note that while there was a significant increase in the number of apoptotic cells in the lungs of *gp130*$^{F/F}$:*Kras*^{G12D} compared to *Kras*^{G12D} mice, as reported previously this is also observed in *gp130*$^{F/F}$ compared to *gp130*$^{+/+}$ mice with wild-type Kras[200], and thus is independent of their Kras mutational status.

We next explored whether the exacerbated Kras-induced lung tumourigenesis in *gp130*$^{F/F}$:*Kras*^{G12D} mice was associated with the upregulated expression of genes encoding key angiogenic factors, namely vascular endothelial growth factor (Vegf), matrix metalloproteinase (Mmp)-2 and -9, and the glutamic acid-leucine-arginine (Elr) motif-containing chemokines Cxcl1 and Cxcl2. It has been shown that Ras mutations mediate

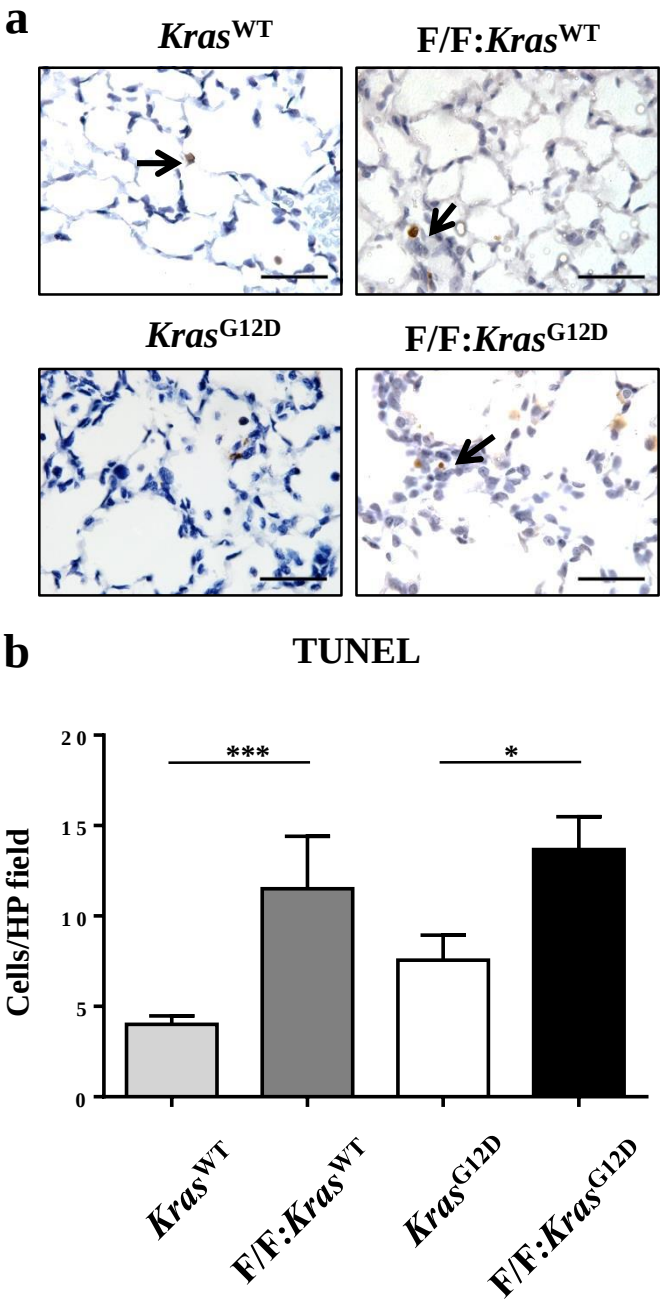

Figure 3.4. Apoptosis does not play a role in exacerbated lung cancer in *gp130*$^{F/F}$:*Kras*^{G12D} mice

(a) Representative photomicrographs of TUNEL-stained lung cross-sections from either *gp130*$^{+/+}$:*Kras*^{WT} (*Kras*^{WT}) and *gp130*$^{F/F}$:*Kras*^{WT} (F/F:*Kras*^{WT}) mice treated with vehicle control for 6 weeks or *gp130*$^{+/+}$:*Kras*^{G12D} (*Kras*^{G12D}) and *gp130*$^{F/F}$:*Kras*^{G12D} (F/F:*Kras*^{G12D}) mice treated with Cre-recombinase for 6 weeks. Scale bar, 50µm. (b) Graph depicts quantitative enumeration of TUNEL positive cells per high powered field (x100 magnification). Data from 4 to 12 mice per genotype expressed as mean ± s.e.m, * $p<0.05$, *** $p<0.005$.

endothelial cell-dependent tumour angiogenesis via Vegf[218], and that in human xenograft models, secretion of IL-8 via Ras signalling activates tumour-associated angiogenesis[219]. Also, that in a LC *Kras*^{G12D} model harbouring a Cre-mediated CC10 mutation Vegf was significantly elevated[57]. However, the expression of these genes was comparable between *gp130*$^{F/F}$:*Kras*^{G12D} and *Kras*^{G12D} mice and their *Kras* wild-type counterparts (Figure 3.5). These data therefore suggest that deregulated gp130 signalling increases the number of apoptotic cells independent of their *Kras* mutational status.

3.5 Exacerbated lung carcinogenesis in *gp130*$^{F/F}$:*Kras*^{G12D} mice is associated with augmented lung cellular proliferation

Uncontrolled cellular proliferation is a hallmark of all malignant tumour growth[93] and we have previously discussed that IL-6 family cytokines play a crucial role in regulating cellular responses including cell proliferation, survival/apoptosis and functional maturation in physiological systems via regulation of Jak/Stat3, mTor, PI3K/Akt, and Erk/Mapk pathways. In Kras mouse models it was shown that constitutive *Kras* signalling can drive exacerbated proliferation in pancreatic ductal carcinoma (PDAC)[175], and that glutaminolysis in Kras-transformed fibroblasts had altered proliferation via the mTor pathway[220].

Since a key cellular process implicated in Kras-driven lung carcinogenesis is cellular proliferation[51], we next examined whether the exacerbated lung tumourigenesis in *gp130*$^{F/F}$:*Kras*^{G12D} mice correlated with a higher proliferative potential in the lung. Indeed, as shown in Figure 3.6a and b, there was a significant 3.5-fold and 2-fold increase in the number of PCNA-positive cells in the lungs of *gp130*$^{F/F}$:*Kras*^{G12D} mice compared to control *gp130*$^{F/F}$:*Kras*^{WT} and *Kras*^{G12D} mice, respectively. This is consistent in histological analysis of *Kras*^{G12D} mice and the presence of AAH being thought to be a proliferation of atypical

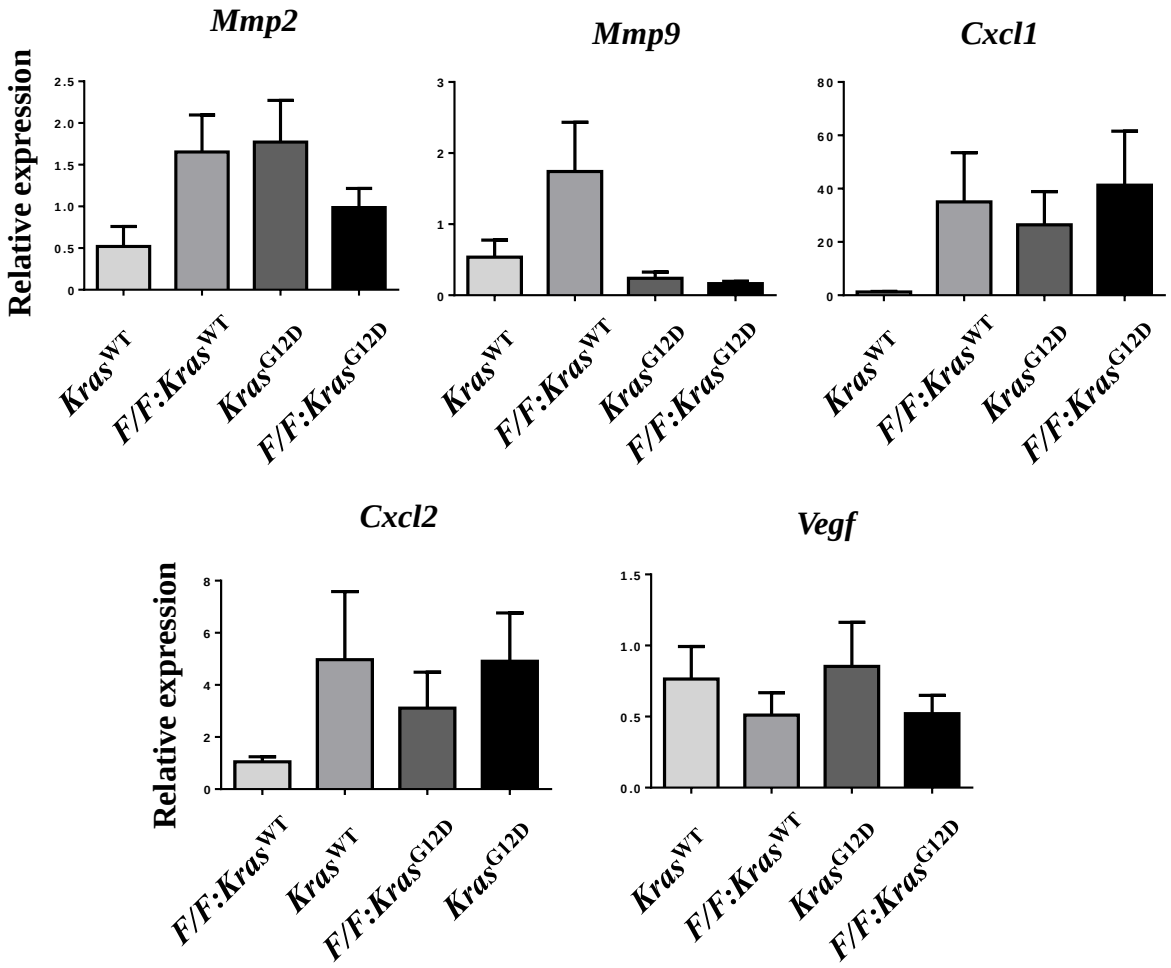

Figure 3.5. *gp130*$^{F/F}$:*Kras*^{G12D} mice show no augmentation in key angiogenic factors

qRT-PCR expression analysis of *Mmp2*, *Mmp9*, *Cxcl1*, *Cxcl2*, and *Vegf* were performed on cDNA derived from the lungs of 3 month old *gp130*$^{+/+}$:*Kras*^{WT} (*Kras*^{WT}), *gp130*$^{F/F}$:*Kras*^{WT} (F/F:*Kras*^{WT}), *gp130*$^{+/+}$:*Kras*^{G12D} (*Kras*^{G12D}) and *gp130*$^{F/F}$:*Kras*^{G12D} (F/F:*Kras*^{G12D}) mice. Expression data are normalized against *18S*, and are presented from 9-12 mice per group as the mean +/- s.e.m.

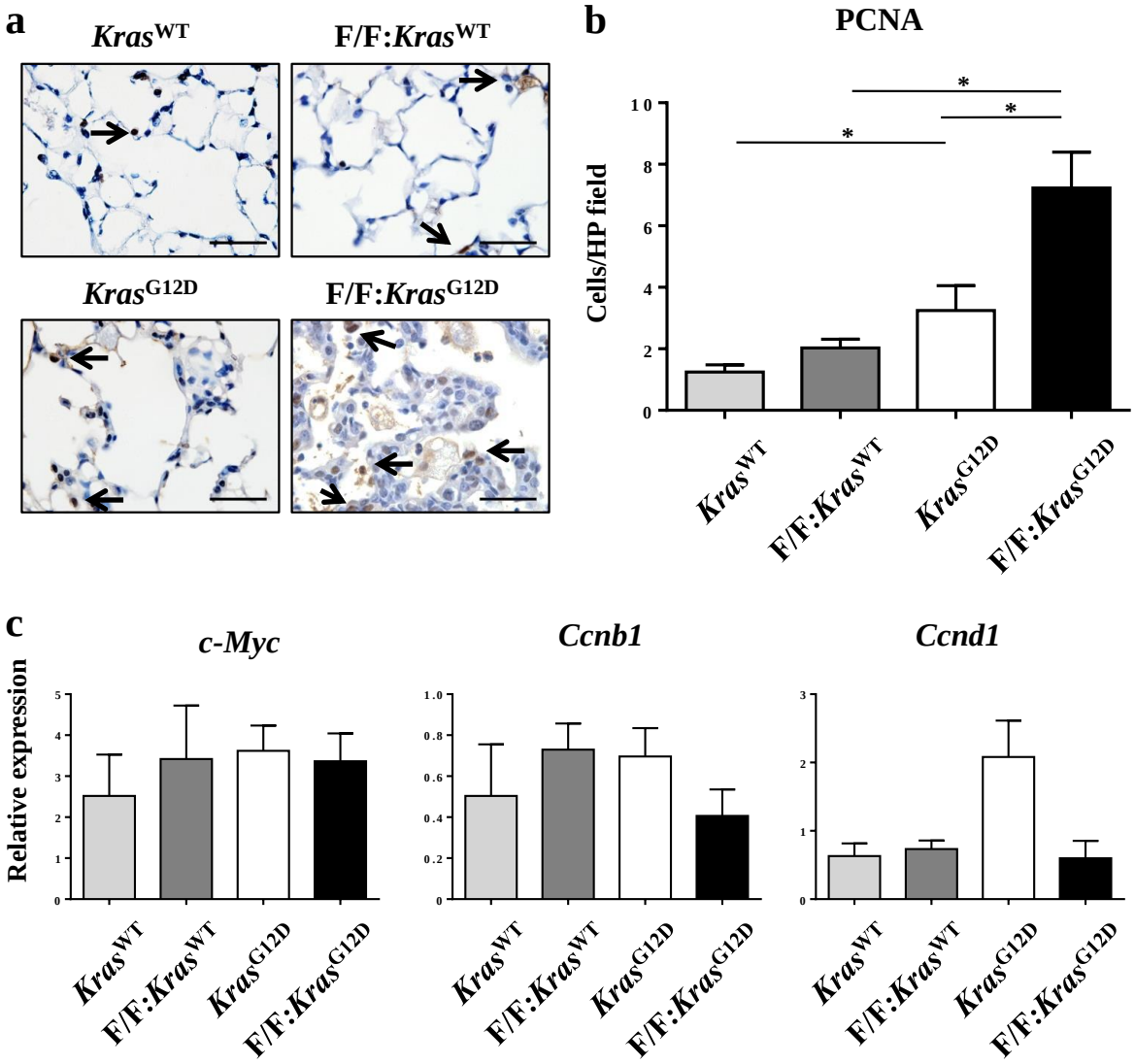

Figure 3.6. *gp130*$^{F/F}$:*Kras*^{G12D} mice show augmented lung cellular proliferation

(a) Representative photomicrographs of PCNA-stained lung cross-sections from either *gp130*$^{+/+}$:*Kras*^{WT} (*Kras*^{WT}) and *gp130*$^{F/F}$:*Kras*^{WT} (F/F:*Kras*^{WT}) mice treated with vehicle control for 6 weeks or *gp130*$^{+/+}$:*Kras*^{G12D} (*Kras*^{G12D}) and *gp130*$^{F/F}$:*Kras*^{G12D} (F/F:*Kras*^{G12D}) treated with Cre-recombinase for 6 weeks. Scale bar, 50µm (b) graph depicts quantitative enumeration of PCNA positive tumour cells per high powered field (x100 magnification). Data from 4 to 12 mice per genotype expressed as mean +/- s.e.m, * $p<0.05$.

epithelial cell growth[51]. Despite this increase, the expression of proliferative genes *c-Myc*, *Ccnb1* and *Ccnd1* was unchanged upon oncogenic activation of Kras (Figure 3.6c).

3.6 Discussion

The IL-6 cytokine family signalling via gp130 receptor has been linked to an extraordinary assortment of cellular functions including, protection from infection, proliferation, apoptosis and promotion of inflammation-associate diseases[132,224] and cancers[148,150]. Notably, several studies have indicated that Kras-induced LAC is likely linked with downstream mediators of gp130 signalling such as Erk/Mapk, PI3K/Akt and Stat3[42,46,63,81], though yet to be formally identified. The identification of gp130 signalling in lung cancer has been hampered due to the lack of tools to formally elucidate whether aberrant gp130 signalling (and any associated lung inflammation) contributes to this disease process. Therefore, we provide evidence that gp130 signalling augmented Kras-induced lung carcinogenesis in *gp130*$^{F/F}$:*Kras*^{G12D} mice, thus this model provided an invaluable genetic tool to formally identify the role of gp130 signalling in lung cancer development. Furthermore, we showed that hyper-activation of gp130 signalling has a causal role in cell proliferation, rather than cell survival or inflammation to promote Kras-induced LAC development. Collectively, our data provided novel insights into how gp130-driven lung cancer cell proliferation might be targeted in primary or secondary prevention of a lethal disease with a large unmet clinical need. However, further studies are required to fully elucidate specific gp130-driven (upstream and downstream mediators) lung diseases.

Perhaps one of the most interesting findings of this chapter was that Kras-driven lung cancer pathogenesis was exacerbated in *gp130*$^{F/F}$:*Kras*^{G12D} mice, in the presence of deregulated gp130 signalling. Our laboratory has previously shown that the *gp130*$^{F/F}$ mouse model develops severe pulmonary inflammation[225], while others have shown that mouse

models genetically engineered to express the oncogenic *Kras*^{G12D} allele conditionally, somatically, or inducibly can develop AAH at 16 weeks post infection[57,62]. Importantly, in our pre-clinical mouse model *gp130*$^{F/F}$:*Kras*^{G12D}, we showed an enhanced degree of extensive AAH, diffuse AIS, and areas of invasive adenocarcinoma in the lungs by 3 months of age (i.e. 6 week old mice exposed to experimentally-induced lung cancer over 6 weeks). Considering these mice develop gp130-driven lung inflammation, this suggests a strong correlation between gp130 signalling to lung cancer. I note that if the induction of lung cancer was from 3 months of age (when there would be well established lung inflammation) as opposed to 6 weeks of age, (prior to lung inflammation) perhaps more pronounced or even, histopathologically, a more severe form of lung pathology might be observed. While there are numerous lung cancer mouse models ranging from transgenic models for oncogenes such as c-myc, c-raf1 and Hras[226], spontaneous or chemically induced models[227,228], and xenograft models, none have shown a direct link for gp130 signalling in LAC. Therefore our mouse model provides an important model to further elucidate the specific gp130 signalling associated with LAC.

In addition, we discovered that gp130 signalling drives cell proliferation to promote Kras-induced LAC in our *gp130*$^{F/F}$:*Kras*^{G12D} mouse model. This is consistent with previous findings in the mouse[51,208] and the human environment[52,165,223,229] in Kras associated LAC. Others have shown that proliferation can drive tumourgenesis in a microenvironment rich in inflammatory cell and growth/survival factors like Stat3, oncogenic *Kras* and Mapk/PI3K signalling, all downstream of gp130 signalling[63,198,210]. In contrast, in a study in our own laboratory we showed that *gp130*$^{F/F}$ mice, on an A/J background, in response to 4-(methylnitrosamino)-1-(3-pyridyl)-1-butanone (Nicotine-derived Nitrosamine Ketone; NNK) developed less and smaller foci of lung adenocarcinoma when compared to *gp130*^{WT} litter mate controls, and this also correlated with a reduction in cellular proliferation[21], suggesting

that specific gp130 signalling pathways have different effects on cell proliferation to exacerbate or ameliorate lung cancer. While the role of inflammation in Kras-induced lung carcinogenesis remains unclear we observed a comparable increase in the number of CD45 positive immune cells in the lungs of both *gp130*$^{F/F}$:*Kras*^{G12D} and *Kras*^{G12D} mice compared with control tumour-free *gp130*$^{F/F}$:*Kras*^{WT} and *Kras*^{WT} mice. In contrast, the numbers of apoptotic cells in the lungs of either *gp130*$^{F/F}$:*Kras*^{G12D} or *Kras*^{G12D} mice compared with their *Kras*^{WT} controls were unchanged. Although these data suggest that oncogenic Kras within the lung epithelium can elicit both a pulmonary inflammatory response and an apoptotic response, this is however not associated with the exacerbated lung tumorigenesis observed in *gp130*$^{F/F}$:*Kras*^{G12D} mice as these results were also observed in *gp130*$^{F/F}$ compared with *gp130*$^{+/+}$ mice with wild-type Kras [200], and thus is independent of their Kras mutational Status.

In conclusion, these data suggest that upregulation of gp130 signalling may enhance the oncogenic potency of activating *Kras* mutants, and gp130 inflammatory pathways within cancer cells can act as oncogenic stimuli to promote cell proliferation. Since therapeutic targeting of Kras has proven difficult, the blockade of specific gp130 signalling pathways (via IL-6) may represent an alternative strategy to treat LAC in humans. In that regard, we will next explore a specific IL-6 cytokine associated with gp130 in promoting Kras-driven LAC.

Chapter 4
IL-6 trans signalling as a driver for Kras associated LAC

4.1 Introduction

In Chapter 3, we discovered that oncogenic Kras engages with gp130 signalling cascades to promote LAC, although the identity of the specific IL-6 family cytokine(s) which promotes Kras-driven lung carcinogenesis remain ill-defined. In that regard, the pleiotropic and potent immunomodulatory cytokine IL-6 is strongly implicated in the pathogenesis of LAC, but not other lung cancer types (e.g. SCLC). For instance, in LAC, IL-6 levels are increased in serum, BALF, and pleural fluid[145,230,231] and polymorphisms in the *IL-6* gene[232] are observed in subjects with LAC. In addition augmented autocrine production of IL-6 is a characteristic of many LAC and a signature of up to 50% of LAC associated with poor prognosis[145]. Interestingly, in primary LAC harbouring activating mutations in the EGFR, upregulated production of IL-6 is also observed[221]. It is also noteworthy that IL-6 is produced in human lung epithelial cells in response to cigarette smoke and protects against apoptosis triggered by smoke-induced DNA damage via Stat3[156]. Given the importance of gp130 signalling in Kras-driven lung cancer as was discovered in Chapter 3, we speculate that IL-6 thus presents as a candidate upstream activator of oncogenic signalling in Kras-driven LAC.

IL-6 signalling occurs via two distinct modes; termed classical and trans signalling. Classical IL-6 signalling occurs when the IL-6 binds to its membrane bound specific receptor (mIL-6R) that is expressed on the surface membrane of a limited number of target cells,

mainly hepatocytes, neutrophils, monocytes/macrophages, and sub-types of lymphocytes[122]. However, recently it has been shown that IL-6 trans signalling facilitates the IL-6 responsiveness of cells which lack mIL-6R, including haemopoietic progenitors, activated T-cells and endothelial cells, via the naturally-occurring sIL-6R through the involvement of ADAM10 and ADAM17 metalloproteases[114].

At a physiological level, sgp130 specifically binds to sIL-6R and thus antagonises signalling from the IL-6/sIL-6R complex without interfering with classical signalling[142]. IL-6 trans signalling has been implicated as the pathogenic mode of IL-6 signalling in many inflammatory diseases and in numerous cancers, such as those of the colon[137,138], pancreas[140] and ovary[233], and while the downstream oncogenic molecular and cellular processes driven by IL-6 trans signalling remain ill-defined, it is presumed that IL-6 trans signalling promotes cell proliferation and survival by activating STAT3[138,140]. In contrast to the above, the involvement of different IL-6 signalling modes in lung cancer is ill-defined. Therefore, there is a clear and urgent need to investigate the causal role of IL-6 trans signalling in lung cancer via the use of sophisticated genetic mouse models and therapeutic strategies to target different modes of IL-6 signalling.

In that regard, our collaborator, Dr W Ferlin (NovImmune, Switzerland) has recently developed a novel series of monoclonal antibodies (mAbs) which selectively target IL-6 trans signalling and/or classical signalling, and demonstrated their efficacy at suppressing inflammatory responses *in vivo* driven by either IL-6 classical signalling or IL-6 trans signalling[170]. Another strategy to inhibit IL-6 trans signalling is to target the IL-6/sIL-6R complex via sgp130. Indeed, another collaborator of ours Professor S Rose-John (University of Kiel, Germany) has generated transgenic sgp130FcTg mice which systemically express sgp130Fc, a fusion protein of sgp130 and the Fc portion of human IgG1 which serves as a specific and potent IL-6 trans-signalling inhibitor[114,132]. Here, we utilised a novel

experimental approach based on the targeted blockade of IL-6 trans signalling and/or classical signalling by mAbs and sgp130FcTg mice in our established genetic LAC mouse model (*gp130*$^{F/F}$:*Kras*^{G12D} mice).

4.2 Increased production of IL-6 is associated with exacerbated lung carcinogenesis in *gp130*$^{F/F}$:*Kras*^{G12D} mice

To examine whether the exacerbated LAC phenotype of *gp130*$^{F/F}$:*Kras*^{G12D} mice was linked to deregulated expression of specific members of the IL-6 cytokine family, qPCR was used to measure the mRNA levels of IL-6 family cytokines during Kras-induced lung carcinogenesis. Among the IL-6 family cytokines examined, namely; IL-27, OSM, LIF, IL-11, and IL-6 only the expression of the *IL-6* gene was significantly elevated in the lungs of *gp130*$^{F/F}$:*Kras*^{G12D} mice compared to *Kras*^{G12D} mice (Figure 4.1a). ELISA on lung lysates revealed that although IL-6 protein levels were elevated (not significant) in the lungs of *gp130*$^{F/F}$:*Kras*^{G12D} mice compared to *gp130*$^{F/F}$:*Kras*^{WT} mice, which was not the case verses *Kras*^{G12D} mice (Figure 4.1b). In addition, no significant changes were observed for the mRNA expression of IL-6 family cytokines and IL-6 protein level in the lungs of control *gp130*$^{F/F}$:*Kras*^{WT} and *Kras*^{WT} mice expressing wild-type *Kras* which were subjected to intranasal inhalation with PBS as a vehicle control (Figure 4.1a and b). Of note is the differences in these data verses data published by Brooks G.D. *et al*, 2016. The data observed in the published works have increased mouse numbers and as such observed significance in of IL-6 protein levels in the lungs of *gp130*$^{F/F}$:*Kras*^{G12D} mice compared to *gp130*$^{F/F}$:*Kras*^{WT} mice [66].

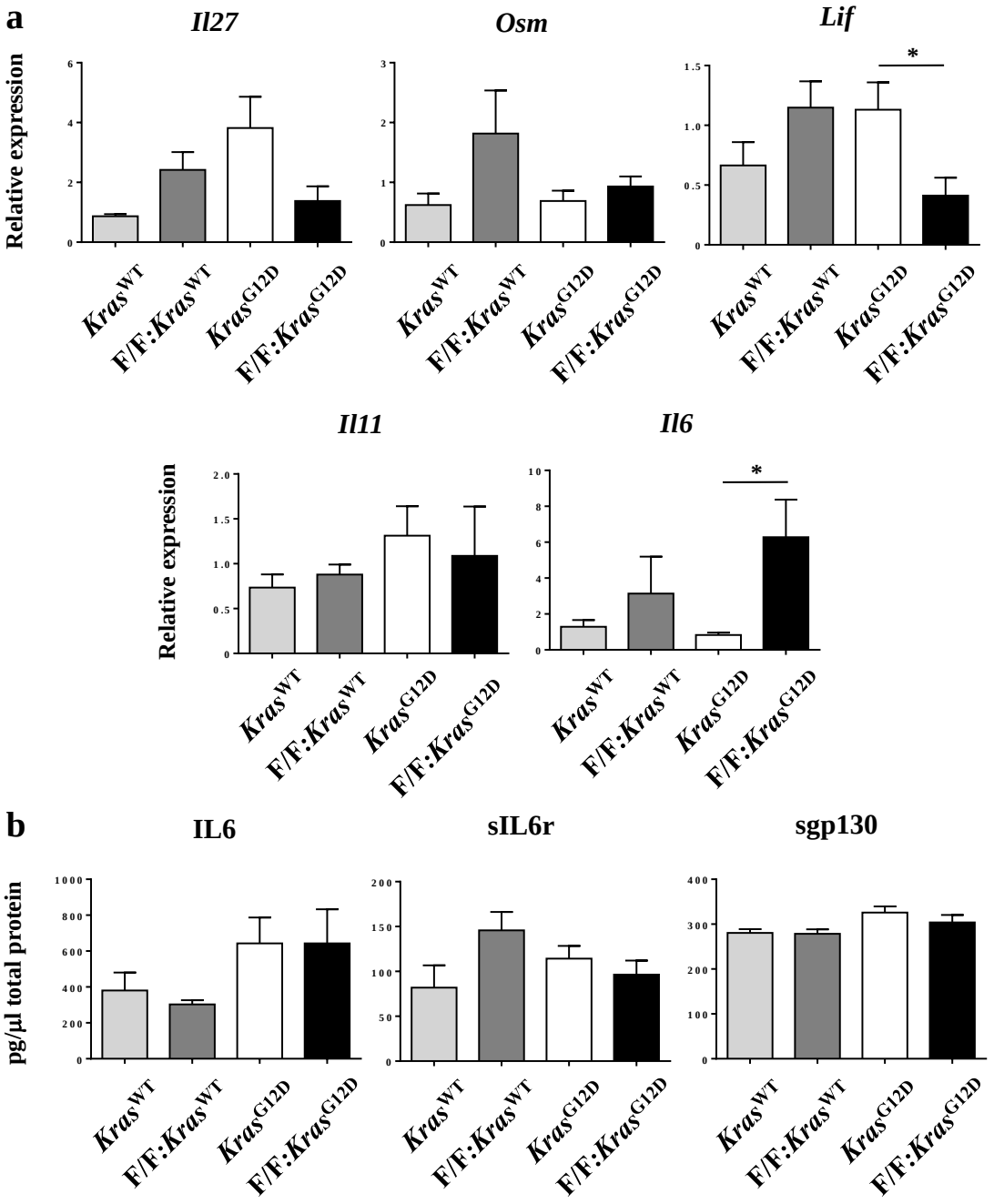

Figure 4.1. Increased production of *IL-6* is associated with exacerbated lung carcinogenesis in *gp130*$^{F/F}$:*Kras*^{G12D} mice

(a) qRT-PCR expression analyses of *Il27*, *Osm*, *Lif*, *Il11* and *IL-6* were performed on cDNA- and (b) IL-6, sIL-6R and sgp130 protein expression analyses by ELISA were performed on whole lung lysates- derived from the lungs of 3 month old *gp130*$^{+/+}$:*Kras*^{WT} (*Kras*^{WT}) and *gp130*$^{F/F}$:*Kras*^{WT} (F/F:*Kras*^{WT}) mice following vehicle inhalation for 6 weeks, or *gp130*$^{+/+}$:*Kras*^{G12D} (*Kras*^{G12D}) and *gp130*$^{F/F}$:*Kras*^{G12D} (F/F:*Kras*^{G12D}) mice following Cre inhalation for 6 weeks. Expression data are normalized against *18S*, and are presented from 4-12 mice per group as the mean +/- s.e.m. * $p<0.05$.

4.3 Ablation of IL-6 from *gp130*$^{F/F}$:*Kras*^{G12D} mice ameliorates lung cancer progression

Based on the findings in section 4.2, we generated *gp130*$^{F/F}$:*Kras*^{G12D}:*IL-6*$^{-/-}$ mice to explore whether IL-6 deficiency would suppress the severity of the LAC phenotype in *gp130*$^{F/F}$:*Kras*^{G12D} mice. These mice were generated by back-crossing *gp130*$^{F/F}$:*Kras*^{G12D} mice with homozygous null for *IL-6* to produce *gp130*$^{F/F}$:*Kras*^{G12D}:*IL-6*$^{-/-}$ mutant mice (as described in 2.1.1). Indeed, the area of lung parenchyma containing AAH and AIS lesions in *gp130*$^{F/F}$:*Kras*^{G12D}:*IL-6*$^{-/-}$ mice (Figure 4.2a) was significantly reduced compared to *gp130*$^{F/F}$:*Kras*^{G12D} mice. The amelioration of LAC in the lungs of *gp130*$^{F/F}$:*Kras*^{G12D}:*IL-6*$^{-/-}$ mice was reduced almost 2 fold, returning to similar levels of *Kras*^{G12D} mice (Figure 4.2a and b). The architecture of *gp130*$^{F/F}$:*Kras*^{G12D}:*IL-6*$^{-/-}$ mice was also reflective of *Kras*^{G12D} mice with LAC seen in the peribronchial and peripheral lung, the foci were small and sporadic throughout the whole parenchyma, however they were more discrete than originally observed in *Kras*^{G12D} mice. By contrast, IL-6 deficiency in *Kras*^{G12D}:*IL-6*$^{-/-}$ mice after 6 weeks of Kras oncogenic activation did not suppress lung carcinogenesis (Figure 4.2c) and histologically similar to *Kras*^{G12D} mice.

In support of the above findings, immunohistochemical evaluation with TTF-1 indicated a significant 2-fold decrease in the number of TTF-1 positive cells in the lungs of *gp130*$^{F/F}$:*Kras*^{G12D}:*IL-6*$^{-/-}$ compared to *gp130*$^{F/F}$:*Kras*^{G12D} mice, which was similar to that seen in *Kras*^{G12D} and *Kras*^{G12D}:*IL-6*$^{-/-}$ mice (Figure 4.3). In addition, we also confirmed that cellular proliferation was the main cellular process associated with amelioration of LAC in *gp130*$^{F/F}$:*Kras*^{G12D}:*IL-6*$^{-/-}$ mice. Specifically there was a 2-fold decrease in the number of

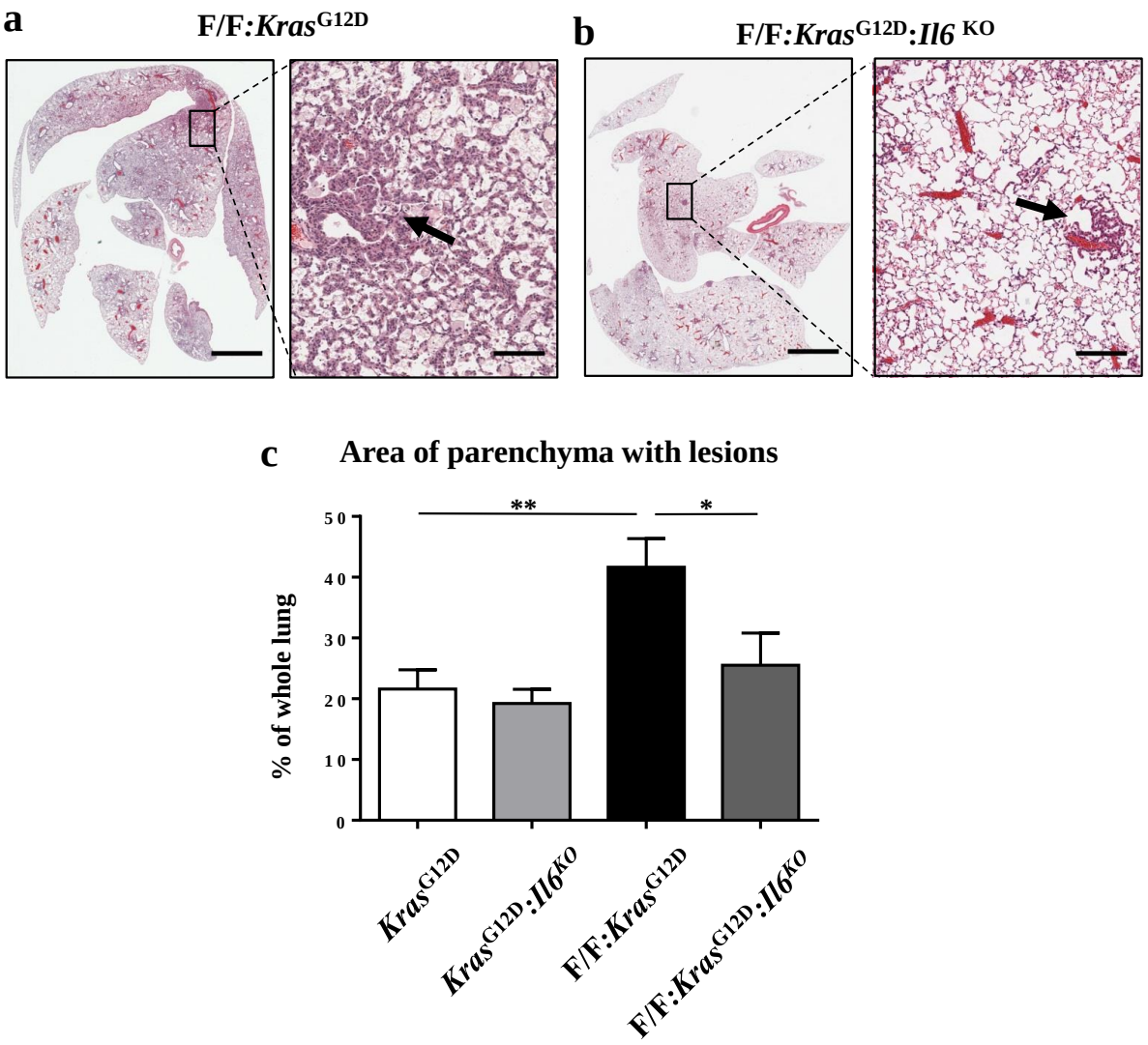

Figure 4.2. Ablation of *IL-6* in *gp130*$^{F/F}$:*Kras*^{G12D} mice ameliorates *in situ* adenocarcinoma

Representative lower-power (left) and high-power (right) photomicrographs showing haemotoxylin and eosin-stained lung cross-sections from either (a) *gp130*$^{F/F}$:*Kras*^{G12D} (F/F:*Kras*^{G12D}) and (b) *gp130*$^{F/F}$:*Kras*^{G12D}:*IL-6*$^{-/-}$ (F/F:*Kras*^{G12D}:*IL-6*^{KO}) mice treated with Cre-recombinase for 6 weeks. Arrows indicate discrete AIS. Scale bar, 3mm left pane, 300µm right pane. (c) Graph depicts quantification of lung parenchyma area occupied by AIS lesions for indicated genotypes for whole lung at 10x magnification. Data from 5 to 9 mice per genotype expressed as mean +/- s.e.m, * $p<0.05$, ** $p<0.01$.

PCNA-positively stained cells in the lungs of *gp130*$^{F/F}$:*Kras*^{G12D}:*IL-6*$^{-/-}$ mice compared to the experimental *gp130*$^{F/F}$:*Kras*^{G12D} genotype, correlating with the decreased levels of tumourigenesis in the lungs of *gp130*$^{F/F}$:*Kras*^{G12D}:*IL-6*$^{-/-}$ mice (Figure 4.4). By contrast, IL-6 deficiency in *Kras*^{G12D}:*IL-6*$^{-/-}$ mice after 6 weeks of Kras oncogenic activation did not suppress cellular lung proliferation. Of note is that cellular inflammation and cellular apoptosis was not altered in the lungs of *Kras*^{G12D} or *gp130*$^{F/F}$:*Kras*^{G12D} (Figures 3.3 and 3.4 respectively) suggesting that these cellular mechanisms do not play a role in IL-6 driven Kras-induced LAC in *gp130*$^{F/F}$:*Kras*^{G12D} mice. Collectively, these data therefore confirm that augmented expression of IL-6 can potentiate cellular proliferation in the lung, and thus augment *Kras*-induced LAC by cellular proliferation in the lung in *gp130*$^{F/F}$:*Kras*^{G12D} mice.

4.4 IL-6 trans signalling exacerbates lung carcinogenesis in *gp130*$^{F/F}$:*Kras*^{G12D} mice

We next assessed the mode of IL-6 signalling involved in IL-6-driven LAC in our mouse model. To examine whether IL-6 trans signalling promoted the exacerbated LAC phenotype in *gp130*$^{F/F}$:*Kras*^{G12D} mice, we crossed *gp130*$^{F/F}$:*Kras*^{G12D} mice with transgenic *sgp130Fc*$^{tg/tg}$ mice that systemically express high levels of sgp130Fc protein, a fusion protein of sgp130 and the Fc portion of human IgG1 which serves as a specific and potent inhibitor of IL-6 trans signalling[132].

Notably, sgp130Fc-mediated blockade of IL-6 trans signalling in the lungs of *gp130*$^{F/F}$:*Kras*^{G12D}:*sgp130Fc*$^{tg/tg}$ mice suppressed the extent of AAH and AIS lesion development which was associated with significant reduction in the area of lung parenchyma containing LAC compared to *gp130*$^{F/F}$:*Kras*^{G12D} mice (Figure 4.6). This reduction of tumourgenesis in the lungs of *gp130*$^{F/F}$:*Kras*^{G12D}:*sgp130Fc*$^{tg/tg}$ mice was similar to the amelioration in *gp130*$^{F/F}$:*Kras*^{G12D}:*IL-6*$^{-/-}$ mice seen in Figure 4.2. It is also of note that

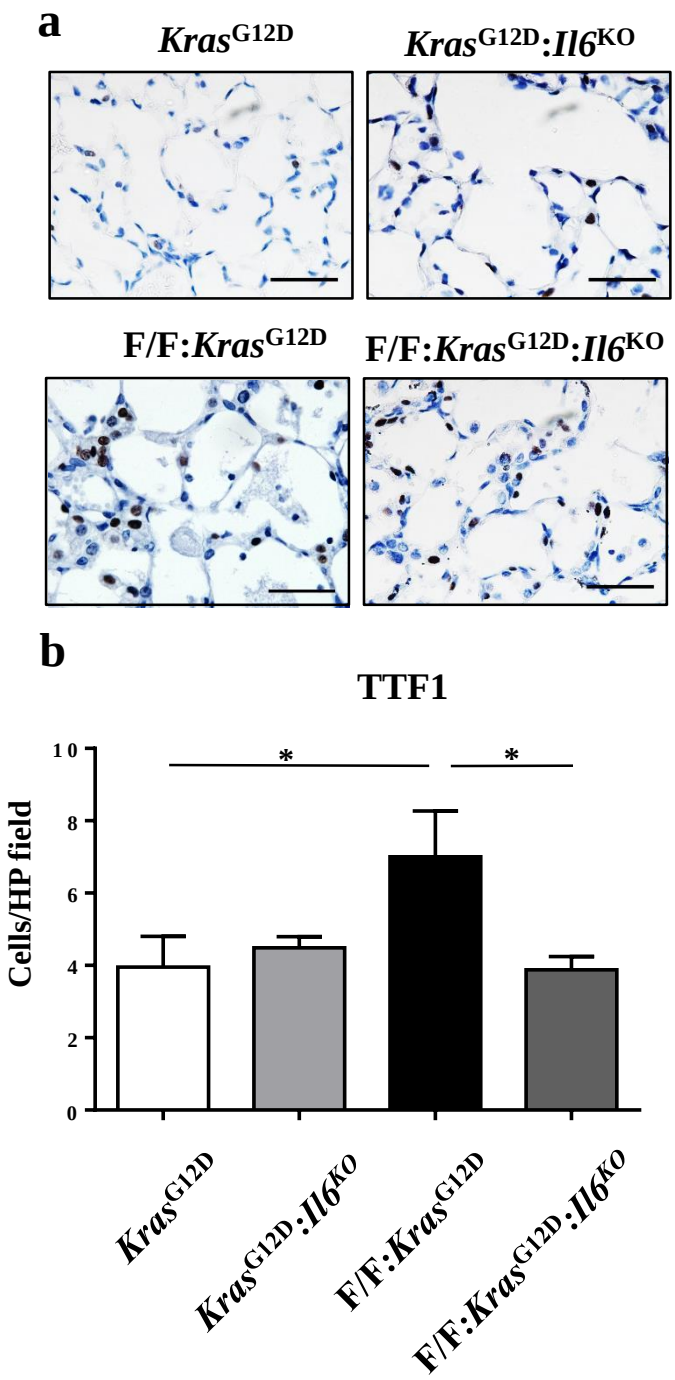

Figure 4.3. The lungs of *gp130*$^{F/F}$:*Kras*^{G12D}:*IL-6*^{KO} mice show decreased Thryoid transcription factor (TTF)-1 staining

(a) Representative high-power photomicrographs of TTF-1-stained lung cross-sections from *gp130*$^{+/+}$:*Kras*^{G12D} (*Kras*^{G12D}), *gp130*$^{+/+}$:*Kras*^{G12D}:*IL-6*$^{-/-}$ (*Kras*^{G12D}:*IL-6*^{KO}), *gp130*$^{F/F}$:*Kras*^{G12D} (F/F:*Kras*^{G12D}) and *gp130*$^{F/F}$:*Kras*^{G12D}:*IL-6*$^{-/-}$ (F/F:*Kras*^{G12D}:*IL-6*^{KO}) mice treated with Cre-recombinase for 6 weeks. Scale bar, 50µm (b) Graph depicts quantification of TTF-1 positive cells per high powered field (100x magnification) in the lungs of the indicated mice. Data from 5 to 9 mice per genotype expressed as mean +/- s.e.m, * $p<0.05$, ** $p<0.01$.

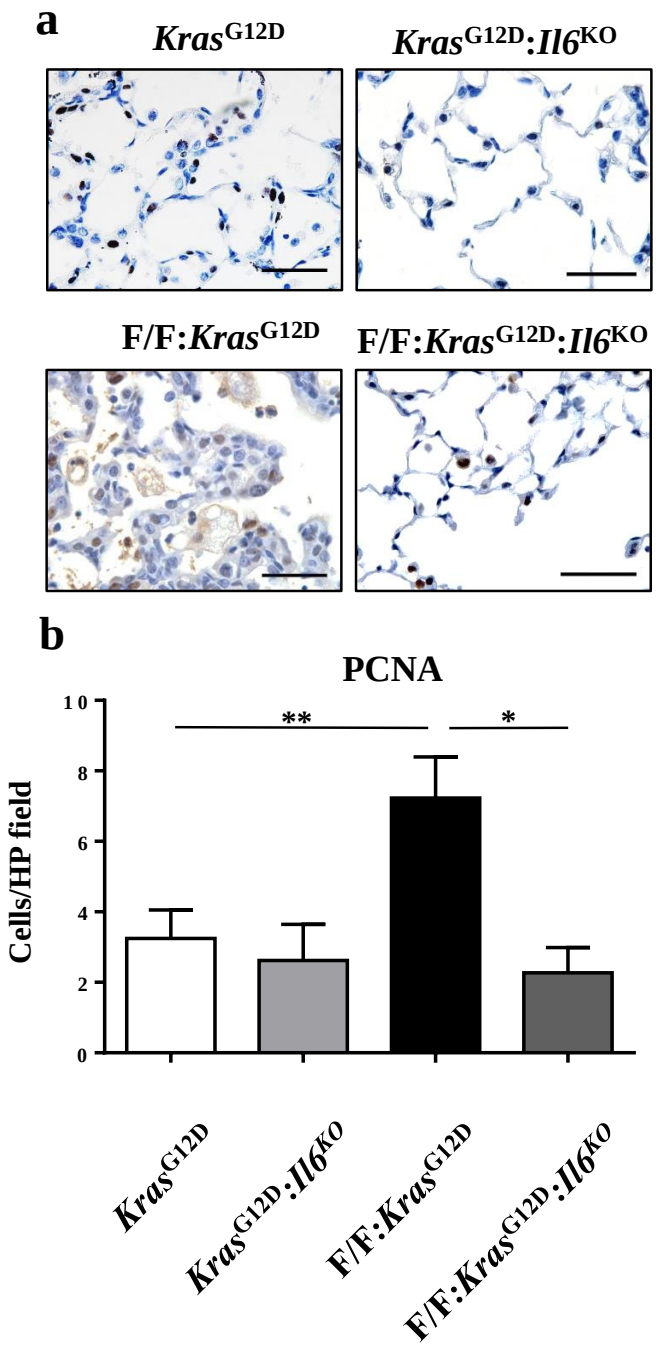

Figure 4.4. The lungs of *gp130*$^{F/F}$:*Kras*^{G12D}:*IL-6*^{KO} mice show decreased cellular proliferation

(a) Representative high-power photomicrographs of PCNA-stained lung cross-sections from *gp130*$^{+/+}$:*Kras*^{G12D} (*Kras*^{G12D}), *gp130*$^{+/+}$:*Kras*^{G12D}:*IL-6*$^{-/-}$ (*Kras*^{G12D}:*IL-6*^{KO}), *gp130*$^{F/F}$:*Kras*^{G12D} (F/F:*Kras*^{G12D}) and *gp130*$^{F/F}$:*Kras*^{G12D}:*IL-6*$^{-/-}$ (F/F:*Kras*^{G12D}:*IL-6*^{KO}) mice treated with Cre-recombinase for 6 weeks. Scale bar, 50μm (b) Graph depicts quantification of PCNA-positive cells per high powered field (100x magnification) in the lungs of the indicated mice. Data from 5 to 9 mice per genotype expressed as mean +/- s.e.m, * $p<0.05$, ** $p<0.01$.

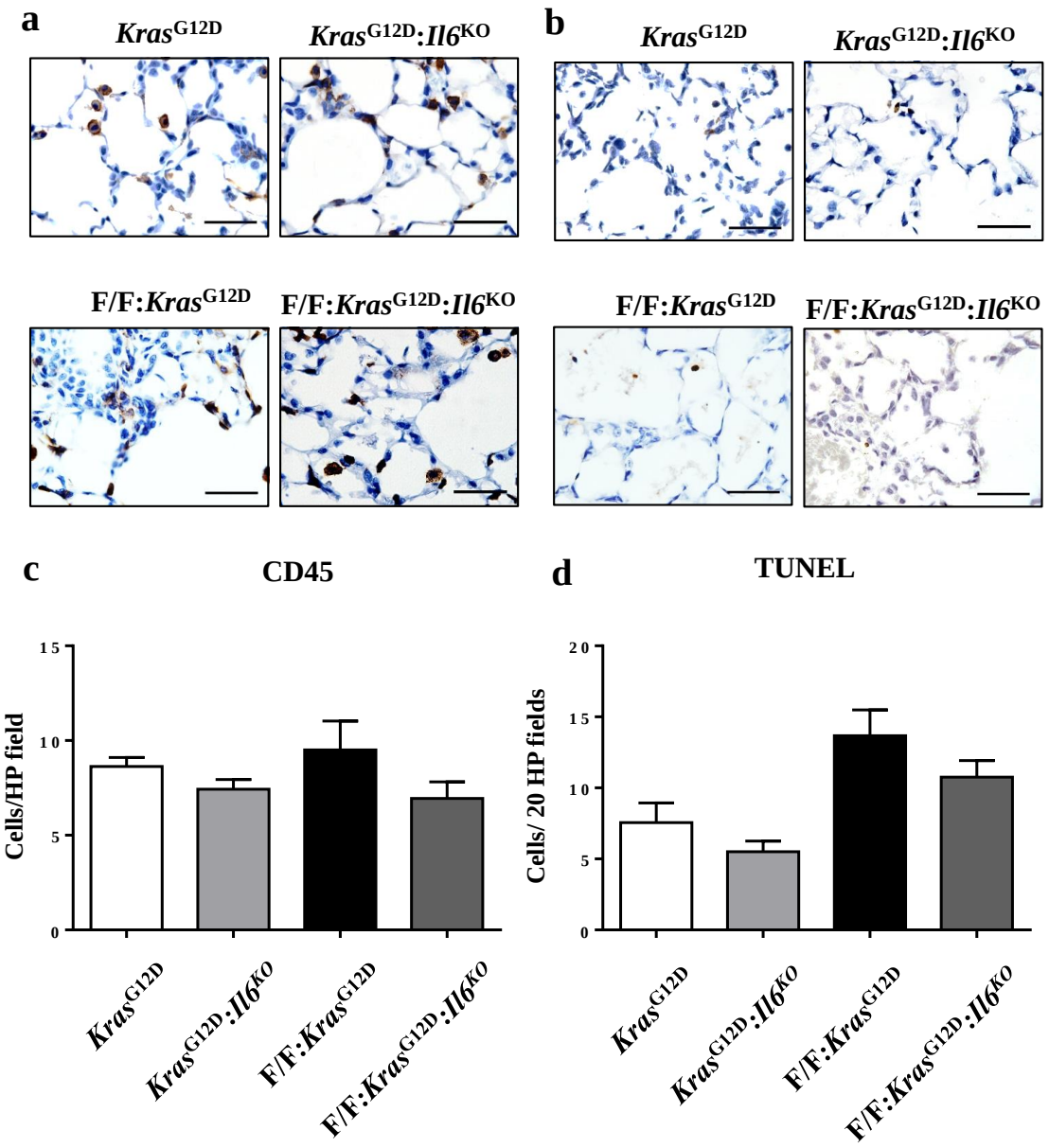

Figure 4.5. Unaltered cellular inflammation and apoptosis in the lungs of *gp130*$^{F/F}$:*Kras*^{G12D}:*IL-6*^{KO} mice display ameliorated AIS

(a) Representative high-power photomicrographs of (a) CD45 stained- and (b) TUNEL-stained lung cross-sections from *gp130*$^{+/+}$:*Kras*^{G12D} (*Kras*^{G12D}), *gp130*$^{+/+}$:*Kras*^{G12D}:*IL-6*$^{-/-}$ (*Kras*^{G12D}:*IL-6*^{KO}), *gp130*$^{F/F}$:*Kras*^{G12D} (F/F:*Kras*^{G12D}) and *gp130*$^{F/F}$:*Kras*^{G12D}:*IL-6*$^{-/-}$ (F/F:*Kras*^{G12D}:*IL-6*^{KO}) mice treated with Cre-recombinase for 6 weeks. Scale bar, 50μm (b) graph depicts quantification of (c) CD45- positive cells per high powered field and (d) TUNEL-positive cells per 20 high powered fields (100x magnification) in the lungs of the indicated mice. Data from 4 to 9 mice per genotype expressed as mean +/- s.e.m.

we observed a slight, albeit insignificant, alleviation of the mild LAC phenotype in *Kras*^{G12D}:*sgp130Fc*$^{tg/tg}$ mice compared to *Kras*^{G12D} mice after 6 weeks of Kras oncogenic activation (Figure 4.6a, b, and e). In addition, the suppressed lung lesion development in *gp130*$^{F/F}$:*Kras*^{G12D}:*sgp130Fc*$^{tg/tg}$ mice was associated with reduced numbers of TTF-1 (Figure 4.7, though significance was not achieved) and PCNA stained cells (Figure 4.8) compared to *gp130*$^{F/F}$:*Kras*^{G12D} mice.

Since the generation of sIL-6R occurs by either proteolytic cleavage of mIL-6Rα by A disintegrin and metalloproteinase domain-containing protein ADAM10 and ADAM17[127] or alternative splicing of IL-6Rα mRNA, I next assessed their gene expression levels. Of note, my preliminary analysis indicated that *Adam10* and *Adam17* gene expression in the lungs of *gp130*$^{F/F}$:*Kras*^{G12D} was not altered compared to *Kras*^{G12D} mice (Figure 4.9). Interestingly this contrasts the observed increase in Adam17 levels reported in the lungs of 6 month old emphysematous, gp130$^{F/F}$ mice, in which IL-6 trans signalling drives emphysema [222]. Therefore, it remains to be seen from future studies whether ADAM17 plays a role in this lung cancer model, or alternatively, if the sIL-6R is being produced through alternative splicing. Nonetheless, these data suggests a critical role for IL-6 trans signalling in Kras-dependent LAC development.

4.5 IL-6 trans signalling as a therapeutic target for lung adenocarcinoma

Only one major humanised anti-IL-6R monoclonal antibody (mAb), Tocilizumab, is currently approved for clinical treatment Tocilizumab is used in more than 100 countries for the treatment of RA, Crohn's disease and other autoinflammatory diseases[214,234]. However a

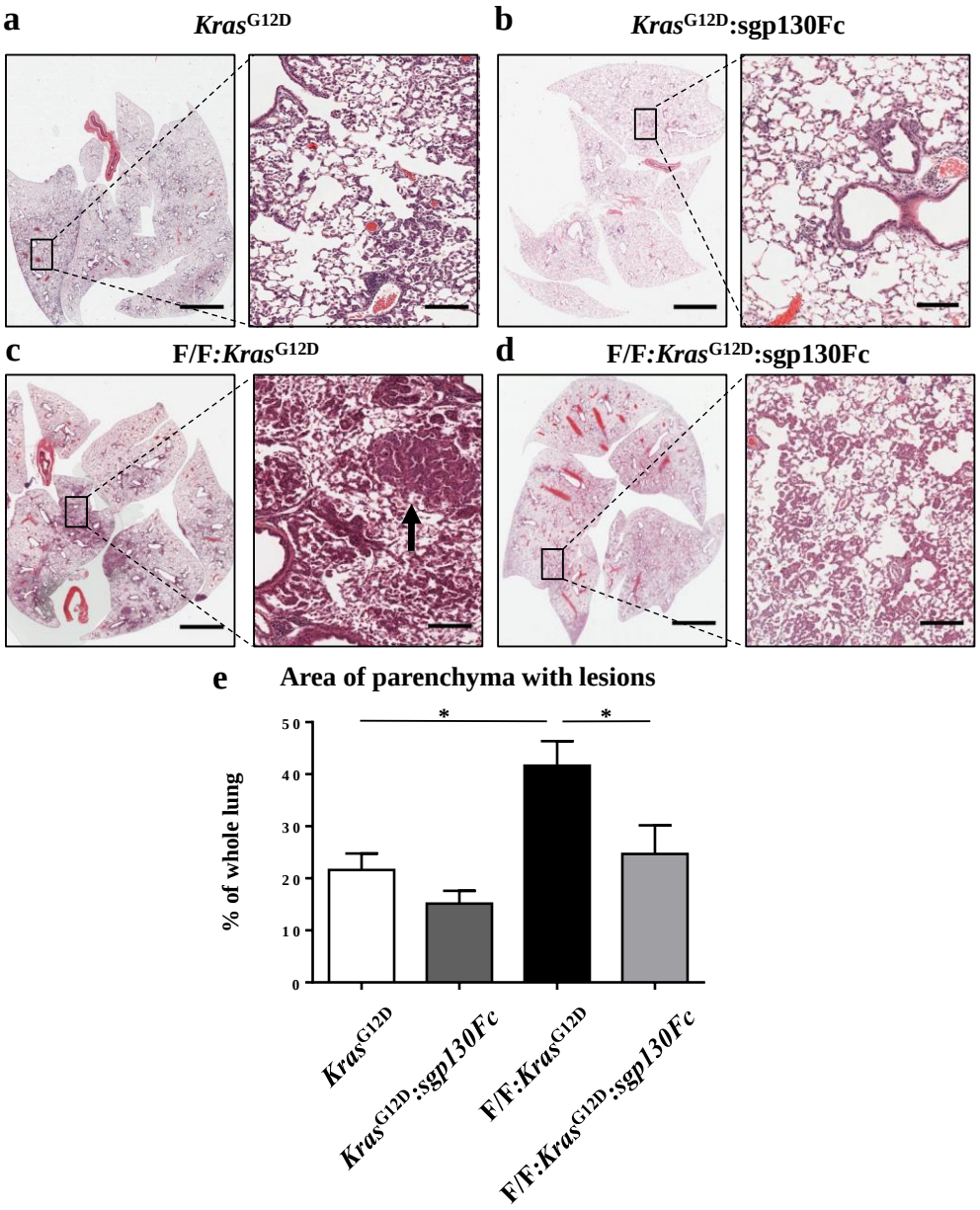

Figure 4.6. Ablation of IL-6 trans signalling in *gp130*$^{F/F}$:*Kras*^{G12D} mice ameliorates *in situ* adenocarcinoma

Representative low-power (left) and high-power (right) photomicrographs showing haemotoxylin and eosin-stained lung cross-sections from (a) *gp130*$^{+/+}$:*Kras*^{G12D} (*Kras*^{G12D}), (b) *gp130*$^{+/+}$:*Kras*^{G12D}:*sgp130Fc*$^{tg/tg}$ (*Kras*^{G12D}:*sgp130Fc*), (c) *gp130*$^{F/F}$:*Kras*^{G12D} (F/F:*Kras*^{G12D}) and (d) *gp130*$^{F/F}$:*Kras*^{G12D}:*sgp130Fc*$^{tg/tg}$ (F/F:*Kras*^{G12D}:*sgp130Fc*) mice treated with Cre-recombinase for 6 weeks. Arrow, a discrete AIS lesion. Scale bar, 3mm left pane, 300µm right pane. (e) Graph depicts quantification of lung parenchyma area occupied by AIS lesions for indicated genotypes for whole lung at 10x magnification. Data from 5 to 9 mice per genotype expressed as mean +/- s.e.m, * $p<0.05$.

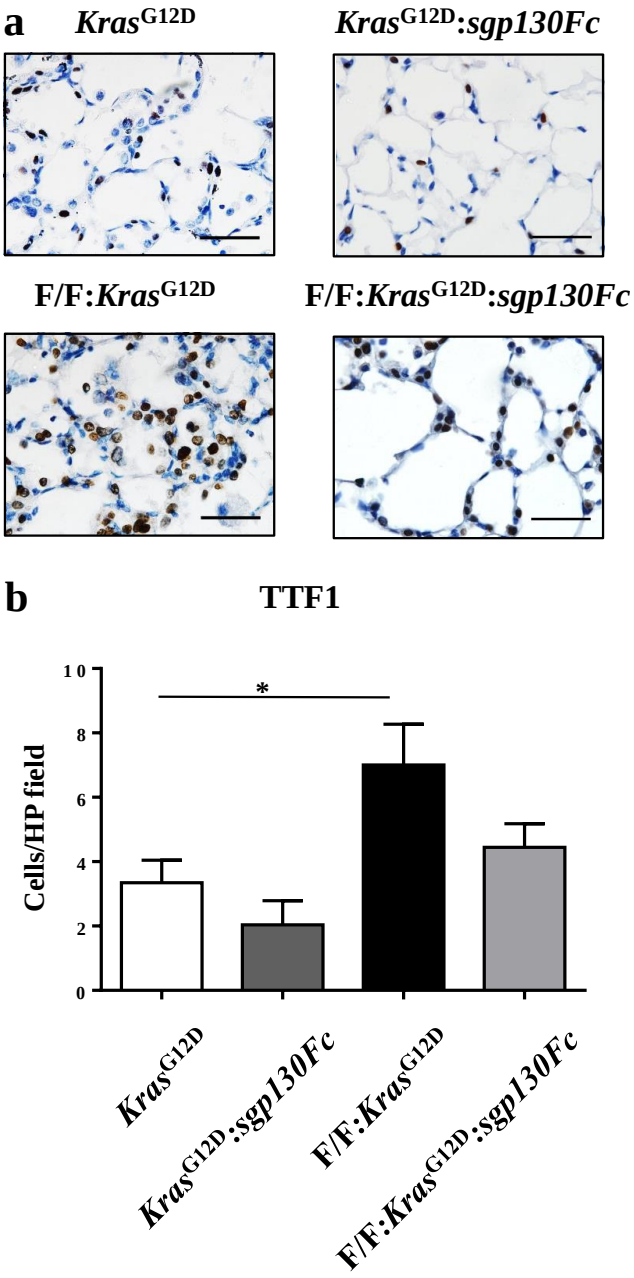

Figure 4.7. Reduction of TTF-1 stained epithelial cells in the lungs of *gp130*$^{F/F}$:*Kras*^{G12D}:*sgp130Fc* mice

(a) Representative high-power photomicrographs of TTF-1-stained lung cross-sections from *gp130*$^{+/+}$:*Kras*^{G12D} (*Kras*^{G12D}), *gp130*$^{+/+}$:*Kras*^{G12D}:*sgp130Fc*$^{tg/tg}$ (*Kras*^{G12D}:*sgp130Fc*), *gp130*$^{F/F}$:*Kras*^{G12D} (F/F:*Kras*^{G12D}) and *gp130*$^{F/F}$:*Kras*^{G12D}:*sgp130Fc*$^{tg/tg}$ (F/F:*Kras*^{G12D}:*sgp130Fc*) mice treated Cre-recombinase for 6 weeks. Scale bar, 50µm (b) Graph depicts quantification of TTF-1 positive cells per high powered field (100x magnification) in the lungs of the indicated mice. Data from 4 to 9 mice per genotype expressed as mean +/- s.e.m, * $p<0.05$.

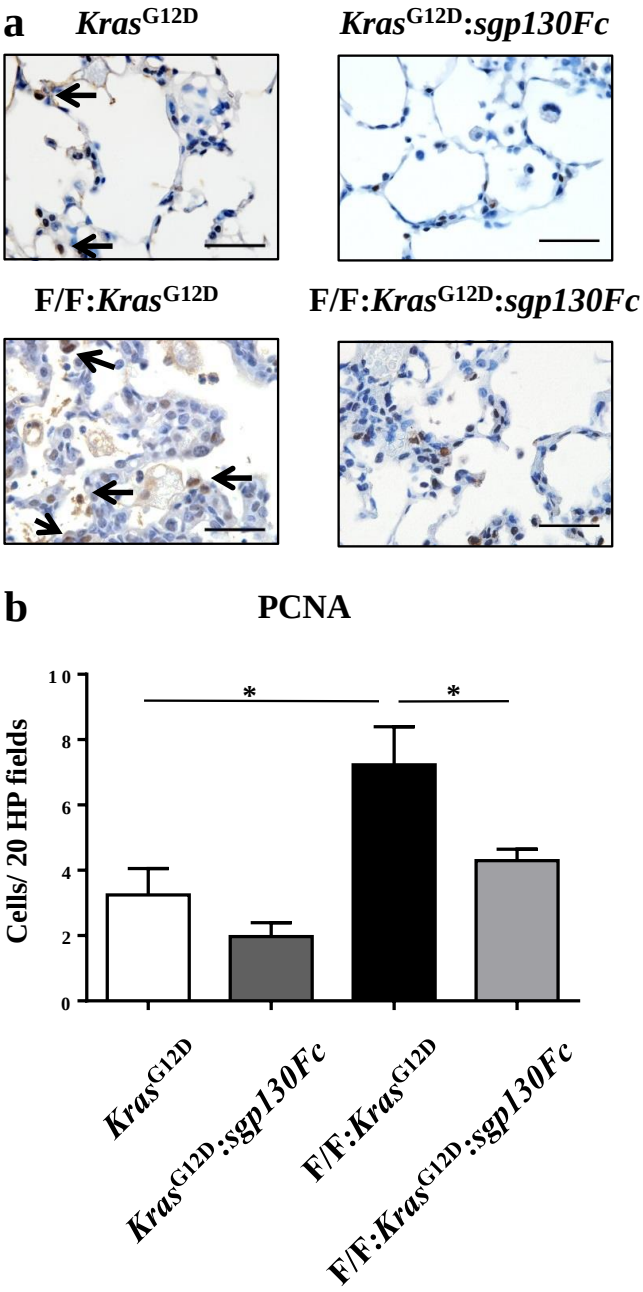

Figure 4.8. Cellular proliferation is reduced in the lungs of *gp130*$^{F/F}$:*Kras*^{G12D}:*sgp130Fc* mice

(a) Representative high-power photomicrographs of PCNA-stained lung cross-sections from *gp130*$^{+/+}$:*Kras*^{G12D} (*Kras*^{G12D}), *gp130*$^{+/+}$:*Kras*^{G12D}:*sgp130Fc*$^{tg/tg}$ (*Kras*^{G12D}:*sgp130Fc*), *gp130*$^{F/F}$:*Kras*^{G12D} (F/F:*Kras*^{G12D}) and *gp130*$^{F/F}$:*Kras*^{G12D}:*sgp130Fc*$^{tg/tg}$ (F/F:*Kras*^{G12D}:*sgp130Fc*) mice treated with Cre-recombinase for 6 weeks. Scale bar, 50μm (b) Graph depicts quantification of PCNA- positive cells per high powered field (100x magnification) in the lungs of the indicated mice. Data from 4 to 9 mice per genotype expressed as mean +/- s.e.m, * $p<0.05$.

drawback associated with this anti-IL-6 therapeutics is the numerous adverse events, including infections[37], most likely a consequence of suppressing the "immuno-protective" classical IL-6 signalling pathway, as well as trans signalling. While the clinical benefits of such an approach against LAC are yet unknown, an inherent issue that may arise again revolves around targeting "protective" IL-6 classical signaling, therefore selective targeting of IL-6 trans signalling will ameliorate disease while minimising the occurrence of side effects.

In that regard, to determine whether IL-6 trans signalling can serve as a *bona fide* therapeutic target for Kras-driven LAC, we treated *gp130*$^{F/F}$:*Kras*^{G12D} mice with 2 anti-IL-6R single-chain variable fragment mAbs, 25F10 and IF7, which efficiently block IL-6 trans signalling in the mouse. These antibodies, which were kindly provided by our collaborator Dr W.Ferlin, (NovoImmune, Switzerland), were administered to *gp130*$^{F/F}$:*Kras*^{G12D} mice at 10mg/kg injection twice a week over 6 weeks with the initial injection given the day after Cre inhalation (Section 2.1.4). Notably, the treatment of *gp130*$^{F/F}$:*Kras*^{G12D} mice with either 25F10 or IF7 significantly suppressed the identical exacerbated LAC phenotype observed in untreated *gp130*$^{F/F}$:*Kras*^{G12D} mice, as determined by significantly reduced the area of lung parenchyma (Figure 4.10). Consistent with these observations, TTF-1- and PCNA-positive cell numbers were also reduced in the lungs of gp130$^{F/F}$:*Kras*^{G12D} mice treated with either 25F10 or 1F7 (Figure 4.11). Interestingly, significantly lower numbers of TTF-1- and PCNA-positive cells were also present in the lungs of Kras^{G12D} mice treated with 1F7 compared with isotype control, and this was associated with a reduction in the area of lung parenchyma–containing lesions, albeit not significant. Collectively, these data reveal that therapeutic blockade of IL-6 trans signalling suppresses *Kras*-driven LAC.

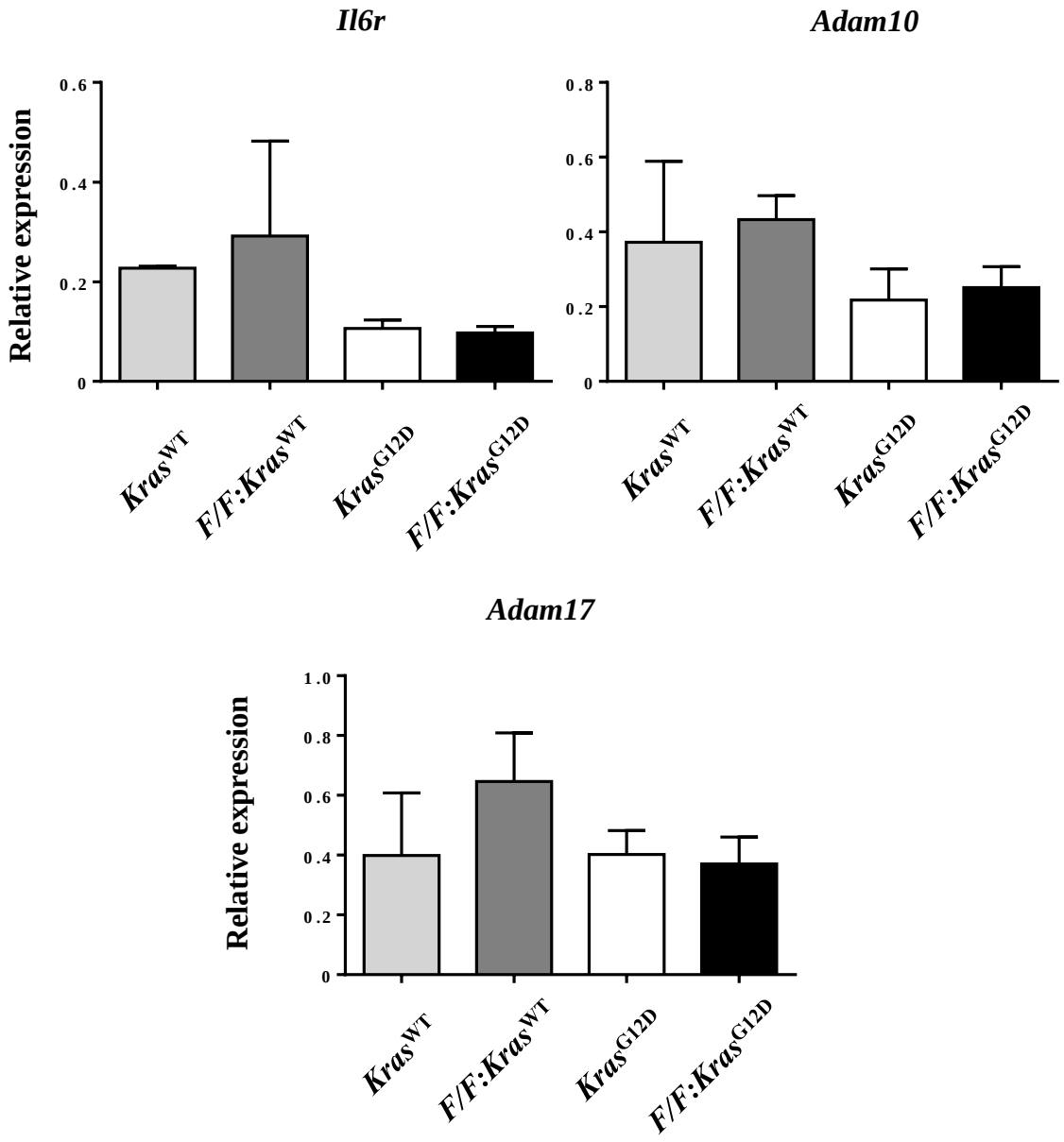

Figure 4.9. Generation of sIL-6R is not dependent on ADAM10 and ADAM17-dependent proteolytic cleavage

qPCR gene expression analyses for *IL-6r*, *Adam10*, and *Adam17* on lung cDNA from *gp130*$^{+/+}$:*Kras*^{G12D} (*Kras*^{G12D}) or *gp130*$^{F/F}$:*Kras*^{G12D} (F/F:*Kras*^{G12D}) mice and control *gp130*$^{+/+}$:*Kras*^{WT} (*Kras*^{WT}) or *gp130*$^{F/F}$:*Kras*^{WT} (F/F:*Kras*^{WT}) mice. Expression data are normalized against 18S and are presented from 4 to 9 mice per genotype expressed as mean +/- s.e.m.

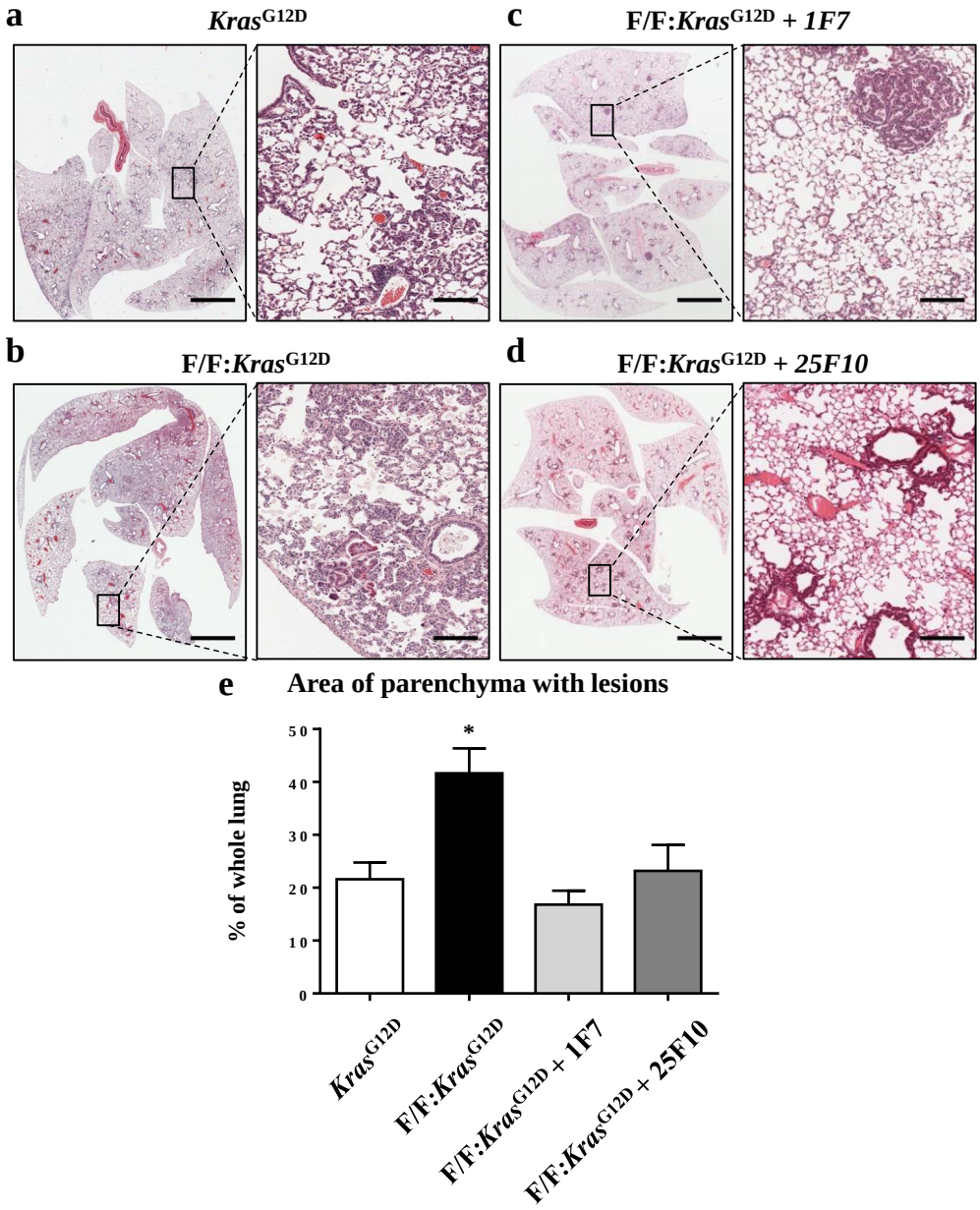

Figure 4.10. Antibody-mediated blockade of IL-6 trans signalling in *gp130*$^{F/F}$ mice supresses *Kras*^{G12D}-induced AIS

Representative low-power (left) and high-power (right) photomicrographs showing haemotoxylin and eosin-stained lung cross-sections from (a) *gp130*$^{+/+}$:*Kras*^{G12D} (*Kras*^{G12D}), (b) *gp130*$^{F/F}$:*Kras*^{G12D} (F/F:*Kras*^{G12D}), (c) F/F:*Kras*^{G12D} mice treated with 1F7 Ab and (d) *gp130*$^{F/F}$:*Kras*^{G12D} (F/F:*Kras*^{G12D}) treated with 25F10 Ab. Mice were treated with Cre-recombinase for 6 weeks. Arrows, show discrete AIS lesion. Scale bar, 3mm left pane, 300µm right pane. (e) Graph depicts quantification of lung parenchyma area occupied by AIS lesions for indicated genotypes for whole lung at 10x magnification. Data from 5 to 9 mice per genotype expressed as mean +/- s.e.m, * $p<0.05$.

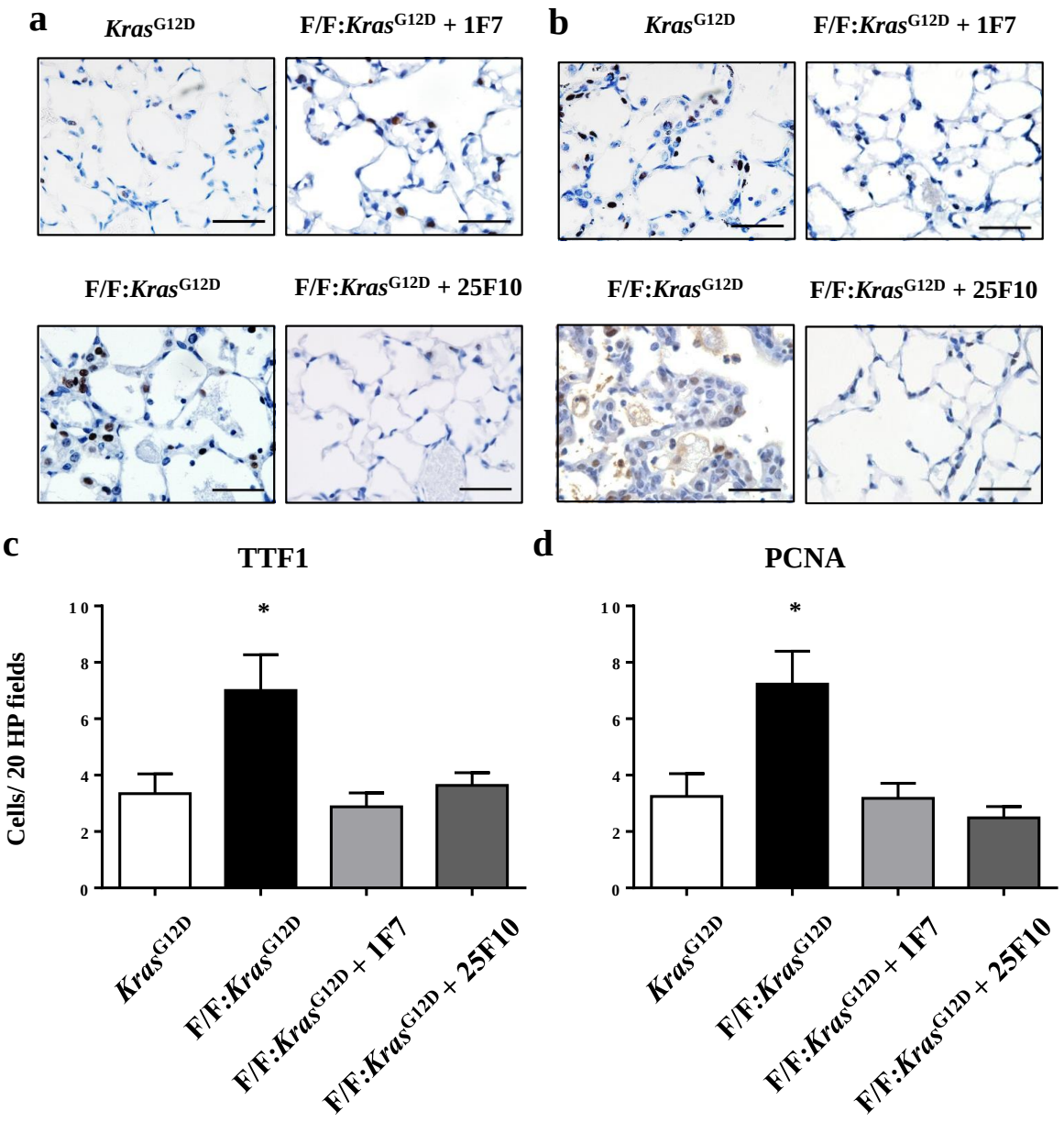

Figure 4.11. Antibody-mediated blockade of IL-6 trans signalling in *gp130*$^{F/F}$ mice supresses *Kras*^{G12D}-induced epithelial cell proliferation

Representative high-power photomicrographs of (a) TTF-1 stained and (b) PCNA-stained lung cross-sections from *gp130*$^{+/+}$:*Kras*^{G12D} (*Kras*^{G12D}), *gp130*$^{F/F}$:*Kras*^{G12D} (F/F:*Kras*^{G12D}), F/F:*Kras*^{G12D} mice treated with 1F7 and or 25F10 mice for 6 weeks. Scale bar, 50µm. Graph depicts quantification of either (c) TTF-1 or (d) PCNA positive cells per high powered field in the lungs of the indicated mice. Data from 4 to 9 mice per genotype expressed as mean +/- s.e.m, * $p<0.05$.

4.6 Discussion

In this chapter, I reveal that among IL-6 family cytokines, augmented levels of only IL-6 is associated with exacerbated LAC in *Kras*^{G12D}-driven lung carcinogenesis in mice. However, further research to these findings in our lab showed that the essential IL-6 trans signalling receptor subunit, sIL-6R, was also shown to be reduced [66]. The discrepancies between data presented here and data published is due to further mouse number being published. I also showed a reduction in cellular proliferation and epithelial cell development which correlated with the amelioration of IL-6 trans signalling driven lung cancer progression. Again, expanding on research done in this thesis, published works showed comparable high levels of naturally occurring sgp130 in the lungs of both *Kras*^{G12D} and gp130$^{F/F}$:*Kras*^{G12D} mice, the 2-fold increase in sIL-6R levels in gp130$^{F/F}$:*Kras*^{G12D} mouse lungs [66], without any increase in sgp130 levels, means that endogenous sgp130 levels are insufficient to block pathologic trans-signalling[235] in the lungs. This is in contrast with the administration of sgp130Fc, which is approximately 10 to 100 times more effective than sgp130 alone at blocking IL-6 trans signalling[142].

IL-6 trans signalling is emerging as a key pro-inflammatory factor driving many innate and auto immune diseases [236]. I have shown that in the gp130$^{F/F}$:*Kras*^{G12D} model for lung cancer, of the many cytokine involved in the IL-6 family of cytokines only IL-6 is up-regulated in these mice utilising the IL-6 “trans signalling” mode of signalling. IL-6 is the only cytokine that can be involved in this “trans signalling” mode of signalling as the soluble form of the IL-6R (sIL-6R), which interestingly enough was identified before the IL-6 cytokine, and is required for IL-6 trans signalling to occur through the proteolytic cleavage[237] or from alternatively spliced mRNA[132]

Chapter 5
The role of Stat3 (via IL-6 trans signalling) in Kras-driven LAC development

5.1 Introduction

I have thus far reported that oncogenic *Kras* engages with IL-6 trans signalling via gp130 to promote LAC, although the downstream mediators of gp130/IL-6/*Kras*-induced LAC are yet to be formally identified. Activation of the Stat3 transcription factor, as well as the PI3K and MAPK pathways, has been recently reported as a key pathological element in a conditional *Kras*-driven model of LAC[42,46,81]. Among these signalling mediators, cell autonomous Stat3 signalling clearly has a role in cancer development in models of inflammation–associated cancers, including lung cancer[63].

Consistent with these observations, various Stat3 target genes involved in cell cycle progression, cell survival, and angiogenesis are frequently overexpressed in human lung cancer[145,238,239], and Stat3 has been linked with mediating survival of human NSCLC cells[240]. The importance of Stat3 in lung cancer is suggested by the requirement of Stat3 for Ras-mediated oncogenesis[63], systemically and in lung tumour cells[42,241]. This has been confirmed by showing that a reduction in Stat3 phosphorylation is associated with tumour regression in a *Kras* mouse LAC model[42]. Furthermore, Stat3 is persistently activated in up to 50% of NSCLC[195,242]. Although the upstream mechanisms leading to deregulated Stat3 activity in lung cancer remain ill-defined, elevated Stat3 activity is a critical downstream regulator of tumour cell survival[92,195] triggered by EGFR mutations in a subset of LACs (predominantly never smokers)[100]. More recently, in these tumours it has been proposed that increased

activation of Stat3 is mediated by upregulated expression of IL-6 through the EGFR receptor[221].

In this Chapter I will examine whether enhanced activation of Stat3 (via IL-6 signalling) can augment the oncogenic potency of activated *Kras*^{G12D} carcinogenesis. As I have previously demonstrated that genetic ablation of IL-6 in the lungs of gp130$^{F/F}$ mice normalizes the activation levels of Stat3[217], whose hyper-activation is a common feature of human lung adenocarcinoma[145,233]. Also, it has also been shown that the IL-6/gp130/Stat3 signalling pathway is associated with pulmonary inflammation and LAC in mice[42,63,90]. So to examine whether Stat3 hyperactivation in gp130$^{F/F}$ mice exacerbated *Kras*^{G12D}–induced LAC, we crossed *gp130*$^{F/F}$:*Stat3*$^{-/+}$ mice, displaying normalised pulmonary Stat3 activation[146], with *Kras*^{G12D} mice.

5.2 Augmented Stat3 in *gp130*$^{F/F}$:*Kras*^{G12D} mice is associated with lung cancer

Expression of the Stat3 target gene *Socs3*, which is a *bona fide* read out of Stat3 activity, is shown to be augmented in the lungs of *gp130*$^{F/F}$:*Kras*^{G12D} mice compared to *Kras*^{G12D} mice, however the downstream apoptotic gene, *Bcl2*, was not activated by Stat3 in any of our mouse models (Figure 5.1a). There was however a trend for increased expression in *gp130*$^{F/F}$:*Kras*^{WT} mice compared to *Kras*^{WT} consistent with previous findings[243]. I next looked at the activation of Stat3 within lesions of *gp130*$^{F/F}$:*Kras*^{G12D} mice and showed that nuclear staining of pY-Stat3 was frequently observed within epithelial cells of the lungs (Figure 5.1b).

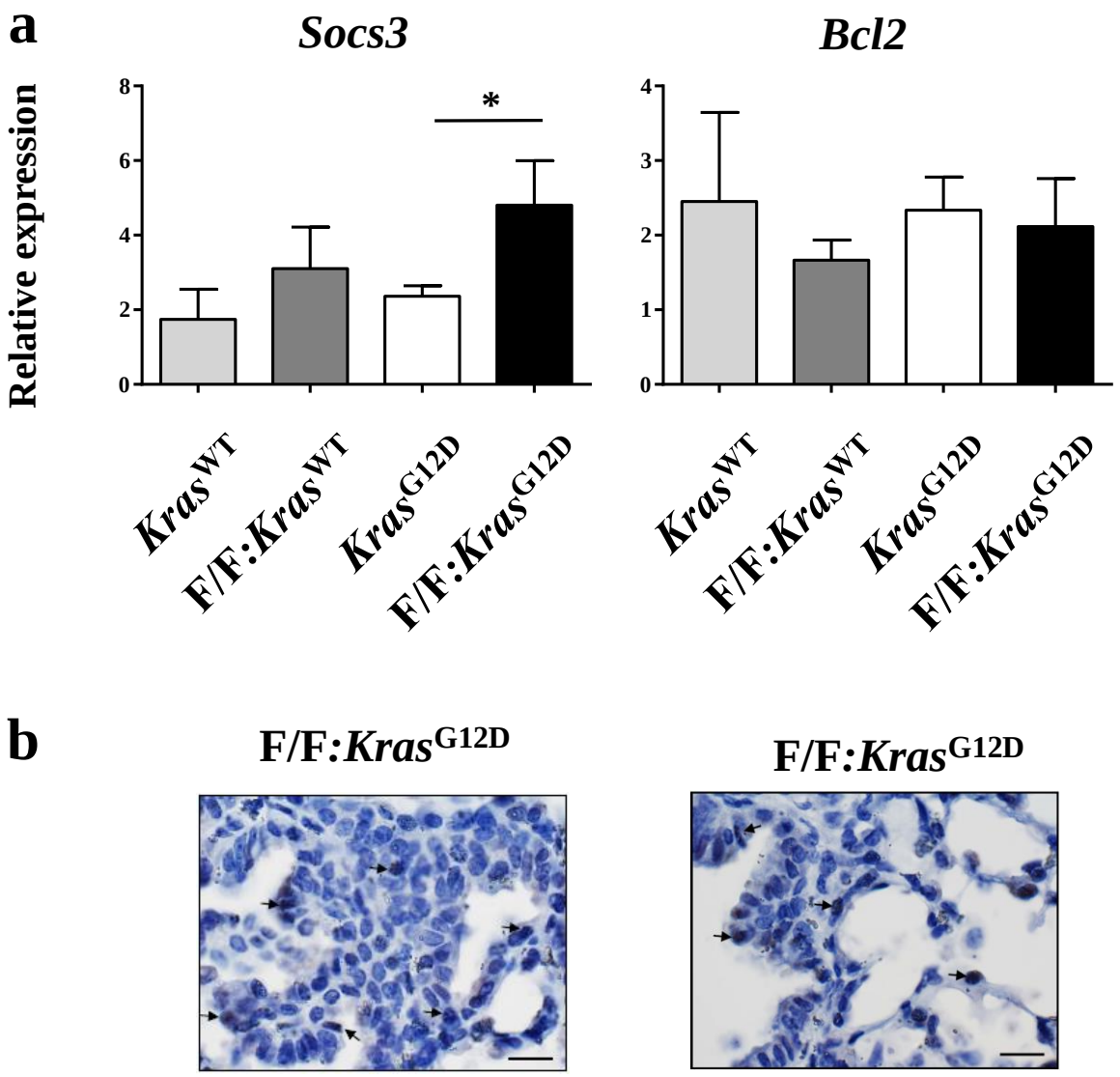

Figure 5.1. Stat3 target gene expression is augmented in *gp130*$^{F/F}$:*Kras*^{G12D} mice

(a) qPCR expression analysis of *Socs3* and *Bcl2* from cDNA derived from the lungs of 3 month old *gp130*$^{+/+}$:*Kras*^{WT} (*Kras*^{WT}) and *gp130*$^{F/F}$:*Kras*^{WT} (F/F:*Kras*^{WT}) mice treated with vehicle control for 6 weeks or *gp130*$^{+/+}$:*Kras*^{G12D} (*Kras*^{G12D}) and *gp130*$^{F/F}$:*Kras*^{G12D} (F/F:*Kras*^{G12D}) mice treated with Cre-recombinase for 6 weeks. Data from 4 to 12 mice per genotype expressed as mean +/- s.e.m and normalised for *18S* expression. * $p<0.05$. (b) Representative high power photomicrographs of nuclear expression of pY-Stat3 in the epithelial lesions in the lungs of F/F:*Kras*^{G12D} mice treated with Cre-recombinase for 6 weeks. Arrows point to representative cells displaying the characteristic punctate nuclear immunostaining of pY-Stat3. Scale bar 10μm.

5.3 Heterozygous ablation of Stat3 in *gp130*$^{F/F}$:*Kras*^{G12D} mice suppresses *Kras*-induced lung cancer

Based on the above findings and to further examine whether Stat3 hyper-activation in *gp130*$^{F/F}$:*Kras*^{G12D} mice exacerbated Kras-induced LAC, *gp130*$^{F/F}$:*Stat3*$^{-/+}$ mice displaying normal levels of pulmonary Stat3 activation[217] were back-crossed onto the *Kras*^{G12D} mice to produce *gp130*$^{F/F}$:*Kras*^{G12D}:*Stat3*$^{-/+}$ mice (as described in 2.1.1).

The area of parenchyma containing LAC in *gp130*$^{F/F}$:*Kras*^{G12D}:*Stat3*$^{-/+}$ mice was significantly reduced compared to *gp130*$^{F/F}$:*Kras*^{G12D} mice (Figure 5.2a and c). While this reduction is reflective of that found in *Kras*^{G12D} mice, the architecture of *gp130*$^{F/F}$:*Kras*^{G12D}:*Stat3*$^{-/+}$ mice was more similar to that found in human lung cancer patients with AAH, a precursor to AIS[203]. The foci were small, round, and sporadic throughout the whole parenchyma, however while the area of parenchyma was similar to that of the *Kras*^{G12D} mice (Figure 5.2c), the lesions were larger and more developed.

5.4 Amelioration of lung cancer development in *gp130*$^{F/F}$:*Kras*^{G12D}:*Stat3*$^{-/+}$ mice correlated with a reduction in cell proliferation

As previously discussed, increases in the alveolar epithelial type II cell marker, TTF-1, correlated with increased tumourgenesis in *gp130*$^{F/F}$:*Kras*^{G12D} mice (Section 3.3). As such, immunohistochemical evaluation was performed and indicated a significant 2-fold decrease in the number of TTF-1 positive cells in the lungs of *gp130*$^{F/F}$:*Kras*^{G12D}:*Stat3*$^{-/+}$ compared to *gp130*$^{F/F}$:*Kras*^{G12D} mice (Figure 5.3), confirming not only that this is a LAC phenotype but also that the development of LAC in the lungs of *gp130*$^{F/F}$:*Kras*^{G12D} mice is influenced by

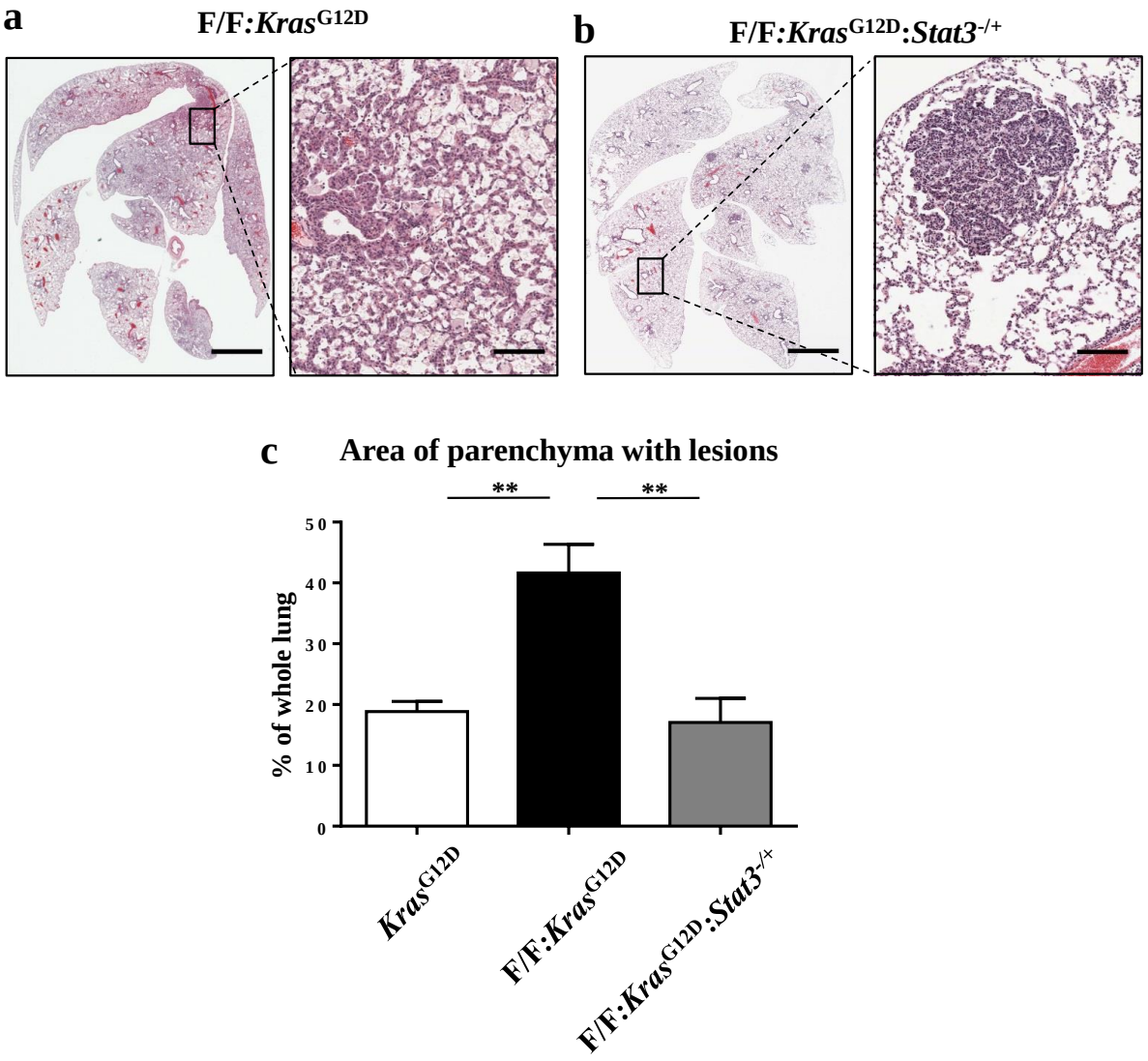

Figure 5.2. Heterozygous ablation of *Stat3* in *gp130*$^{F/F}$:*Kras*^{G12D} mice ameliorates AIS

Representative low-power (left) and high-power (right) photomicrographs showing haemotoxylin and eosin-stained lung cross-sections from either (a) *gp130*$^{F/F}$:*Kras*^{G12D} (F/F:*Kras*^{G12D}) and (b) *gp130*$^{F/F}$:*Kras*^{G12D}:*Stat3*$^{-/+}$ (F/F:*Kras*^{G12D}:*Stat3*$^{-/+}$) mice treated with Cre-recombinase for 6 weeks. Arrows, a small lesion. Scale bars, 3mm left panes, 300µm right panes (c) Graph depicts percentage of lung parenchyma occupied with AIS lesions. Whole lung and 10x magnification displayed. Data from 5 and 9 mice per genotype expressed as mean +/- s.e.m, ** $p<0.01$.

the activation of the IL-6 trans signalling/gp130/Stat3 pathway. By contrast, Stat3 deficiency in *Kras*^{G12D}:*Stat3*$^{-/+}$ mice after 6 weeks of Kras oncogenic activation did not change number of TTF-1 positive cells similar to *Kras*^{G12D} mice (Figure 5.3).

In addition to confirmation of the AIS phenotype of *gp130*$^{F/F}$*:Kras*^{G12D}:*Stat3*$^{-/+}$ mice, we also confirmed that cellular proliferation was involved in development, or in this case, amelioration of LAC. It was observed that there is a 4-fold decrease in the number of PCNA-positively stained cells in the lungs of *gp130*$^{F/F}$*:Kras*^{G12D}:*Stat3*$^{-/+}$ mice compared to the *gp130*$^{F/F}$:*Kras*^{G12D} mice, and the level of proliferation (number of PCNA positive cells) remained similar in *Kras*^{G12D}, *Kras*^{G12D}:*Stat3*$^{-/+}$ and *gp130*$^{F/F}$*:Kras*^{G12D}:*Stat3*$^{-/+}$ mice (Figure 5.4). We also note, that cellular inflammation and apoptosis was not changed in the lungs of in *gp130*$^{+/+}$:*Kras*^{G12D}, *gp130*$^{+/+}$:*Kras*^{G12D}:*Stat3*$^{-/+}$, *gp130*$^{F/F}$:*Kras*^{G12D} and *gp130*$^{F/F}$*:Kras*^{G12D}:*Stat3*$^{-/+}$ mice (Figures 5.5c and 5.5d respectively), and this correlated with the IL-6 trans signalling deficiency in these mice (Figure 4.5). These data therefore confirm that augmented IL-6 trans signalling through Stat3 is the mechanism by which Kras-induced LAC in *gp130*$^{F/F}$:*Kras*^{G12D} mice is being potentiated. As gp130/Stat3 signalling has a number of transcriptional effects, I next determined if there was a possible feed forward effect caused by the hyper-activation of Stat3. Indeed, mRNA levels of *IL-6* were markedly reduced in *gp130*$^{F/F}$*:Kras*^{G12D}:*Stat3*$^{-/+}$ mouse lungs when compared to the lungs of *gp130*$^{F/F}$:*Kras*^{G12D} mice (Figure 5.6). Of note, Stat3 is increased in the lungs of *gp130*$^{F/F}$*:Kras*^{G12D}:*Stat3*$^{-/+}$ mice when compared to *gp130*$^{F/F}$:*Kras*^{G12D} mice, albeit not significantly, which is not consistent with Stat3 heterozygous mutants, however I believe this is due to inherent variability within this mouse model.. Thus, these data support the notion that IL-6/gp130/Stat3 hyper-activation can potentiate Kras- induced LAC, and also evoke the existence of a possible feed forward loop whereby gp130/Stat3 hyper-activation augments the transcriptional induction of IL-6.

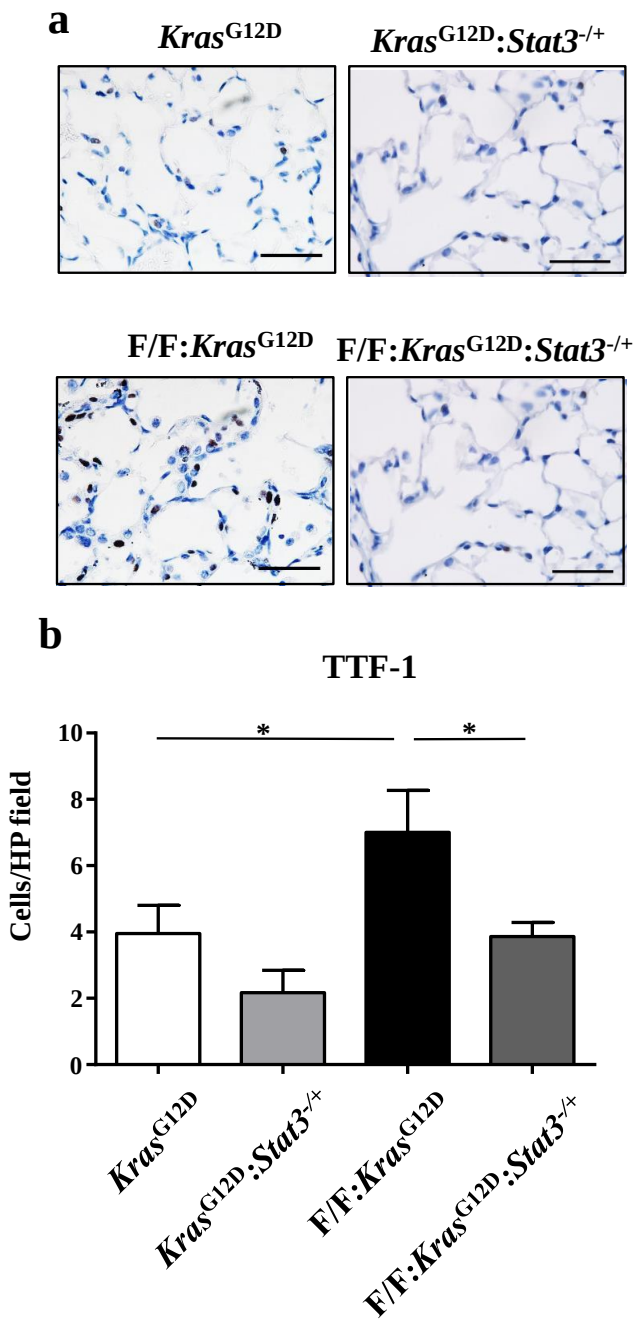

Figure 5.3. *gp130*$^{F/F}$:*Kras*^{G12D}:*Stat3*$^{-/+}$ mice show decreased Thyroid transcription factor (TTF)-1 staining in the lungs (a) Representative high-power photomicrographs of TTF-1-stained lung cross-sections from *gp130*$^{+/+}$:*Kras*^{G12D} (*Kras*^{G12D}), *gp130*$^{+/+}$:*Kras*^{G12D}:*Stat3*$^{-/+}$ (*Kras*^{G12D}:*Stat3*$^{-/+}$), *gp130*$^{F/F}$:*Kras*^{G12D} (F/F:*Kras*^{G12D}) and *gp130*$^{F/F}$:*Kras*^{G12D}: *Stat3*$^{-/+}$ (F/F:*Kras*^{G12D}: *Stat3*$^{-/+}$) mice treated with Cre-recombinase for 6 weeks. Scale bar, 50µm (b) Graph depicts quantification of TTF-1 positive cells per high powered field (100x magnification) in the lungs of the indicated mice. Data from 5 to 9 mice per genotype expressed as mean +/- s.e.m, * $p<0.05$.

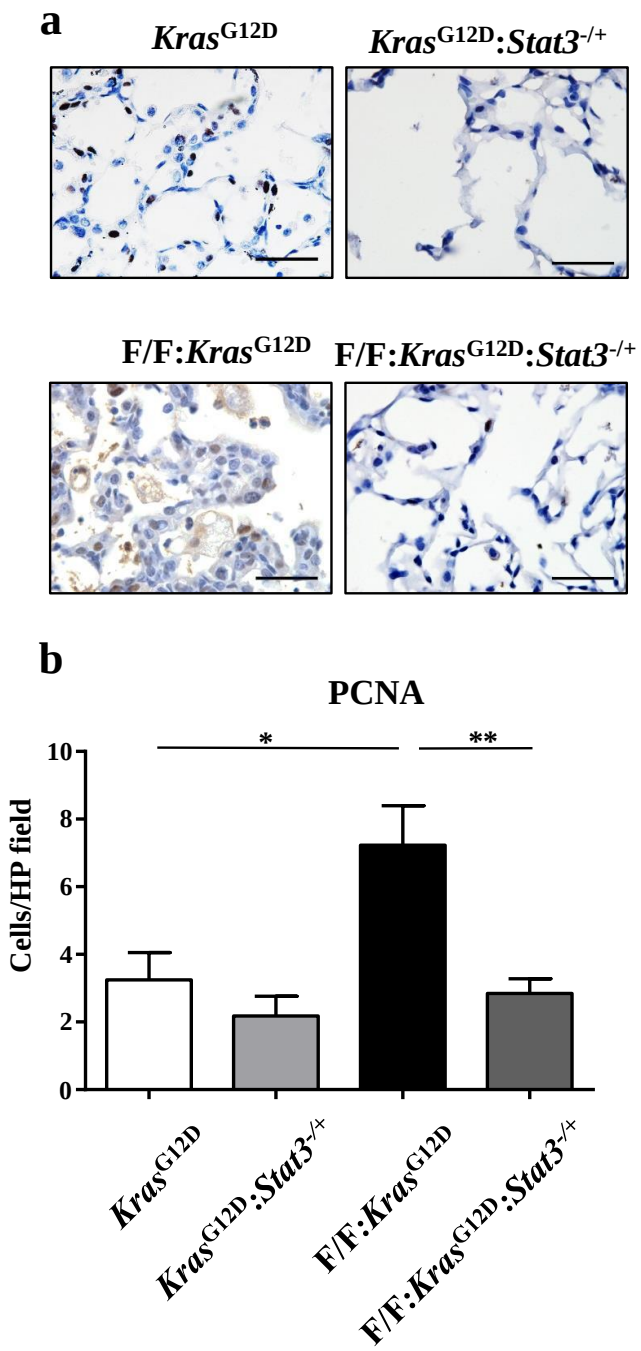

Figure 5.4. The lungs of *gp130*$^{F/F}$:*Kras*^{G12D}:*Stat3*$^{-/+}$ mice show decreased cellular proliferation

(a) Representative high-power photomicrographs of PCNA-stained lung cross-sections from *gp130*$^{+/+}$:*Kras*^{G12D} (*Kras*^{G12D}), *gp130*$^{+/+}$:*Kras*^{G12D}:*Stat3*$^{-/+}$ (*Kras*^{G12D}:*Stat3*$^{-/+}$), *gp130*$^{F/F}$:*Kras*^{G12D} (F/F:*Kras*^{G12D}) and *gp130*$^{F/F}$:*Kras*^{G12D}: *Stat3*$^{-/+}$ (F/F:*Kras*^{G12D}: *Stat3*$^{-/+}$) mice treated with Cre-recombinase for 6 weeks. Scale bar, 50μm (b) graph depicts quantification of PCNA positive cells per high powered field (100x magnification) in the lungs of the indicated mice. Data from 5 to 9 mice per genotype expressed as mean +/- s.e.m, * $p<0.05$.

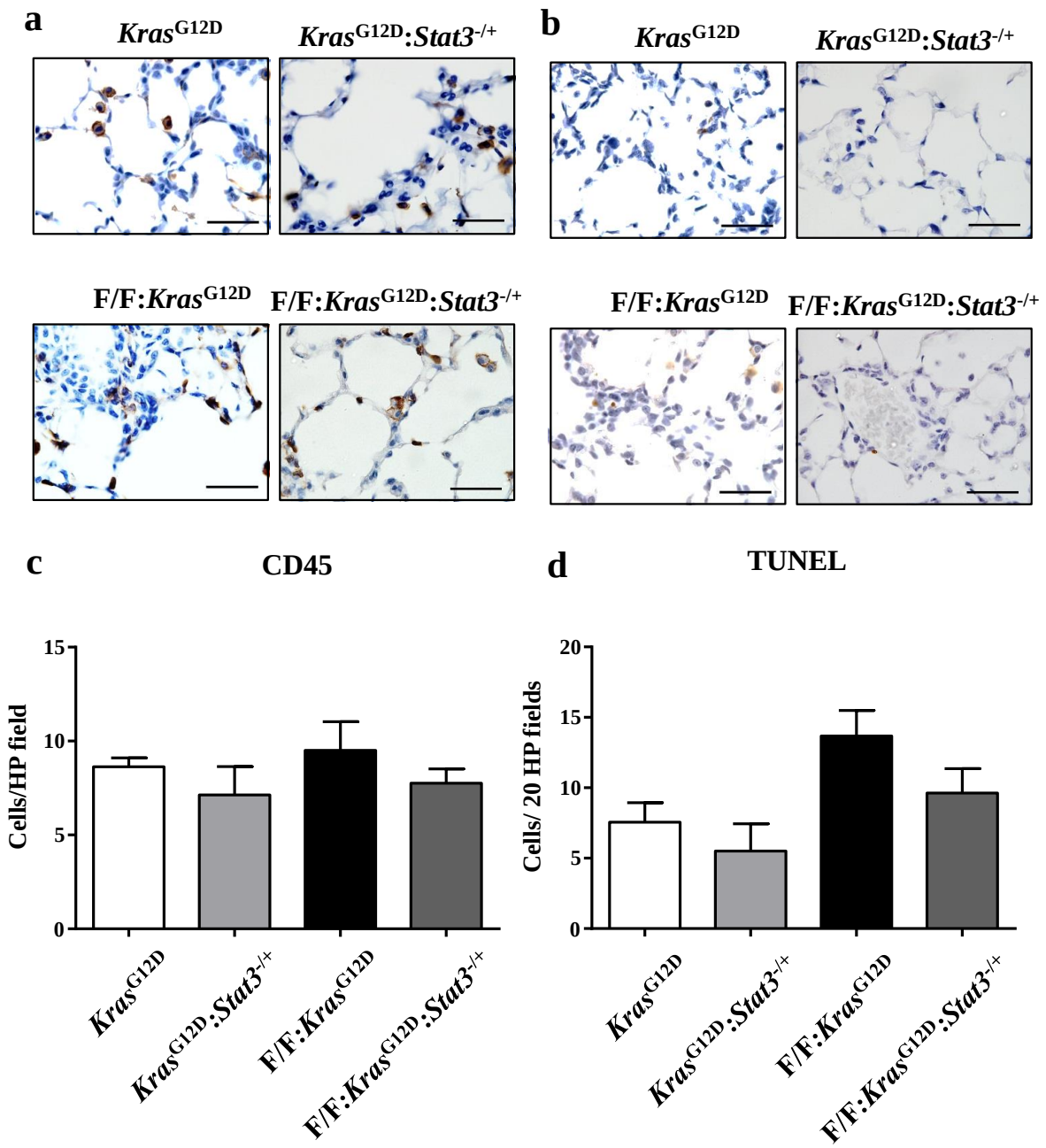

Figure 5.5. Cellular inflammation and apoptosis in the lung is unaffected upon amelioration of AIS in *gp130*$^{F/F}$:*Kras*^{G12D}:*Stat3*$^{-/+}$ mice

(a) Representative high-power photomicrographs of (a) CD45 stained- and (b) TUNEL-stained lung cross-sections from *gp130*$^{+/+}$:*Kras*^{G12D} (*Kras*^{G12D}), *gp130*$^{+/+}$:*Kras*^{G12D}:*Stat3*$^{-/+}$ (*Kras*^{G12D}:*Stat3*$^{-/+}$), *gp130*$^{F/F}$:*Kras*^{G12D} (F/F:*Kras*^{G12D}) and *gp130*$^{F/F}$:*Kras*^{G12D}: *Stat3*$^{-/+}$ (F/F:*Kras*^{G12D}: *Stat3*$^{-/+}$) mice treated with Cre-recombinase for 6 weeks. Scale bar, 50µm (b) Graph depicts quantification of (c) CD45- positive cells per high powered field and (d) TUNEL-positive cells per 20 high powered fields (100x magnification) in the lungs of the indicated mice. Data from 4 to 9 mice per genotype expressed as mean +/- s.e.m.

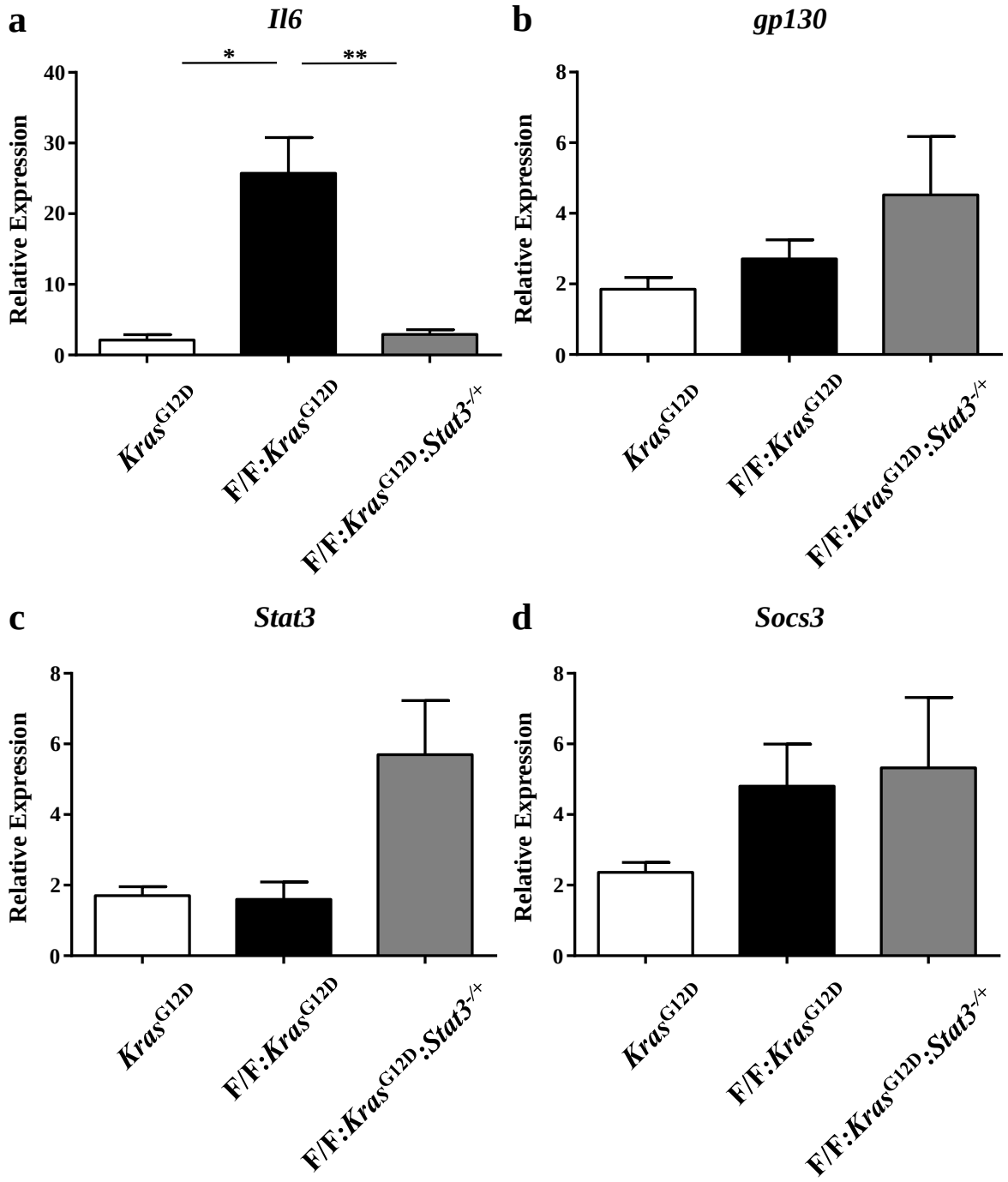

Figure 5.6. Ablation of Stat3 from *gp130*$^{F/F}$:*Kras*^{G12D} mice augments induction of *IL-6*

(a) qPCR expression analysis of *IL-6, gp130, Stat3, and Socs3* was performed on cDNA derived from the lungs of 3 month old *gp130*$^{+/+}$:*Kras*^{G12D} (*Kras*^{G12D}), *gp130*$^{F/F}$:*Kras*^{G12D} (F/F:*Kras*^{G12D}) and *gp130*$^{F/F}$:*Kras*^{G12D}: *Stat3*$^{-/+}$ (F/F:*Kras*^{G12D}:*Stat3*$^{-/+}$) treated with Cre-recombinase for 6 weeks. Relative expression data from 4 to 12 mice per genotype expressed as mean +/- s.e.m and normalised for *18S* expression are shown. * $p<0.05$.

5.5 Discussion

In this chapter, I show that the gp130-dependent signalling pathway that exacerbates adenocarcinoma development in *gp130*$^{F/F}$:*Kras*^{G12D} mice is through the IL-6/gp130/Stat3 signalling axis and that this augmentation of cytokine signalling in lung cancer development may evoke a number transcriptional alterations within the tumour foci. We showed that a reduction of proliferation and epithelial cell development correlated with the amelioration of Stat3 mediated Kras-induced lung cancer development.

Although the downstream mediators of Kras-induced lung adenocarcinoma remain ill-defined, my data here suggest that enhanced activation of Stat3 can augment the oncogenic potency of the activating *Kras*^{G12D} mutant. The combined observations that tyrosine-phosphorylated (activated) Stat3 resides primarily in the respiratory epithelium (where the oncogenic *Kras*^{G12D} mutant is expressed from its endogenous promoter) of *gp130*$^{F/F}$:*Kras*^{G12D} mouse lungs, and the exacerbated lung adenocarcinoma phenotype in *gp130*$^{F/F}$:*Kras*^{G12D} mice is not associated with any further increase in leukocyte infiltrates, support the notion that gp130$^{F/F}$-dependent oncogenic cellular responses in the lung are driven by the epithelium, as has been previously reported for the epithelium of other tissues from *gp130*$^{F/F}$ mice[244]. I also note that these current findings are consistent with the previous report that IL-6 trans signalling and Stat3 are required for tumorigenesis in a *Kras*^{G12D}-induced pancreatic adenocarcinoma mouse model[139]. Furthermore, autocrine IL-6/Stat3 signalling can promote the Kras-dependent cell survival and proliferation *in vitro* of human LAC cell lines[245], albeit the specific role of IL-6 trans signalling was not addressed in this paper.

Although collectively these observations imply that Stat3 via IL-6 trans signalling can augment the oncogenic potential of Kras mutations in lung adenocarcinoma, recently it was reported that the lung epithelial-specific inactivation of Stat3 exacerbates *Kras*^{G12D}-driven

lung adenocarcinoma[208]. The tumour-suppressive activity of Stat3 is observed by its ability to regulate cytoplasmic NFkB and inhibit transcription of the proangiogenic chemokine Cxcl1 which has been shown to alter tumour vascularization and growth[66]. While in this thesis the cytokines responsible for upstream Stat3-activating were also not identified, these findings are reminiscent of previous studies using Stat3 conditional ablation in mice[133]. As IL-6 trans signalling also activates Stat3 heterodimers with Stat1[133] modulating a different network of gene targets it is not surprising that Cxcl1 gene expression was unchanged in the lungs of *gp130*$^{F/F}$:*Kras*^{G12D} mice displaying exacerbated LAC as Stat3 modulates by other cytokines, such as IL-10, which activates Stat3 homodimers.

Collectively, these data show an important pathogenic role for Stat3 downstream of IL-6 in exacerbated AIS in the lungs of *gp130*$^{F/F}$:*Kras*^{G12D} mice. These data therefore further support the previous knowledge that Stat3 is intimately linked to IL-6-dependent cancers and specifically the pro-inflammatory element of IL-6 trans signalling. This also raises the fundamental question about the role the IL-6/Stat3/gp130 pathway is playing in human lung cancer development. As such in the next chapter I touch on the important factors impacting IL-6 trans signalling-driven LAC development in the human environment.

Chapter 6
Validation of augmented IL-6 trans signalling/STAT3 components in human lung cancer

6.1 Introduction

An important extension of pre-clinical mouse models is to further investigate those mechanisms of IL-6 and Stat3 and their downstream consequences on oncogenic cellular processes to the human environment. IL-6 has been shown to be increased in patients with NSCLC systemically when BALF, serum or pleural fluid is examined[145,230,231,246]. Importantly, elevated levels of IL-6 are intimately linked to higher levels of mortality and morbidity[155,247] suggesting that IL-6 plays an important role in lung cancer development and progression. To investigate this our laboratory utilised human non-immortalised primary airway epithelial cells and immortalised NSCLC cell lines, in addition to human biopsy samples form patients presenting to the Monash Hospital, Clayton, Victoria with some form of lung disease including chronic obstructive pulmonary disease (COPD) or LC. Several clinical observation support a link between IL-6 trans signalling and lung cancer development[111,158,208], however human models to further investigate the mechanisms and downstream processes on inflammatory and oncogenic cellular processes *in vitro* are impractical. The use of human cells provides the key advantage of confirming species conservation in these processes, which is an integral step for the future translation of our mechanistic findings in the pathogenesis of lung disease.

The above findings support the potential interaction between oncogenic Kras and IL-6/gp130/Stat3 signalling in human cancers, however this has not being fully studied for lung cancer, nor the interaction between *Kras* and specific IL-6 cytokine signalling modes. My above findings show an important involvement of IL-6 trans signalling through the Stat3 signalling in the *Kras*^{G12D}-induced mouse model for lung cancer. So to study this in the human environment our laboratory obtained samples from LAC patients and COPD patients from the Monash Medical Centre, Clayton, Victoria, Australia, in order to assess the genetic and molecular phenotypes of these patients and relate it to our own data *in vivo*. We obtained a total of 24 LAC samples with a 1:3 male:female ratio, and 80% of these had been smokers previously (Table 6.1). A control cohort comprised of individuals presenting with various lung diseases, including COPD and interstitial pneumonia, in total there were 5 control samples with a 3 males and 2 females, and 80% had previously smoked (Table 6.1).

6.2 IL-6/STAT3 signalling activation in human lung cancer cell lines

To validate our mouse data showing that IL-6 trans signalling via STAT3 plays an important role in LAC development (Chapters 3-5), two lung cancer bronchial epithelial cell lines that harbour either mutant *Kras* or wild type *Kras* alleles, A549[248] and H838[249] respectively, were used. Gene expression levels were compared to that of A549 cells as these human lung cells were originally cultured from explanted malignant tissue[250] but maintain characteristics of type II pneumocytes[251]. In addition, they have been well characterised and have been established as a standard in human lung cell. Since IL-6 and STAT3 activation varies markedly in unstimulated human NSCLC cell lines[252]. Therefore, firstly I determined the gene expression levels of *IL-6*, *STAT3* and *SOCS3* were assessed and found to be readily detectable in these 2 independent human cell lines, containing either mutant or WT *Kras* (Figure 6.1). Furthermore, A549

Table 6.1: Clinical features of LAC patients and control LAC free individuals.

Patient characteristics	**LAC**	**Control**
n	24	5
Mean age (range in years)	66 (45-85)	62(47-75)
Gender		
Male, n (%)	8 (33)	3 (60)
Female, n (%)	16 (67)	2 (40)
Smoking history		
Never smokers, n (%)	5 (21)	1 (20)
Smokers, n (%)	19 (79)	4 (80)
Packs per year (mean)	42	32

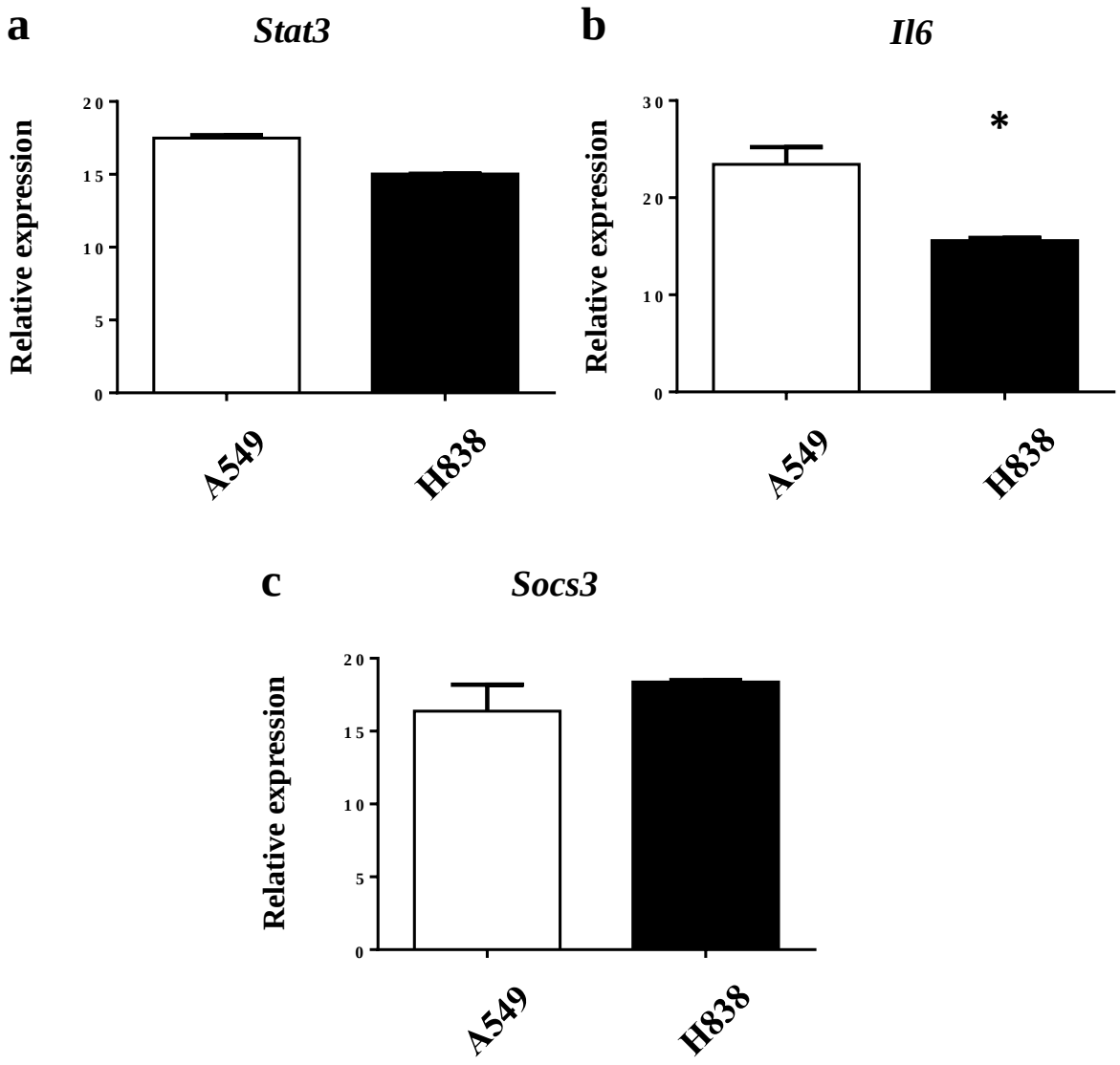

Figure 6.1. mRNA expression levels of *IL-6* and *STAT3* signalling genes in human LAC cell lines.

qPCR gene expression analyses for *IL-6*, *STAT3*, and *SOCS3* on lung cDNA from A549 and H838 human LAC cell lines. Expression data are normalized against 18S and are presented from 3 independent experiments expressed as mean +/- s.e.m, * $p<0.05$.

showed increased level of IL-6 gene expression compared to H838 (Figure 6.1b), however Stat3 and Socs3 levels were unchanged (Figure 6.1a and c respectively), suggesting that while A549 may have increased basal *IL-6*, both *STAT3* and *SOCS3* have a similar basal level of downstream gp130 genes.

In addition, basal levels of a number of tumour suppressor genes, *p53* and *Tsc2*; *Cdkn1b* and *MyD88* implicated in exacerbated lung cancer development[21,229]; and *Ikbke* and *Map2k4*, two Stat3 target genes, were assessed, and found that they were also readily detectable in these two LC cell lines (Figure 6.2). However, no changes were seen from a basal level between the *Kras* mutant cell line and the wild type cell lines.

I then used these A549 and H838 cell lines which had been serum starved for 24 hours and stimulated with IL-6 at 100nM; this was based on a concentration curve previously determined (data not shown). At this concentration of *IL-6* there was no discernible activation of *Stat3* gene expression in these two cell lines, but there were early increases of *IL-6* and *Socs3* gene expressions at 1hr, thus confirming that IL-6 can induce Stat3 signalling these cells (Figure 6.3). Further to this, we found that IL-6 stimulation did not induce gene expressions of tumour suppressors *p53* and *Tsc2*, *Cdkn1b*, and *MyD88* in A549 (Figure 6.4) or H838 (Figure 6.5) indicating that IL-6, in these cell lines, does not activate tumour suppressor genes. This is most likely due to these cell lines being human lung adenocarcinoma cell lines and as such these genes will already have been augmented.

6.3 Augmented levels of *IL-6* and *Socs3*, in human LAC patients

Given the reported involvement of IL-6 and its downstream targets in the regulation of cellular proliferation, survival, and differentiation, it is not surprising that IL-6 signalling has also been

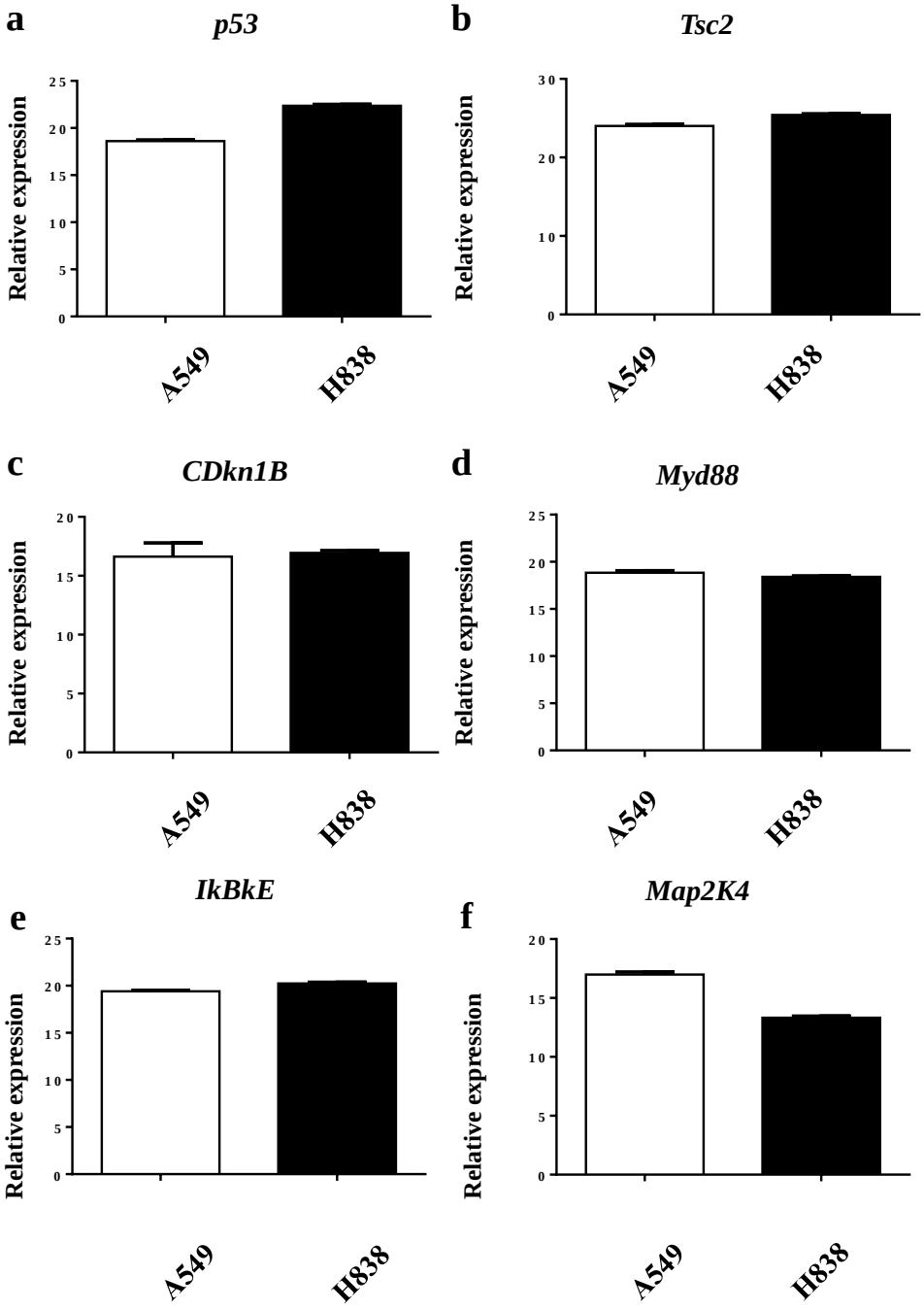

Figure 6.2. mRNA expression levels of tumour suppressor and STAT3 target genes in human LAC cell lines.

qPCR gene expression analyses for *p53*, *Tsc2*, *IkBkE*, *Ma2K4*, *CDkn1B*, and *Myd88* on lung cDNA from A549 and H838 human lung adenocarcinoma cell lines. Expression data are normalized against 18S and are presented from 3 independent experiments expressed as mean +/- s.e.m.

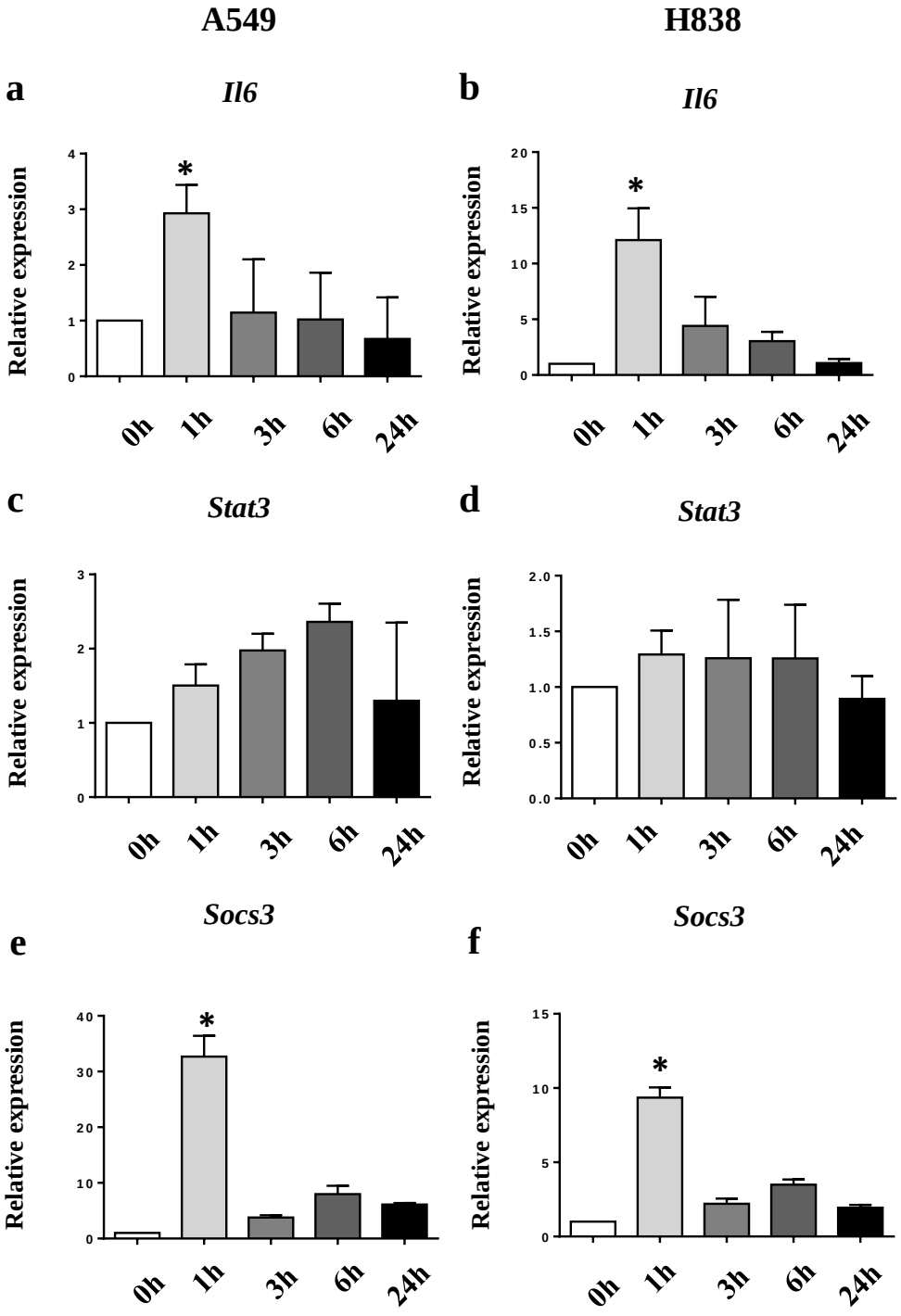

Figure 6.3. IL-6-induced gene regulation of STAT3 target genes

qPCR gene expression analyses for *IL-6, STAT3,* and *SOCS3* on lung cDNA from A549 and NCI-H838 human lung adenocarcinoma cell lines. Expression data are normalized against 18S and 0h time point. Data are presented from 3 independent experiments expressed as mean +/- s.e.m.

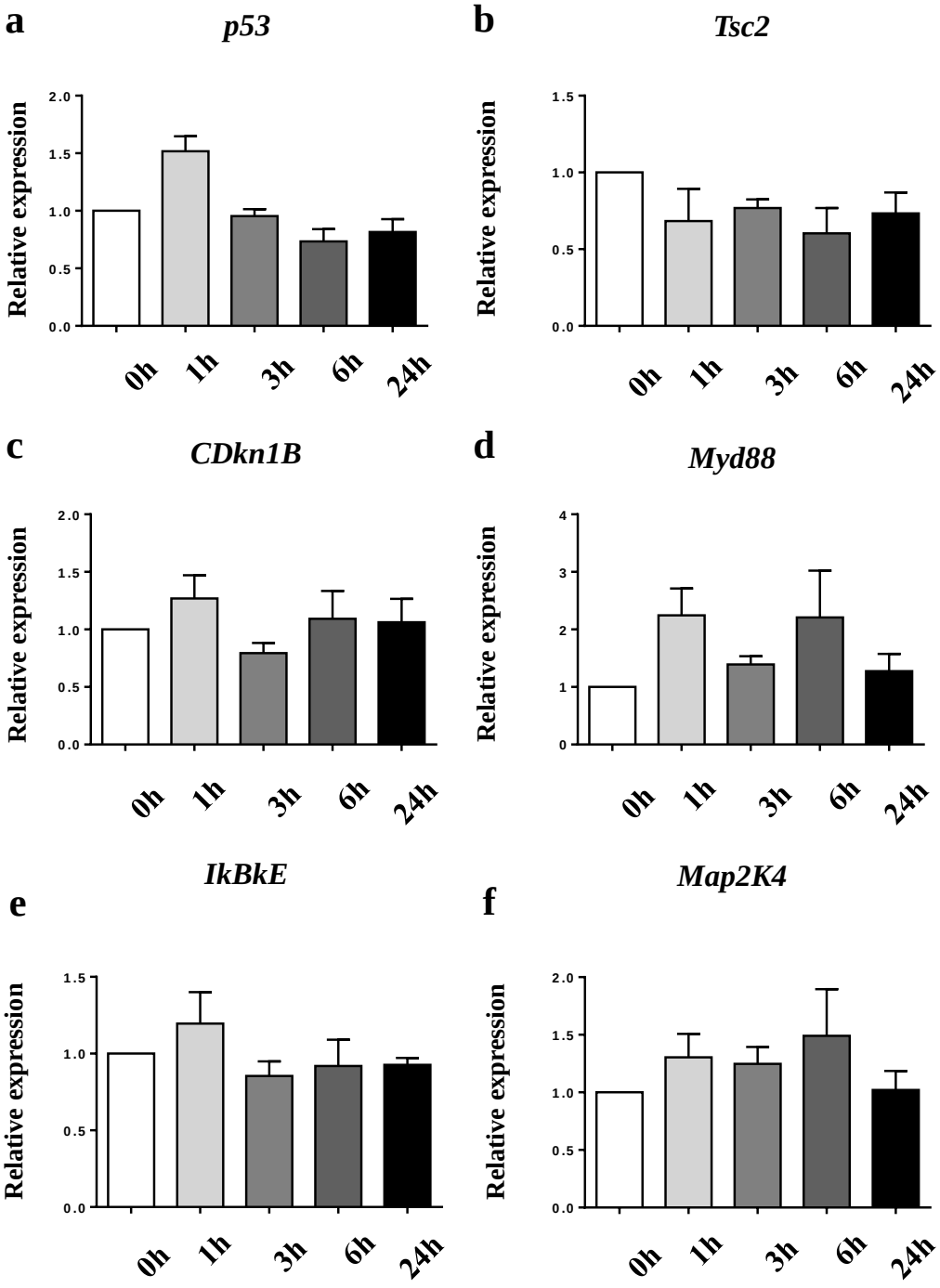

Figure 6.4. IL-6-induced regulation of tumour suppressor and STAT3 target genes in A549 cell lines

qPCR gene expression analyses for *p53, tsc2, cdkn1b, myd88, ikbke,* and *map2k4* on lung cDNA from A549 human lung adenocarcinoma cell lines. Expression data are normalized against 18S and 0h time point. Data are presented from 3 independent experiments expressed as mean +/- s.e.m.

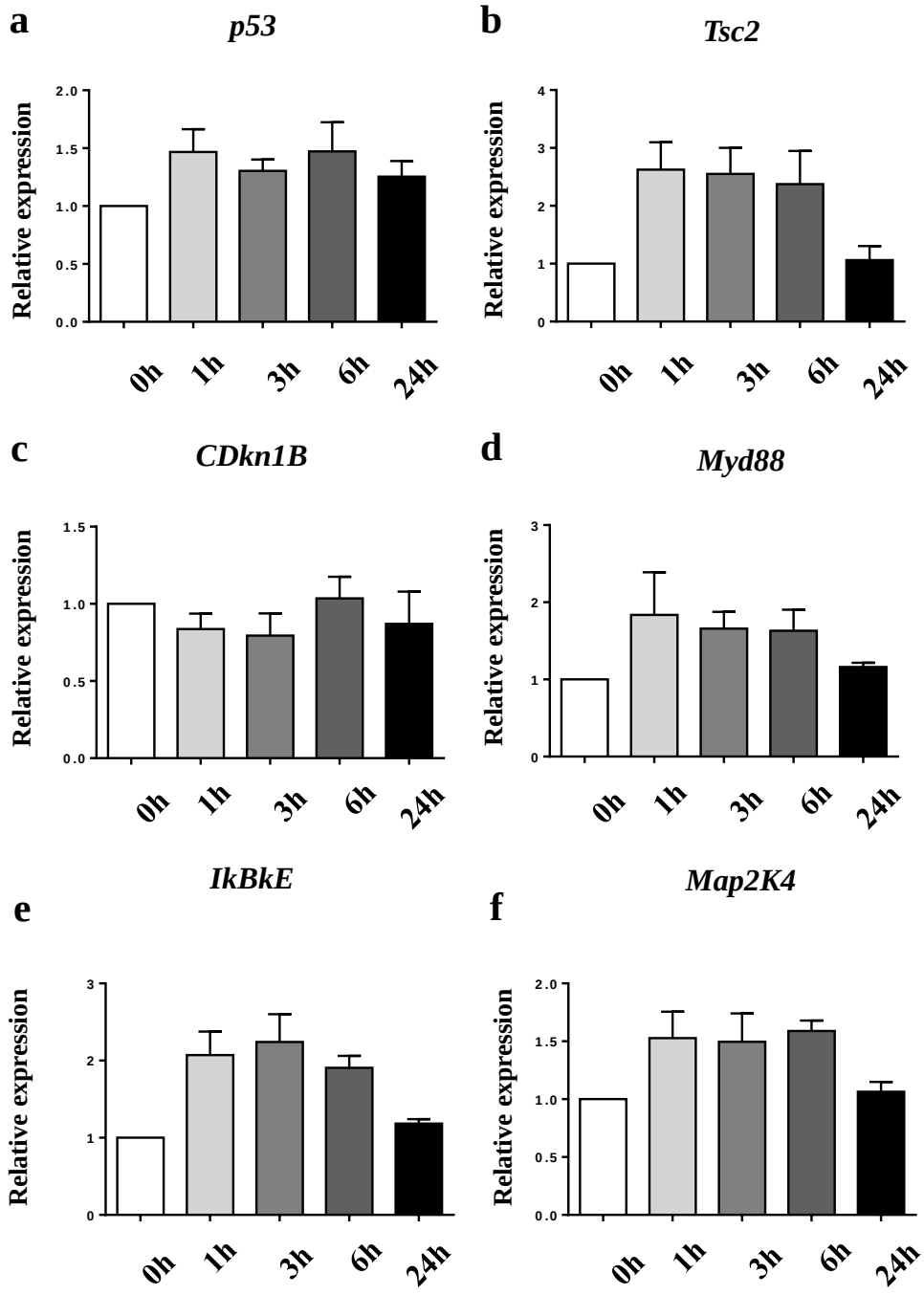

Figure 6.5. IL-6-induced regulation of tumour suppressor and STAT3 target genes in H838 cell lines

qPCR gene expression analyses for *p53, tsc2, cdkn1b, myd88, ikbke,* and *map2k4* on lung cDNA from NCI-H838 human lung adenocarcinoma cell lines. Expression data are normalized against 18S and 0h time point. Data are presented from 3 independent experiments expressed as mean +/- s.e.m.

implicated in tumorigenesis[69,253], this deregulated cytokine signalling via gp130, the critical co-receptor for the IL-6 cytokine family, is implicated in human airway inflammation, and lung carcinogenesis[145,216,254]. There have also been multiple studies that show high IL-6 serum levels in patients with LAC correlated with poor clinical prognosis[183,247,255]. These data suggest an oncogenic role for IL-6 in LAC development, however this was not studied.

My supervisor, Dr Saleela Ruwanpura, determined the mRNA levels for *Socs3*, whose expression is indicative of Stat3 activity, in patients with LAC patients and found that there was a 4-fold increase among LAC patients compared to control individuals (Figure 6.6a). Among the IL-6 family of cytokines, only mRNA levels of *IL-6* were significantly (13-fold) increased in lung adenocarcinoma patients compared to control individuals (Figure 6.6b)[66]. Of note is that these data correlated with data found in *gp130*$^{F/F}$:*Kras*^{G12D} mice when compared to *Kras*^{G12D} mice (Figure 4.1a).

6.4 Increased IL-6 trans signalling components in LAC patients

Since it was shown that there is a significant increase in the production of IL-6 in LAC patients, I next looked at whether this was specific to IL-6 trans signalling[66]. Indeed, the protein expression of IL-6 in both the lung parenchyma and serum of lung adenocarcinoma patients was almost 2-fold increased in the lungs (Figure 6.7a) and an almost 4-fold increase in the serum (Figure 6.7c). Importantly however, was there was an in sIL-6R levels in the lungs (Figure 6.7b) and a 2-fold increase in the serum (Figure 6.7d) of LAC patients compared to control individuals. It was next studied whether increased IL-6 production also correlated with sIL-6R levels in both the lung parenchyma (Figure 6.7e) and serum (Figure 6.7f). Indeed, the production of IL-6 in these LAC patients correlated with the increased

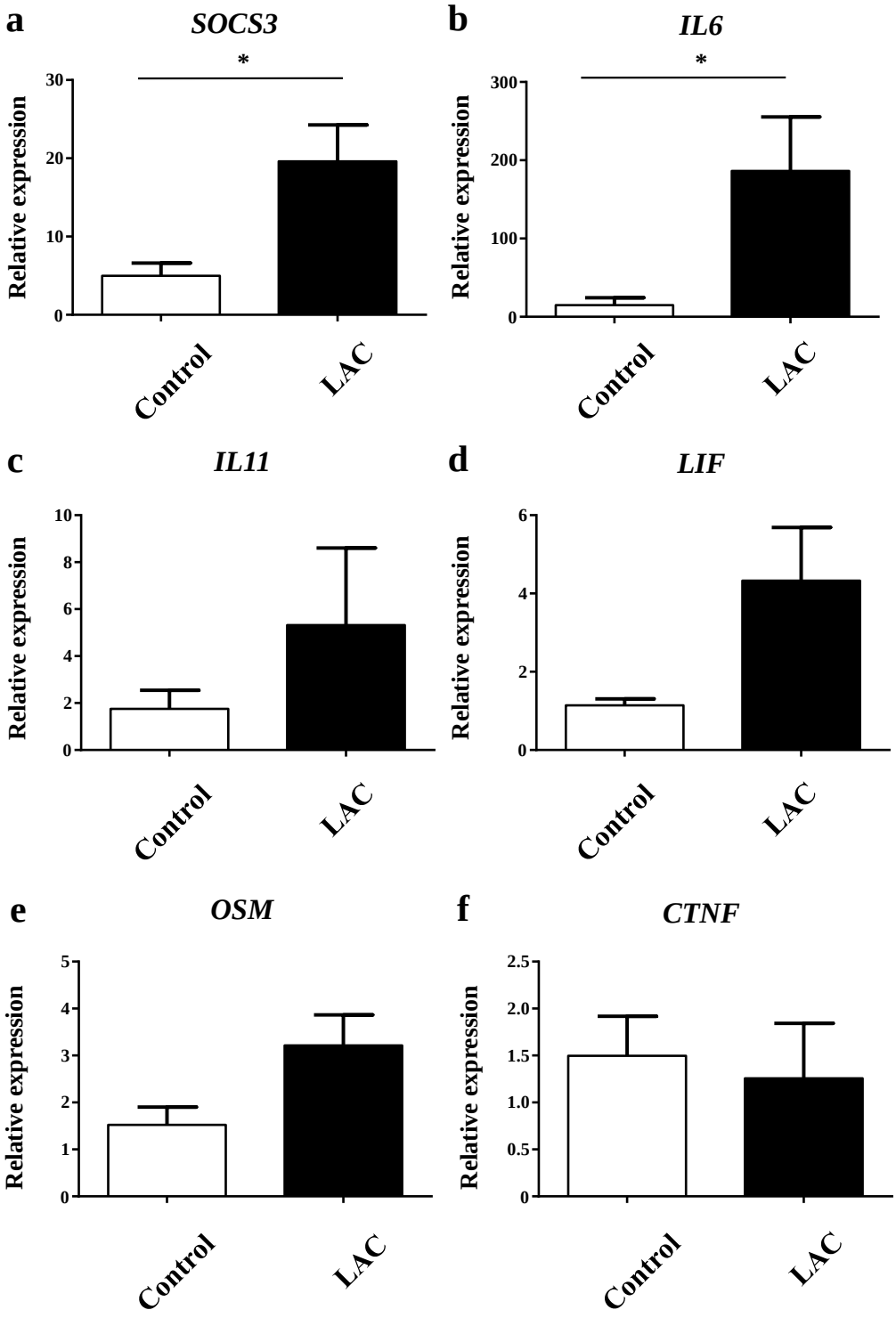

6.6. Augmented mRNA levels on IL-6/STAT3 signalling genes in human LAC tissues qPCR expression analysis from human LAC patients (n=24) or control (n=5) of (a) *SOCS3,* (b) *IL-6,* (c) *IL11,* (d) *LIF,* (e) *OSM, and* (f) *CTNF* were performed on cDNA. Relative expression data expressed as mean +/- s.e.m and normalised for *18S* expression are shown. * $p<0.05$. (reprinted from data collected by Saleela Ruwanpura[66])

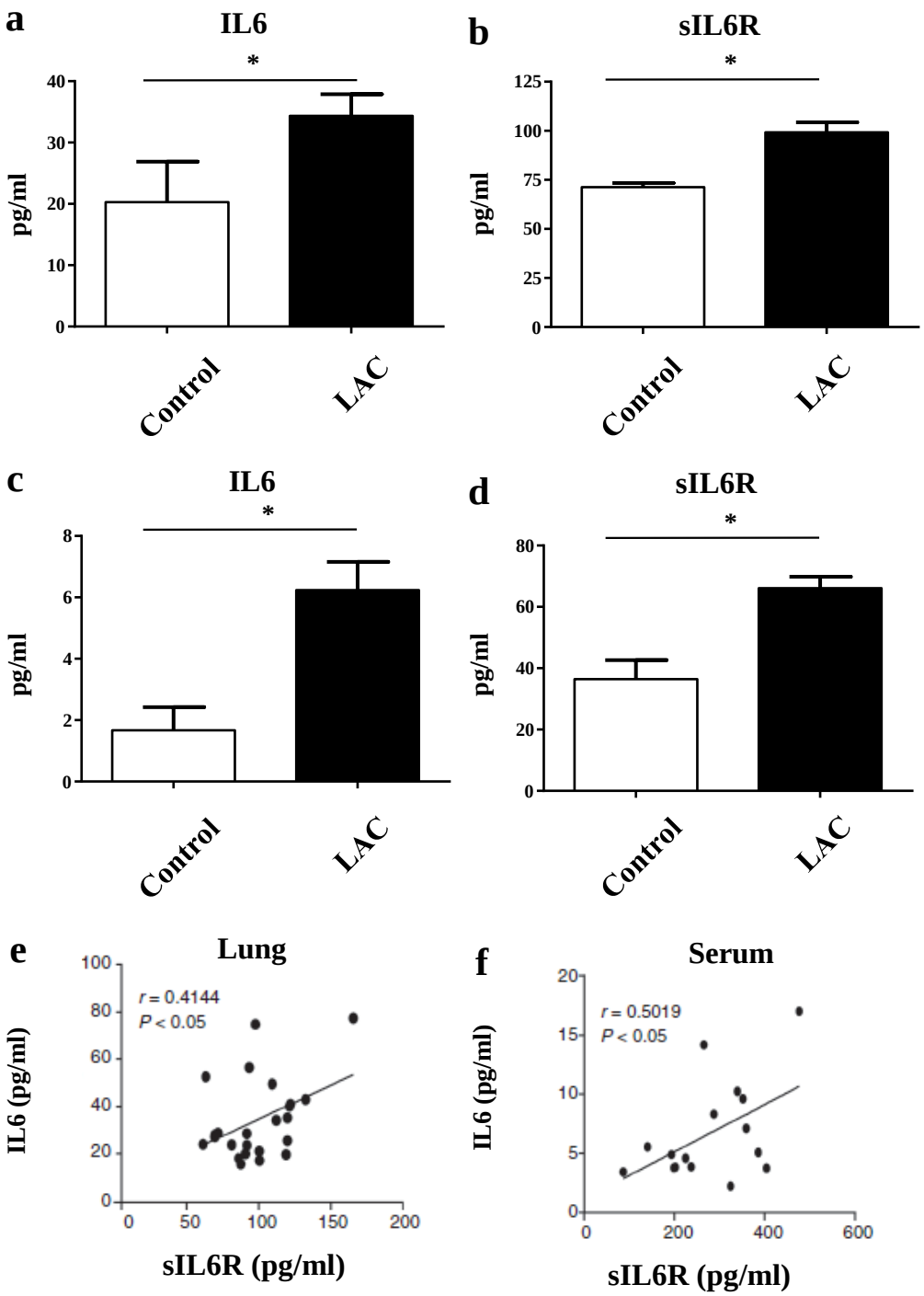

Figure 6.7. Augmented protein levels of IL-6 trans signalling components in human LAC tissue

IL-6 and sIL-6R protein levels on (a) lung lysates and (b) Serum from LAC patients (n=24) and control (n=5) groups. Relative expression data expressed as mean +/- s.e.m and normalised for *18S* expression are shown. * p<0.05. (reprinted from data collected by Saleela Ruwanpura[66])

production of the sIL-6, thus strongly supporting the concept that IL-6 trans signalling is playing an important role in the pathogenesis of lung cancer.

6.5 Discussion

In this chapter, I showed using both human lung cancer cell lines as well as tissue and serum from LAC patients to report that augmented mRNA levels for *SOCS3* and *IL-6* in patients with LAC, but not other IL-6 family cytokines. Not surprisingly these data also led to the transcription and production of IL-6 trans signalling co-factors, IL-6 and sIL-6R, both systemically throughout the patient and locally within the lungs suggesting that there is a strong role for IL-6 trans signalling in the progression of LAC. I also showed that there is a role for IL-6 in the augmentation IL-6/gp130 target genes in human lung adenocarcinoma cell lines.

In vitro work from other laboratories show that IL-6 secretion varies between NSCLC cell lines, suggesting that the growth of human NSCLC cells is likely to be governed by both IL-6 dependent and independent mechanisms[223]. In that regards our laboratory has shown that specific blockade of IL-6 trans signalling upon treatment of these cell lines with sgp130Fc[114,132], which also acts on human cells, would negate growth in cell culture. They show basal levels of IL-6 and sIL-6R in NCI-H23 and A549 human lung cancer cell lines are readily detectable in the culture supernatant, and MMT cell viability assays[66] revealed that sgp130Fc significantly suppressed the growth of both A549 and NCI-H23 cell lines. The role for IL-6 trans signalling in human LAC is currently being researched with vigour as recently our laboratory showed that protein expression on IL-6 and the sIL-6R is observed in human LAC patients[66]. In addition, variable expression of pSTAT3is seen at baseline in NSCLC cell lines[65,256], and clinical data shows constitutive activation of STAT3 in approximately 50% of

NSCLC[195,257]. Bihl et al. found that serum starvation of A549 cells for 24 hours lead to a significant reduction in IL-6 production, consistent with the observed reduction in pSTAT3 with prolonged serum starvation (Figure 4.2) but others have found the converse[65,223]. This difference is not explained by cell type or culture conditions, as both publications included A549 cells, showing different results, and all cells were grown in RPMI-1640 media. The only difference was the percentage of FCS/FBS used, but this would not explain such divergent changes when this serum was taken away. Notable however, it has been found that patients with emphysema were characterised with excessive production of sIL-6R by hyperactivation of the mTORC1 pathway[173], known to be down-stream of the IL-6/gp130 pathway[80]. Anti-IL-6 therapy as a whole has been shown to reduce inflammation, hepatic acute phase proteins, and anaemia[258] and is effective at treating RA[158]. A number of anti-IL-6 therapeutics are currently clinically registered including, siltuximab, an anti-IL-6 mAb, and tocilizumab, an anti-IL-6R mAb and as such are safe and useful in inflammatory disease treatment.

These data show, that there is a strong association with the development of LAC and an increase in the production of IL-6 trans signalling factors both localised within the lungs and systemically throughout the body. Importantly these data correlated closely with findings from our animal models both the LAC phenotypic *gp130*$^{F/F}$:*Kras*^{G12D} mice and those mice receiving IL-6 trans signalling inhibitors.

Chapter 7
Discussion

7.1 Discussion

My project aimed to determine the specific signalling pathway associated with the development of lung cancer using a sophisticated animal model displaying deregulated gp130 signalling. Here, I utilised our *gp130*$^{F/F}$ mouse model for pulmonary inflammation and associated upregulated IL-6 production, leading to exaggerated activation of gp130/STAT3. I have generated *gp130*$^{F/F}$ mice onto the well-defined *Kras*^{G12D} LAC model to examine the role of gp130 signalling in lung cancer. Finally, I also reported human LAC cell lines and human biopsies to validate findings on the mouse model in clinical setting and to examine the activation of key oncogenic signalling pathways. The main findings of the project are as follows:

1. Deregulated gp130 signalling leads to augmented cellular proliferation to exacerbate adenocarcinoma *in situ* in the lungs of *gp130*$^{F/F}$:*Kras*^{G12D} mice.
2. Increased IL-6 production via IL-6 trans signalling mode exacerbates lung carcinogenesis in *gp130*$^{F/F}$:*Kras*^{G12D} mice.
3. Augmented IL-6/gp130/Stat3 activation is associated with exacerbated lung carcinogenesis in *gp130*$^{F/F}$:*Kras*^{G12D} mice.
4. IL-6 trans signalling components are upregulated in human lung adenocarcinoma.

Lung cancer is the most leading cause of death worldwide which in Australia alone accounts for more than 7000 deaths annually [2]. Cigarette smoking plays a causal role in 80-90% of

LAC, the most common form of lung cancer, and represents the major cause of lung inflammation associated with LAC[13,259]. One of the most established disease-associated consequences of the genotoxic effects of cigarette-derived carcinogens is activating mutations in the *Kras* proto-oncogene[4,5]. LAC is often diagnosed at an advanced stage with treatment options mainly restricted to surgery, chemotherapy and/or radiation therapy. However, current treatment strategies are associated with a high risk of tumour re-occurrence and poor patient survival rates (5-year relative survival rate for lung cancer is ~15%)[1,3]. In the last 5 years, the identification of EGFR activating mutations in LAC patients, albeit a minority of cases mainly comprising never smoking women, has paved the way for effective targeted therapy with tyrosine kinase inhibitors[10]. By contrast, effective therapies for LAC with more typical mutation profiles, especially those associated with smoking, are yet to be identified, thus highlighting the need for a better understanding of the molecular and genetic alterations involved in the initiation and progression of LAC.

As I have described in Chapter 3, lung cancer pathogenesis is exacerbated in *gp130*$^{F/F}$:*Kras*^{G12D} mice, in the presence of deregulated gp130 cytokine signalling. To reiterate, the *gp130*$^{F/F}$ mouse provides a model of endogenous increased IL-6 and hyper-activated Stat3 signalling, in the absence of pathways downstream of SHP2, specifically PI3K/Akt and MAPK/ERK signalling. My laboratory has previously shown that the *gp130*$^{F/F}$ mouse model develops severe pulmonary inflammation[260], where gene expression of key inflammatory cytokines implicated in lung cancer, including TNF-α, IL-1β and IL-6, are all elevated in the *gp130*$^{F/F}$ mouse lung[200,259]. Similarly, gene expression of granulocyte-attracting chemokines CXCL-1 and -2, and T cell-attracting chemokines CCL-2 and -5 are elevated in the *gp130*$^{F/F}$ mouse lung, and have previously been associated with lung cancer[261,262]. This appeared to be mediated by IL-6 through Stat3 as evidenced by normalised expression levels of these genes in *gp130*$^{F/F}$:IL-6$^{-/-}$ and *gp130*$^{F/F}$:Stat3$^{-/+}$ mice. Other have shown that mouse models genetically

engineered to express the oncogenic *Kras*^{G12D} allele conditionally, somatically, or inducibly can develop AAH[57,62]. Importantly, the development of exacerbated *in situ* adenocarcinoma within 6 weeks of Cre-mediated infection in *gp130*$^{F/F}$:*Kras*^{G12D} mice shows a critical role for gp130 in lung adenocarcinoma development and progression. In *gp130*$^{F/F}$:*Kras*^{G12D} mice, I showed an enhanced degree of AAH in the lungs by 3 months of age (i.e. 6 week old mice exposed to experimentally-induced lung cancer over 6 weeks), and considering these mice develop lung inflammation, this suggests a strong correlation between those co-factors and the predisposition to lung cancer. I note that if the induction of lung cancer was from 3 months of age (when there would be well established lung inflammation) as opposed to 6 weeks of age, (prior to lung inflammation) perhaps the spread of AAH in the lung may be more pronounced or even, histopathologically, a more severe form of lung pathology (such as severe adenocarcinoma) might be observed. Of note is the severe and early onset of LAC at 6 weeks of age after treatment, in the initial *Kras*^{G12D} model [51] these mice were treated with Cre-recombinase for 12 weeks. As augmented IL-6 trans signalling in these mice let to severe tumour burden we were required to end the experiments at 6 weeks after treatment. While the interactions of gp130 signalling have been widely studied here, in the context of lung carcinogenesis, we have utilised the *gp130*$^{F/F}$ model as the advantage of this over other previously established mouse models is the endogenously deregulated gp130 activation. In this respect, this model enables clear attribution of any actions of hyper-activated gp130-regulated signalling pathways.

Perhaps one of the most novel findings of this thesis (as described in Chapter 4 and 6), was that increased IL-6 production via IL-6 “trans signalling” exacerbates lung carcinogenesis in *gp130*$^{F/F}$:*Kras*^{G12D} mice. This was also validated for human LAC. The IL-6 cytokine is a diverse and complex protein, being both a pro- and anti-inflammatory, it has been linked to an extraordinary assortment of molecular functions including, protection from

infection, proliferation, apoptosis and promotion of inflammation-associate diseases[132,224] and cancers[148,150]. Notably, the role for IL-6 in the pathogenesis of LAC has been suggested by both clinical data (Chapter 6) demonstrating that IL-6 levels are augmented in human LAC patients[145,154,221], as well as an oncogenic *Kras*^{G12D}-driven mouse LAC model whereby genetic ablation of IL-6 alleviates lung tumorigenesis (Chapter 4). The involvement of other members of the IL-6 cytokine family in Kras-driven lung carcinogenesis, as well as the mode of signalling by which IL-6 promotes LAC, remains unknown. Although, IL-6 trans signalling is implicated in a number of other diseases including RA[111], colon cancer[263], and pulmonary emphysema[173], the link between lung cancer and IL-6 trans signalling is yet unidentified. Here, I also revealed for the first time that among IL-6 family cytokines, IL-6 was only involved in the development of LAC in our mouse model. In addition, I demonstrated first time that IL-6 trans-signalling receptor subunit, sIL-6R was associated with exacerbated LAC in *Kras*^{G12D}-driven lung carcinogenesis in mice. We showed that despite the comparable high levels of naturally occurring sgp130 in the lungs of both *Kras*^{G12D} and *gp130*$^{F/F}$:*Kras*^{G12D} mice, the 2-fold increase in sIL-6R levels in *gp130*$^{F/F}$:*Kras*^{G12D} mouse lungs, without any increase in sgp130 levels, means that endogenous sgp130 levels are insufficient to block pathologic trans-signalling[235]. This is in contrast with the administration of sgp130Fc, which is approximately 10 to 100 times more effective than sgp130 alone at blocking IL-6 trans-signalling[142]. Amelioration of LAC in *gp130*$^{F/F}$:*Kras*^{G12D} mice by transgenic overexpression of sgp130Fc is of clinical significance as sgp130Fc has successfully passed phase I clinical trials in Europe in patients with inflammatory bowel disease[149]. Recently my laboratory has demonstrated that the sgp130Fc-mediated blockade of IL-6 trans signalling suppressed the growth of human LAC cell lines[66], by suggesting this inhibitor can have therapeutic benefits for LAC.

My data also demonstrated that two anti-IL-6R monoclonal antibodies (mAb)s, which act in the mouse to target trans-signalling, can reduce the severity of *Kras*^{G12D}-induced LAC, indicating that humanized variants of such mAbs could provide a rational therapeutic approach for human lung adenocarcinoma patients displaying augmented IL-6 and sIL-6R levels. Recently, siltuximab, a chimeric mouse/human mAb, has shown promise in inhibiting the growth of tumours in preclinical LAC cell line xenograft models[64] and trials using a humanized neutralizing mAb against IL-6, ALD-518, which like siltuximab targets systemic IL-6 signalling, has shown promise in ameliorating cachexia associated with advanced metaStatic non–small cell lung cancer, although the antitumor effects of such therapy were not reported[165]. Although the efficacy of using systemic anti-IL-6 mAbs to suppress tumour growth in LAC remains unknown, the inherent issue involves targeting "immune-protective" IL-6 classical signalling. My data presented here showing that two anti-IL-6R mAbs, which act in the mouse to target trans-signalling, can reduce the severity of KrasG12D-induced lung adenocarcinoma, indicating that humanized variants of such mAbs could provide a rational therapeutic approach for subset human lung adenocarcinoma patients.

We have previously demonstrated that genetic ablation of IL-6 in the lungs of gp130$^{F/F}$ mice normalizes the activation levels of Stat3[217], whose hyper-activation is a common feature of human lung adenocarcinoma[145,233]. It has also been shown that the IL-6/gp130/Stat3 signalling pathway is associated with pulmonary inflammation and LAC in mice[42,63,90], so to examine whether Stat3 hyperactivation in gp130$^{F/F}$ mice exacerbated *Kras*^{G12D}–induced LAC, we crossed gp130$^{F/F}$:*Stat3*$^{-/+}$ mice, displaying normalised pulmonary Stat3 activation[146], with *Kras*^{G12D} mice. Our data here suggest that enhanced activation of Stat3 (via IL-6 trans signalling, and as occurs in *gp130*$^{F/F}$ mice) can augment the oncogenic potency of the activating *Kras*^{G12D} mutant. The combined observations that tyrosine-phosphorylated (i.e., activated) Stat3 resides primarily in the respiratory epithelium (where

the oncogenic *Kras*^{G12D} mutant is expressed from its endogenous promoter) of *gp130*$^{F/F}$:*Kras*^{G12D} mouse lungs, and the exacerbated lung adenocarcinoma phenotype in *gp130*$^{F/F}$:*Kras*^{G12D} mice is not associated with any further increase in leukocyte infiltrates, support the notion that gp130$^{(Y757F)}$-dependent oncogenic cellular responses in the lung are driven by the epithelium, as our lab has reported previously for the epithelium of other tissues from *gp130*$^{F/F}$ mice, such as the stomach[244]. I also note that our current findings are consistent with the previous report that IL-6 trans signalling and Stat3 are required for tumorigenesis in a *Kras*^{G12D}-induced pancreatic adenocarcinoma mouse model[139]. Furthermore, autocrine IL-6/Stat3 signalling can promote the Kras-dependent cell survival and proliferation in vitro of human LAC cell lines, although the specific role of IL-6 trans signalling was not addressed[245]. In addition, IL-6 has been shown to be required for Ras-driven tumorigenesis in multiple cell types; however, its role in LAC was not investigated [264]. Although collectively these observations imply that Stat3 via IL-6 trans signalling can augment the oncogenic potential of mutant Kras in LAC, recently it was reported that the lung epithelial-specific inactivation of Stat3 exacerbates *Kras*^{G12D}-driven lung adenocarcinoma[208]. The tumour-suppressive activity of Stat3 was assigned to its ability to sequester cytoplasmic NF-kB and inhibit NF-kB–induced transcription of the proangiogenic chemokine Cxcl1, thus suppressing tumour vascularization and growth. While the cytokines responsible for upstream Stat3-activating were also not identified, these findings are similar to previous studies using Stat3 conditional ablation in mice[133]. As IL-6 trans signalling also activates Stat3 heterodimers with Stat1[133] modulating a different network of gene targets it is not surprising that Cxcl1 gene expression was unchanged in the lungs of *gp130*$^{F/F}$:*Kras*^{G12D} mice displaying exacerbated LAC as Stat3 modulates by other cytokines, such as IL-10, which activates Stat3 homodimers.

As lung cancer is the number one cause of cancer related deaths per year[265], there is a real need to fully elucidate the role of IL-6 signalling in adaptive and innate immunity and the link to inflammatory disorders and cancer of the lung. More specifically there is an urgent need to determine the role of IL-6 trans signalling associated with deregulated IL-6/gp130/Stat3 cytokine signalling in the pathogenesis of lung cancer. In summary, I provide for the first time strong evidence that IL-6 trans signalling is a major contributor to the pathogenesis of LAC and that this is a targetable signalling pathway for therapeutics in human LAC. Furthermore, this thesis provides rational for a number of anti-IL-6R mAbs, which act on IL-6 trans signalling, to be further studied for development of a therapeutic approach for human lung cancer patients displaying augmented IL-6 levels.

In conclusion, mouse model data revealing that specific targeting of IL-6 trans signalling suppresses LAC pathogenesis, together with clinical data showing positive correlations between elevated sIL-6R and IL-6 levels in tumours and sera of LAC patients, have translational potential for biomarker discovery and early disease detection, as well as patient stratification for potential responders that may benefit from selective anti-IL-6 trans-signalling therapies. Based on our findings, it will now be of interest to examine whether IL-6 trans signalling contributes to the pathogenesis of Kras-independent lung cancer subtypes in which IL-6 has been implicated.

References

1. Jemal, A.*, et al.* Global cancer statistics. *CA: a cancer journal for clinicians* **61**, 69-90 (2011).
2. Welfare, A.I.o.H.a. Australia's Health. (2012).
3. AIHW. Australia's Health 2014. in *Australia's Health series*, Vol. 14 (2014).
4. Warren, C.W., Jones, N.R., Eriksen, M.P., Asma, S. & Global Tobacco Surveillance System collaborative, g. Patterns of global tobacco use in young people and implications for future chronic disease burden in adults. *Lancet* **367**, 749-753 (2006).
5. WHO. The world health report 1999: making a difference. *Report* (1999).
6. Travis, W.D., World Health Organization., International Agency for Research on Cancer., International Association for the Study of Lung Cancer. & International Academy of Pathology. *Pathology and genetics of tumours of the lung, pleura, thymus and heart*, (IARC Press

Oxford University Press (distributor), Lyon

Oxford, 2004).
7. Hickinson, D.M.*, et al.* AZD8931, an equipotent, reversible inhibitor of signaling by epidermal growth factor receptor, ERBB2 (HER2), and ERBB3: a unique agent for simultaneous ERBB receptor blockade in cancer. *Clin Cancer Res* **16**, 1159-1169 (2010).
8. Brandao, G.D., Brega, E.F. & Spatz, A. The role of molecular pathology in non-small-cell lung carcinoma-now and in the future. *Curr Oncol* **19**, S24-32 (2012).
9. A genomics-based classification of human lung tumors. *Science translational medicine* **5**, 209ra153 (2013).
10. Flanders, W.D., Lally, C.A., Zhu, B.P., Henley, S.J. & Thun, M.J. Lung cancer mortality in relation to age, duration of smoking, and daily cigarette consumption: results from Cancer Prevention Study II. *Cancer Res* **63**, 6556-6562 (2003).
11. Doll, R. & Peto, R. Cigarette smoking and bronchial carcinoma: dose and time relationships among regular smokers and lifelong non-smokers. *Journal of epidemiology and community health* **32**, 303-313 (1978).
12. Ahrendt, S.A.*, et al.* Cigarette smoking is strongly associated with mutation of the K-ras gene in patients with primary adenocarcinoma of the lung. *Cancer* **92**, 1525-1530 (2001).
13. Walser, T.*, et al.* Smoking and lung cancer: the role of inflammation. *Proc Am Thorac Soc* **5**, 811-815 (2008).
14. Sasco, A.J., Secretan, M.B. & Straif, K. Tobacco smoking and cancer: a brief review of recent epidemiological evidence. *Lung cancer* **45 Suppl 2**, S3-9 (2004).
15. Youlden, D.R., Cramb, S.M. & Baade, P.D. The International Epidemiology of Lung Cancer: geographical distribution and secular trends. *Journal of thoracic oncology : official publication of the International Association for the Study of Lung Cancer* **3**, 819-831 (2008).
16. Proctor, R.N. Tobacco and the global lung cancer epidemic. *Nature reviews. Cancer* **1**, 82-86 (2001).
17. Hecht, S.S. Lung carcinogenesis by tobacco smoke. *International journal of cancer* **131**, 2724-2732 (2012).
18. Hecht, S.S. Biochemistry, biology, and carcinogenicity of tobacco-specific N-nitrosamines. *Chem Res Toxicol* **11**, 559-603 (1998).
19. Wiener, D., Doerge, D.R., Fang, J.L., Upadhyaya, P. & Lazarus, P. Characterization of N-glucuronidation of the lung carcinogen 4-(methylnitrosamino)-1-(3-pyridyl)-1-butanol (NNAL) in human liver: importance of UDP-glucuronosyltransferase 1A4. *Drug Metab Dispos* **32**, 72-79 (2004).
20. Akopyan, G. & Bonavida, B. Understanding tobacco smoke carcinogen NNK and lung tumorigenesis. *Int J Oncol* **29**, 745-752 (2006).

21. Miller, A., Brooks, G.D., McLeod, L., Ruwanpura, S. & Jenkins, B.J. Differential involvement of gp130 signalling pathways in modulating tobacco carcinogen-induced lung tumourigenesis. *Oncogene* **34**, 1510-1519 (2015).
22. Wakamatsu, N., Devereux, TR, Hong, HH, Sills, RC. Overview of the molecular carcinogenesis of mouse lung tumor models of human lung cancer. *Toxicol Pathol.* **35**, 75-80. (2007).
23. Wiener, D., Doerge, DR, Fang, JL, Upadhyaya, P, Lazarus, P. Characterization of N-glucuronidation of the lung carcinogen 4-(methylnitrosamino)-1-(3-pyridyl)-1-butanol (NNAL) in human liver: importance of UDP-glucuronosyltransferase 1A4. *Drug Metab Dispos* **32**, 72-79 (2004).
24. Akopyan G, B.B. Understanding tobacco smoke carcinogen NNK and lung tumorigenesis. *Int J Oncol.* **29**, 745-752. (2006).
25. Cloutier, J., Drouin, R, Weinfeld, M, O'Connor, TR, Castonguay, A. Characterization and mapping of DNA damage induced by reactive metabolites of 4-(methylnitrosamino)-1-(3-pyridyl)-1-butanone (NNK) at nucleotide resolution in human genomic DNA. *J Mol Biol.* **313**, 539-557 (2001).
26. Ho, Y., et al. Tobacco-specific carcinogen 4-(methylnitrosamino)-1-(3-pyridyl)-1-butanone (NNK) induces cell proliferation in normal human bronchial epithelial cells through NFkappaB activation and cyclin D1 up-regulation. *Toxicol Appl Pharmacol.* **205**, 133-148 (2005).
27. Churg, A.*, et al.* Expression of profibrotic mediators in small airways versus parenchyma after cigarette smoke exposure. *Am J Respir Cell Mol Biol* **40**, 268-276 (2009).
28. Bhalla, S.*, et al.* PCI-24781 induces caspase and reactive oxygen species-dependent apoptosis through NF-kappaB mechanisms and is synergistic with bortezomib in lymphoma cells. *Clin Cancer Res* **15**, 3354-3365 (2009).
29. Adcock, I.M., Caramori, G. & Barnes, P.J. Chronic obstructive pulmonary disease and lung cancer: new molecular insights. *Respiration* **81**, 265-284 (2011).
30. Medzhitov, R. Origin and physiological roles of inflammation. *Nature* **454**, 428-435 (2008).
31. Maeda, H. & Akaike, T. Nitric oxide and oxygen radicals in infection, inflammation, and cancer. *Biochemistry. Biokhimiia* **63**, 854-865 (1998).
32. Cook, T.*, et al.* Nitric oxide and ionizing radiation synergistically promote apoptosis and growth inhibition of cancer by activating p53. *Cancer Res* **64**, 8015-8021 (2004).
33. Esme, H.*, et al.* High levels of oxidative stress in patients with advanced lung cancer. *Respirology* **13**, 112-116 (2008).
34. Härting, F.H. & Hesse, W. Lung cancer, the disease of miners in the Schneberg mines. *Vjschr. gericht. Med. off. Sank.* **1**, 296-309 (1879).
35. Greenberg, M. & Selikoff, I.J. Lung cancer in the Schneeberg mines: a reappraisal of the data reported by Harting and Hesse in 1879. *The Annals of occupational hygiene* **37**, 5-14 (1993).
36. Choi, H. & Mazzone, P. Radon and lung cancer: assessing and mitigating the risk. *Cleveland Clinic journal of medicine* **81**, 567-575 (2014).
37. Narayanan, P.K., Goodwin, E.H. & Lehnert, B.E. Alpha particles initiate biological production of superoxide anions and hydrogen peroxide in human cells. *Cancer Res* **57**, 3963-3971 (1997).
38. O'Reilly, K.M., McLaughlin, A.M., Beckett, W.S. & Sime, P.J. Asbestos-related lung disease. *American family physician* **75**, 683-688 (2007).
39. Husgafvel-Pursiainen, K.*, et al.* Lung cancer and past occupational exposure to asbestos. Role of p53 and K-ras mutations. *Am J Respir Cell Mol Biol* **20**, 667-674 (1999).
40. Jaurand, M.C. Mechanisms of fiber-induced genotoxicity. *Environmental health perspectives* **105 Suppl 5**, 1073-1084 (1997).
41. Liddell, F.D. The interaction of asbestos and smoking in lung cancer. *The Annals of occupational hygiene* **45**, 341-356 (2001).

42. Tran, P.T.*, et al.* Combined Inactivation of MYC and K-Ras oncogenes reverses tumorigenesis in lung adenocarcinomas and lymphomas. *PloS one* **3**, e2125 (2008).
43. Le Calvez, F.*, et al.* TP53 and KRAS mutation load and types in lung cancers in relation to tobacco smoke: distinct patterns in never, former, and current smokers. *Cancer Res* **65**, 5076-5083 (2005).
44. Sanchez-Cespedes, M.*, et al.* Inactivation of LKB1/STK11 is a common event in adenocarcinomas of the lung. *Cancer Res* **62**, 3659-3662 (2002).
45. Keedy, V.L.*, et al.* American Society of Clinical Oncology provisional clinical opinion: epidermal growth factor receptor (EGFR) Mutation testing for patients with advanced non-small-cell lung cancer considering first-line EGFR tyrosine kinase inhibitor therapy. *Journal of clinical oncology : official journal of the American Society of Clinical Oncology* **29**, 2121-2127 (2011).
46. Yang, Y.*, et al.* Phosphatidylinositol 3-kinase mediates bronchioalveolar stem cell expansion in mouse models of oncogenic K-ras-induced lung cancer. *PloS one* **3**, e2220 (2008).
47. Gabrielson, E. Worldwide trends in lung cancer pathology. *Respirology.* **11**, 533-538 (2006).
48. Spira, A., Beane, J, Shah, V, Liu, G, Schembri, F, Yang, X, Palma, J, Brody, JS. Effects of cigarette smoke on the human airway epithelial cell transcriptome. *Proc Natl Acad Sci U S A.* **101**, 10143-10148. (2004).
49. Spira, A., Beane, JE, Shah, V, Steiling, K, Liu, G, Schembri, F, Gilman, S, Dumas, YM, Calner, P, Sebastiani, P, Sridhar, S, Beamis, J, Lamb, C, Anderson, T, Gerry, N, Keane, J, Lenburg, ME, Brody, JS. Airway epithelial gene expression in the diagnostic evaluation of smokers with suspect lung cancer. *Nat Med.* **13**, 361-366 (2007).
50. Imielinski, M.*, et al.* Mapping the hallmarks of lung adenocarcinoma with massively parallel sequencing. *Cell* **150**, 1107-1120 (2012).
51. Jackson, E.L.*, et al.* Analysis of lung tumor initiation and progression using conditional expression of oncogenic K-ras. *Genes Dev* **15**, 3243-3248 (2001).
52. Brose, M.S.*, et al.* BRAF and RAS mutations in human lung cancer and melanoma. *Cancer Res* **62**, 6997-7000 (2002).
53. Lantuejoul, S., Salameire, D., Salon, C. & Brambilla, E. Pulmonary preneoplasia--sequential molecular carcinogenetic events. *Histopathology* **54**, 43-54 (2009).
54. Ji, B.T.*, et al.* Tobacco smoking and colorectal hyperplastic and adenomatous polyps. *Cancer Epidemiol Biomarkers Prev* **15**, 897-901 (2006).
55. Moghaddam, S.J.*, et al.* Promotion of lung carcinogenesis by chronic obstructive pulmonary disease-like airway inflammation in a K-ras-induced mouse model. *Am J Respir Cell Mol Biol* **40**, 443-453 (2009).
56. Johnson, L.*, et al.* Somatic activation of the K-ras oncogene causes early onset lung cancer in mice. *Nature* **410**, 1111-1116 (2001).
57. Ji, H.*, et al.* K-ras activation generates an inflammatory response in lung tumors. *Oncogene* **25**, 2105-2112 (2006).
58. Wislez, M.*, et al.* High expression of ligands for chemokine receptor CXCR2 in alveolar epithelial neoplasia induced by oncogenic kras. *Cancer Res* **66**, 4198-4207 (2006).
59. Rodenhuis, S. & Slebos, R.J. The ras oncogenes in human lung cancer. *The American review of respiratory disease* **142**, S27-30 (1990).
60. Tong, L.A.*, et al.* Structural differences between a ras oncogene protein and the normal protein. *Nature* **337**, 90-93 (1989).
61. Wakamatsu, N., Devereux, T.R., Hong, H.H. & Sills, R.C. Overview of the molecular carcinogenesis of mouse lung tumor models of human lung cancer. *Toxicologic pathology* **35**, 75-80 (2007).
62. DuPage, M., Dooley, A.L. & Jacks, T. Conditional mouse lung cancer models using adenoviral or lentiviral delivery of Cre recombinase. *Nat Protoc* **4**, 1064-1072 (2009).

63. Gough, D.J*., et al.* Mitochondrial STAT3 supports Ras-dependent oncogenic transformation. *Science* **324**, 1713-1716 (2009).
64. Song, L., Rawal, B., Nemeth, J.A. & Haura, E.B. JAK1 activates STAT3 activity in non-small-cell lung cancer cells and IL-6 neutralizing antibodies can suppress JAK1-STAT3 signaling. *Mol Cancer Ther* **10**, 481-494 (2011).
65. Looyenga, B.D*., et al.* STAT3 is activated by JAK2 independent of key oncogenic driver mutations in non-small cell lung carcinoma. *PloS one* **7**, e30820 (2012).
66. Brooks, G.D*., et al.* IL6 Trans-signaling Promotes KRAS-Driven Lung Carcinogenesis. *Cancer Res* **76**, 866-876 (2016).
67. Linggi, B. & Carpenter, G. ErbB receptors: new insights on mechanisms and biology. *Trends in cell biology* **16**, 649-656 (2006).
68. Cohen, S. The epidermal growth factor (EGF). *Cancer* **51**, 1787-1791 (1983).
69. Herbst, R.S. Review of epidermal growth factor receptor biology. *International journal of radiation oncology, biology, physics* **59**, 21-26 (2004).
70. Akca, H., Tani, M., Hishida, T., Matsumoto, S. & Yokota, J. Activation of the AKT and STAT3 pathways and prolonged survival by a mutant EGFR in human lung cancer cells. *Lung cancer* **54**, 25-33 (2006).
71. Sasaki, T., Hiroki, K. & Yamashita, Y. The role of epidermal growth factor receptor in cancer metastasis and microenvironment. *BioMed research international* **2013**, 546318 (2013).
72. Sattler, M., Abidoye, O. & Salgia, R. EGFR-targeted therapeutics: focus on SCCHN and NSCLC. *TheScientificWorldJournal* **8**, 909-919 (2008).
73. Engelman, J.A. & Janne, P.A. Mechanisms of acquired resistance to epidermal growth factor receptor tyrosine kinase inhibitors in non-small cell lung cancer. *Clin Cancer Res* **14**, 2895-2899 (2008).
74. Paez, J.G*., et al.* EGFR mutations in lung cancer: correlation with clinical response to gefitinib therapy. *Science* **304**, 1497-1500 (2004).
75. Marchetti, A*., et al.* EGFR mutations in non-small-cell lung cancer: analysis of a large series of cases and development of a rapid and sensitive method for diagnostic screening with potential implications on pharmacologic treatment. *Journal of clinical oncology : official journal of the American Society of Clinical Oncology* **23**, 857-865 (2005).
76. Lynch, C.C., Crawford, H.C., Matrisian, L.M. & McDonnell, S. Epidermal growth factor upregulates matrix metalloproteinase-7 expression through activation of PEA3 transcription factors. *Int J Oncol* **24**, 1565-1572 (2004).
77. Gerber, D.E. EGFR Inhibition in the Treatment of Non-Small Cell Lung Cancer. *Drug development research* **69**, 359-372 (2008).
78. Maemondo, M*., et al.* Gefitinib or chemotherapy for non-small-cell lung cancer with mutated EGFR. *N Engl J Med* **362**, 2380-2388 (2010).
79. Wang, S., Tsui, S.T., Liu, C., Song, Y. & Liu, D. EGFR C797S mutation mediates resistance to third-generation inhibitors in T790M-positive non-small cell lung cancer. *Journal of hematology & oncology* **9**, 59 (2016).
80. Thiem, S*., et al.* mTORC1 inhibition restricts inflammation-associated gastrointestinal tumorigenesis in mice. *J Clin Invest* **123**, 767-781 (2013).
81. Engelman, J.A*., et al.* Effective use of PI3K and MEK inhibitors to treat mutant Kras G12D and PIK3CA H1047R murine lung cancers. *Nat Med* **14**, 1351-1356 (2008).
82. Yamamoto, H*., et al.* PIK3CA mutations and copy number gains in human lung cancers. *Cancer Res* **68**, 6913-6921 (2008).
83. Scheffler, M*., et al.* PIK3CA mutations in non-small cell lung cancer (NSCLC): genetic heterogeneity, prognostic impact and incidence of prior malignancies. *Oncotarget* **6**, 1315-1326 (2015).
84. Surget, S., Khoury, M.P. & Bourdon, J.C. Uncovering the role of p53 splice variants in human malignancy: a clinical perspective. *OncoTargets and therapy* **7**, 57-68 (2013).

85. Meylan, E.*, et al.* Requirement for NF-kappaB signalling in a mouse model of lung adenocarcinoma. *Nature* **462**, 104-107 (2009).
86. Xue, W.*, et al.* Response and resistance to NF-kappaB inhibitors in mouse models of lung adenocarcinoma. *Cancer discovery* **1**, 236-247 (2011).
87. Cellurale, C.*, et al.* Requirement of c-Jun NH(2)-terminal kinase for Ras-initiated tumor formation. *Mol Cell Biol* **31**, 1565-1576 (2011).
88. Levy, D.E. & Lee, C.K. What does Stat3 do? *J Clin Invest* **109**, 1143-1148 (2002).
89. Bromberg, J.F.*, et al.* Stat3 as an oncogene. *Cell* **98**, 295-303 (1999).
90. Gao, H. & Ward, P.A. STAT3 and suppressor of cytokine signaling 3: potential targets in lung inflammatory responses. *Expert Opin Ther Targets* **11**, 869-880 (2007).
91. Hirano, T., Ishihara, K. & Hibi, M. Roles of STAT3 in mediating the cell growth, differentiation and survival signals relayed through the IL-6 family of cytokine receptors. *Oncogene* **19**, 2548-2556 (2000).
92. Alvarez, J.V., Greulich, H., Sellers, W.R., Meyerson, M. & Frank, D.A. Signal transducer and activator of transcription 3 is required for the oncogenic effects of non-small-cell lung cancer-associated mutations of the epidermal growth factor receptor. *Cancer Res* **66**, 3162-3168 (2006).
93. Hanahan, D. & Weinberg, R.A. The hallmarks of cancer. *Cell* **100**, 57-70 (2000).
94. Yeh, H., Lai, WW, Chen, HH, Liu, HS, Su, WC. Autocrine IL-6-induced Stat3 activation contributes to the pathogenesis of lung adenocarcinoma and malignant pleural effusion. *Oncogene.* **25**, 4300-4309 (2006).
95. Kren, L., Brazdil, J, Hermanova, M, Goncharuk, VN, Kallakury, BV, Kaur, P, Ross, JS. Prognostic significance of anti-apoptosis proteins survivin and bcl-2 in non-small cell lung carcinomas: a clinicopathologic study of 102 cases. *Appl Immunohistochem Mol Morphol.* **12**, 44-49 (2004).
96. Ratschiller, D., Heighway, J, Gugger, M, Kappeler, A, Pirnia, F, Schmid, RA, Borner, MM, Betticher, DC. Cyclin D1 overexpression in bronchial epithelia of patients with lung cancer is associated with smoking and predicts survival. *J Clin Oncol.* **21**, 2085-2093 (2003).
97. Broers, J., Viallet, J, Jensen, SM, Pass, H, Travis, WD, Minna, JD, Linnoila, RI. Expression of c-myc in progenitor cells of the bronchopulmonary epithelium and in a large number of non-small cell lung cancers. *Am J Respir Cell Mol Biol.* **9**, 33-43 (1993).
98. Gao, J., McConnell, MJ, Yu, B, Li, J, Balko, JM, Black, EP, Johnson, JO, Lloyd, MC, Altiok, S, Haura, EB. MUC1 is a downstream target of STAT3 and regulates lung cancer cell survival and invasion. *Int J Oncol.* **35**, 337-345. (2009).
99. Song, L., Turkson, J, Karras, JG, Jove, R, Haura, EB. Activation of Stat3 by receptor tyrosine kinases and cytokines regulates survival in human non-small cell carcinoma cells. *Oncogene.* **22**, 4150-4165. (2003).
100. Pao, W.*, et al.* EGF receptor gene mutations are common in lung cancers from "never smokers" and are associated with sensitivity of tumors to gefitinib and erlotinib. *Proc Natl Acad Sci U S A* **101**, 13306-13311 (2004).
101. Qu, P., Roberts, J, Li, Y, Albrecht, M, Cummings, OW, Eble, JN, Du, H, Yan, C. Stat3 downstream genes serve as biomarkers in human lung carcinomas and chronic obstructive pulmonary disease. *Lung Cancer.* **63**, 341-347 (2009).
102. Li, Y., Du, H, Qin, Y, Roberts, J, Cummings, OW, Yan, C. Activation of the signal transducers and activators of the transcription 3 pathway in alveolar epithelial cells induces inflammation and adenocarcinomas in mouse lung. *Cancer Res.* **67**, 8494-8503 (2007).
103. Ogata H, K.T., Chinen T, Takaki H, Sanada T, Minoda Y, Koga K, Takaesu G, Maehara Y, Iida M, Yoshimura A. . Deletion of the SOCS3 gene in liver parenchymal cells promotes hepatitis-induced hepatocarcinogenesis. *Gastroenterology.* **131**, 179-193. (2006).

104. Kawada M, S.H., Uenoyama Y, Sawabu T, Kanda N, Fukui H, Shimahara Y, Chiba T. . Signal transducers and activators of transcription 3 activation is involved in nuclear accumulation of beta-catenin in colorectal cancer. *Cancer Res.* **66**, 2913-2917. (2006).
105. Kanda, N., Seno, H*., et al.* STAT3 is constitutively activated and supports cell survival in association with survivin expression in gastric cancer cells. *Oncogene.* **23**, 4921-4929 (2004).
106. Qu, P.*, et al.* Stat3 downstream genes serve as biomarkers in human lung carcinomas and chronic obstructive pulmonary disease. *Lung cancer* **63**, 341-347 (2009).
107. Ernst, M. & Jenkins, B.J. Acquiring signalling specificity from the cytokine receptor gp130. *Trends Genet* **20**, 23-32 (2004).
108. Gortz, D*., et al.* Anti-interleukin-6 therapy through application of a monogenic protein inhibitor via gene delivery. *Scientific reports* **5**, 14685 (2015).
109. Taga, T. & Kishimoto, T. Gp130 and the interleukin-6 family of cytokines. *Annu Rev Immunol* **15**, 797-819 (1997).
110. Kastelein, R.A., Hunter, C.A. & Cua, D.J. Discovery and biology of IL-23 and IL-27: related but functionally distinct regulators of inflammation. *Annu Rev Immunol* **25**, 221-242 (2007).
111. Rose-John, S. IL-6 trans-signaling via the soluble IL-6 receptor: importance for the pro-inflammatory activities of IL-6. *International journal of biological sciences* **8**, 1237-1247 (2012).
112. Heinrich, P.C., Behrmann, I., Muller-Newen, G., Schaper, F. & Graeve, L. Interleukin-6-type cytokine signalling through the gp130/Jak/STAT pathway. *The Biochemical journal* **334 (Pt 2)**, 297-314 (1998).
113. Peters, M., Muller, A.M. & Rose-John, S. Interleukin-6 and soluble interleukin-6 receptor: direct stimulation of gp130 and hematopoiesis. *Blood* **92**, 3495-3504 (1998).
114. Rose-John, S., Scheller, J., Elson, G. & Jones, S.A. Interleukin-6 biology is coordinated by membrane-bound and soluble receptors: role in inflammation and cancer. *Journal of leukocyte biology* **80**, 227-236 (2006).
115. Muller-Newen, G. The cytokine receptor gp130: faithfully promiscuous. *Science's STKE : signal transduction knowledge environment* **2003**, PE40 (2003).
116. Heinrich, P.C*., et al.* Principles of interleukin (IL)-6-type cytokine signalling and its regulation. *The Biochemical journal* **374**, 1-20 (2003).
117. Nicholson, S.E*., et al.* Suppressor of cytokine signaling-3 preferentially binds to the SHP-2-binding site on the shared cytokine receptor subunit gp130. *Proc Natl Acad Sci U S A* **97**, 6493-6498 (2000).
118. Cunnick, J.M*., et al.* Regulation of the mitogen-activated protein kinase signaling pathway by SHP2. *The Journal of biological chemistry* **277**, 9498-9504 (2002).
119. Tebbutt, N.C*., et al.* Reciprocal regulation of gastrointestinal homeostasis by SHP2 and STAT-mediated trefoil gene activation in gp130 mutant mice. *Nat Med* **8**, 1089-1097 (2002).
120. Scheller, J., Chalaris, A., Schmidt-Arras, D. & Rose-John, S. The pro- and anti-inflammatory properties of the cytokine interleukin-6. *Biochimica et biophysica acta* **1813**, 878-888 (2011).
121. Elner, V.M*., et al.* Interleukin-6 (IL-6) gene expression and secretion by cytokine-stimulated human retinal pigment epithelial cells. *Experimental eye research* **54**, 361-368 (1992).
122. Scheller, J. & Rose-John, S. Interleukin-6 and its receptor: from bench to bedside. *Med Microbiol Immunol* **195**, 173-183 (2006).
123. Rose-John, S. Interleukin-6 biology is coordinated by membrane bound and soluble receptors. *Acta biochimica Polonica* **50**, 603-611 (2003).
124. Hurst, S.M*., et al.* Il-6 and its soluble receptor orchestrate a temporal switch in the pattern of leukocyte recruitment seen during acute inflammation. *Immunity* **14**, 705-714 (2001).
125. Dann, S.M*., et al.* IL-6-dependent mucosal protection prevents establishment of a microbial niche for attaching/effacing lesion-forming enteric bacterial pathogens. *J Immunol* **180**, 6816-6826 (2008).

126. Lust, J.A.*, et al.* Isolation of an mRNA encoding a soluble form of the human interleukin-6 receptor. *Cytokine* **4**, 96-100 (1992).
127. Rose-John, S. & Heinrich, P.C. Soluble receptors for cytokines and growth factors: generation and biological function. *The Biochemical journal* **300 (Pt 2)**, 281-290 (1994).
128. Garbers, C.*, et al.* Species specificity of ADAM10 and ADAM17 proteins in interleukin-6 (IL-6) trans-signaling and novel role of ADAM10 in inducible IL-6 receptor shedding. *The Journal of biological chemistry* **286**, 14804-14811 (2011).
129. Kyriakou, D.*, et al.* Serum soluble IL-6 receptor concentrations correlate with stages of multiple myeloma defined by serum beta 2-microglobulin and C-reactive protein. *International journal of hematology* **66**, 367-371 (1997).
130. Chalaris, A., Garbers, C., Rabe, B., Rose-John, S. & Scheller, J. The soluble Interleukin 6 receptor: generation and role in inflammation and cancer. *European journal of cell biology* **90**, 484-494 (2011).
131. Chalaris, A.*, et al.* Apoptosis is a natural stimulus of IL6R shedding and contributes to the proinflammatory trans-signaling function of neutrophils. *Blood* **110**, 1748-1755 (2007).
132. Rabe, B.*, et al.* Transgenic blockade of interleukin 6 transsignaling abrogates inflammation. *Blood* **111**, 1021-1028 (2008).
133. Ernst, M.*, et al.* STAT3 and STAT1 mediate IL-11-dependent and inflammation-associated gastric tumorigenesis in gp130 receptor mutant mice. *J Clin Invest* **118**, 1727-1738 (2008).
134. Kallen, K.J. The role of transsignalling via the agonistic soluble IL-6 receptor in human diseases. *Biochimica et biophysica acta* **1592**, 323-343 (2002).
135. Nowell, M.A.*, et al.* Soluble IL-6 receptor governs IL-6 activity in experimental arthritis: blockade of arthritis severity by soluble glycoprotein 130. *J Immunol* **171**, 3202-3209 (2003).
136. Jones, S.A. & Rose-John, S. The role of soluble receptors in cytokine biology: the agonistic properties of the sIL-6R/IL-6 complex. *Biochim Biophys Acta* **1592**, 251-263 (2002).
137. Mitsuyama, K., Sata, M. & Rose-John, S. Interleukin-6 trans-signaling in inflammatory bowel disease. *Cytokine Growth Factor Rev* **17**, 451-461 (2006).
138. Becker, C.*, et al.* TGF-beta suppresses tumor progression in colon cancer by inhibition of IL-6 trans-signaling. *Immunity* **21**, 491-501 (2004).
139. Lesina, M.*, et al.* Stat3/Socs3 activation by IL-6 transsignaling promotes progression of pancreatic intraepithelial neoplasia and development of pancreatic cancer. *Cancer Cell* **19**, 456-469 (2011).
140. Grivennikov, S.*, et al.* IL-6 and Stat3 are required for survival of intestinal epithelial cells and development of colitis-associated cancer. *Cancer Cell* **15**, 103-113 (2009).
141. Narazaki, M.*, et al.* Soluble forms of the interleukin-6 signal-transducing receptor component gp130 in human serum possessing a potential to inhibit signals through membrane-anchored gp130. *Blood* **82**, 1120-1126 (1993).
142. Jostock, T.*, et al.* Soluble gp130 is the natural inhibitor of soluble interleukin-6 receptor transsignaling responses. *Eur J Biochem* **268**, 160-167 (2001).
143. Rose-John, S., Waetzig, G.H., Scheller, J., Grotzinger, J. & Seegert, D. The IL-6/sIL-6R complex as a novel target for therapeutic approaches. *Expert Opin Ther Targets* **11**, 613-624 (2007).
144. Diamant, M.*, et al.* Cloning and expression of an alternatively spliced mRNA encoding a soluble form of the human interleukin-6 signal transducer gp130. *FEBS letters* **412**, 379-384 (1997).
145. Yeh, H.H., Lai, W.W., Chen, H.H., Liu, H.S. & Su, W.C. Autocrine IL-6-induced Stat3 activation contributes to the pathogenesis of lung adenocarcinoma and malignant pleural effusion. *Oncogene* **25**, 4300-4309 (2006).
146. Jenkins, B.J.*, et al.* Hyperactivation of Stat3 in gp130 mutant mice promotes gastric hyperproliferation and desensitizes TGF-beta signaling. *Nat Med* **11**, 845-852 (2005).
147. Greenhill, C.J.*, et al.* IL-6 trans-signaling modulates TLR4-dependent inflammatory responses via STAT3. *J Immunol* **186**, 1199-1208 (2011).

148. Rebouissou, S.*, et al.* Frequent in-frame somatic deletions activate gp130 in inflammatory hepatocellular tumours. *Nature* **457**, 200-204 (2009).
149. Calabrese, L.H. & Rose-John, S. IL-6 biology: implications for clinical targeting in rheumatic disease. *Nature reviews. Rheumatology* **10**, 720-727 (2014).
150. Ochoa, C.E.*, et al.* Interleukin 6, but not T helper 2 cytokines, promotes lung carcinogenesis. *Cancer prevention research* **4**, 51-64 (2011).
151. Tan, X.*, et al.* Loss of p53 attenuates the contribution of IL-6 deletion on suppressed tumor progression and extended survival in Kras-driven murine lung cancer. *PloS one* **8**, e80885 (2013).
152. Pine, S.R.*, et al.* Increased levels of circulating interleukin 6, interleukin 8, C-reactive protein, and risk of lung cancer. *Journal of the National Cancer Institute* **103**, 1112-1122 (2011).
153. Zhou, A.*, et al.* Functional characterization of Crp/Fnr-type global transcriptional regulators in Desulfovibrio vulgaris Hildenborough. *Applied and environmental microbiology* **78**, 1168-1177 (2012).
154. Yanagawa, H.*, et al.* Serum levels of interleukin 6 in patients with lung cancer. *British journal of cancer* **71**, 1095-1098 (1995).
155. Songur, N.*, et al.* Serum interleukin-6 levels correlate with malnutrition and survival in patients with advanced non-small cell lung cancer. *Tumori* **90**, 196-200 (2004).
156. Liu, X. STAT3 activation inhibits human bronchial epithelial cell apoptosis in response to cigarette smoke exposure. *Biochem Biophys Res Commun* **353**, 121-126 (2007).
157. Dougan, M.*, et al.* A dual role for the immune response in a mouse model of inflammation-associated lung cancer. *J Clin Invest* **121**, 2436-2446 (2011).
158. Jones, S.A., Scheller, J. & Rose-John, S. Therapeutic strategies for the clinical blockade of IL-6/gp130 signaling. *J Clin Invest* **121**, 3375-3383 (2011).
159. Rose-John, S. & Schooltink, H. Cytokines are a therapeutic target for the prevention of inflammation-induced cancers. *Recent results in cancer research. Fortschritte der Krebsforschung. Progres dans les recherches sur le cancer* **174**, 57-66 (2007).
160. Jin, Z., Gao, F., Flagg, T. & Deng, X. Tobacco-specific nitrosamine 4-(methylnitrosamino)-1-(3-pyridyl)-1-butanone promotes functional cooperation of Bcl2 and c-Myc through phosphorylation in regulating cell survival and proliferation. *The Journal of biological chemistry* **279**, 40209-40219 (2004).
161. West, K.A., Linnoila, I.R., Belinsky, S.A., Harris, C.C. & Dennis, P.A. Tobacco carcinogen-induced cellular transformation increases activation of the phosphatidylinositol 3'-kinase/Akt pathway in vitro and in vivo. *Cancer Res* **64**, 446-451 (2004).
162. Ho, Y.S.*, et al.* Tobacco-specific carcinogen 4-(methylnitrosamino)-1-(3-pyridyl)-1-butanone (NNK) induces cell proliferation in normal human bronchial epithelial cells through NFkappaB activation and cyclin D1 up-regulation. *Toxicology and applied pharmacology* **205**, 133-148 (2005).
163. Kudo, T., Matsumoto, T., Esaki, M., Yao, T. & Iida, M. Mucosal vascular pattern in ulcerative colitis: observations using narrow band imaging colonoscopy with special reference to histologic inflammation. *International journal of colorectal disease* **24**, 495-501 (2009).
164. Neurath, M.F. & Finotto, S. IL-6 signaling in autoimmunity, chronic inflammation and inflammation-associated cancer. *Cytokine & growth factor reviews* **22**, 83-89 (2011).
165. Bayliss, T.J., Smith, J.T., Schuster, M., Dragnev, K.H. & Rigas, J.R. A humanized anti-IL-6 antibody (ALD518) in non-small cell lung cancer. *Expert opinion on biological therapy* **11**, 1663-1668 (2011).
166. Sommer, J.*, et al.* Constitutively active mutant gp130 receptor protein from inflammatory hepatocellular adenoma is inhibited by an anti-gp130 antibody that specifically neutralizes interleukin 11 signaling. *The Journal of biological chemistry* **287**, 13743-13751 (2012).
167. Tanaka, T., Narazaki, M. & Kishimoto, T. Anti-interleukin-6 receptor antibody, tocilizumab, for the treatment of autoimmune diseases. *FEBS letters* **585**, 3699-3709 (2011).

168. Ogata, A. & Tanaka, T. Tocilizumab for the treatment of rheumatoid arthritis and other systemic autoimmune diseases: current perspectives and future directions. *International journal of rheumatology* **2012**, 946048 (2012).
169. Baldo, B.A. Adverse events to monoclonal antibodies used for cancer therapy: Focus on hypersensitivity responses. *Oncoimmunology* **2**, e26333 (2013).
170. Lissilaa, R.*, et al.* Although IL-6 trans-signaling is sufficient to drive local immune responses, classical IL-6 signaling is obligate for the induction of T cell-mediated autoimmunity. *J Immunol* **185**, 5512-5521 (2010).
171. Casneuf, T.*, et al.* Interleukin-6 is a potential therapeutic target in interleukin-6 dependent, estrogen receptor-alpha-positive breast cancer. *Breast cancer* **8**, 13-27 (2016).
172. Song, L.*, et al.* Antitumor efficacy of the anti-interleukin-6 (IL-6) antibody siltuximab in mouse xenograft models of lung cancer. *Journal of thoracic oncology : official publication of the International Association for the Study of Lung Cancer* **9**, 974-982 (2014).
173. Ruwanpura, S.M.*, et al.* Therapeutic Targeting of the IL-6 Trans-signalling/mTORC1 Axis in Pulmonary Emphysema. *American journal of respiratory and critical care medicine* (2016).
174. Ernst, T., La Rosee, P., Muller, M.C. & Hochhaus, A. BCR-ABL mutations in chronic myeloid leukemia. *Hematology/oncology clinics of North America* **25**, 997-1008, v-vi (2011).
175. Bryant, K.L., Mancias, J.D., Kimmelman, A.C. & Der, C.J. KRAS: feeding pancreatic cancer proliferation. *Trends in biochemical sciences* **39**, 91-100 (2014).
176. Meuwissen, R. & Berns, A. Mouse models for human lung cancer. *Genes Dev* **19**, 643-664 (2005).
177. Meuwissen, R., Linn, S.C., van der Valk, M., Mooi, W.J. & Berns, A. Mouse model for lung tumorigenesis through Cre/lox controlled sporadic activation of the K-Ras oncogene. *Oncogene* **20**, 6551-6558 (2001).
178. Kwon, M.C. & Berns, A. Mouse models for lung cancer. *Molecular oncology* **7**, 165-177 (2013).
179. Bhattacharjee, A.*, et al.* Classification of human lung carcinomas by mRNA expression profiling reveals distinct adenocarcinoma subclasses. *Proc Natl Acad Sci U S A* **98**, 13790-13795 (2001).
180. Linnoila, R.I., Sahu, A., Miki, M., Ball, D.W. & DeMayo, F.J. Morphometric analysis of CC10-hASH1 transgenic mouse lung: a model for bronchiolization of alveoli and neuroendocrine carcinoma. *Experimental lung research* **26**, 595-615 (2000).
181. Linnoila, R.I.*, et al.* The role of CC10 in pulmonary carcinogenesis: from a marker to tumor suppression. *Annals of the New York Academy of Sciences* **923**, 249-267 (2000).
182. Cooper, W.A., Lam, D.C., O'Toole, S.A. & Minna, J.D. Molecular biology of lung cancer. *Journal of thoracic disease* **5 Suppl 5**, S479-490 (2013).
183. Graziano, S.L.*, et al.* Prognostic significance of K-ras codon 12 mutations in patients with resected stage I and II non-small-cell lung cancer. *Journal of clinical oncology : official journal of the American Society of Clinical Oncology* **17**, 668-675 (1999).
184. Castellano, E. & Santos, E. Functional specificity of ras isoforms: so similar but so different. *Genes & cancer* **2**, 216-231 (2011).
185. Tuveson, D.A. & Jacks, T. Modeling human lung cancer in mice: similarities and shortcomings. *Oncogene* **18**, 5318-5324 (1999).
186. Fisher, G.H.*, et al.* Induction and apoptotic regression of lung adenocarcinomas by regulation of a K-Ras transgene in the presence and absence of tumor suppressor genes. *Genes Dev* **15**, 3249-3262 (2001).
187. Guerra, C.*, et al.* Tumor induction by an endogenous K-ras oncogene is highly dependent on cellular context. *Cancer Cell* **4**, 111-120 (2003).
188. Politi, K.*, et al.* Lung adenocarcinomas induced in mice by mutant EGF receptors found in human lung cancers respond to a tyrosine kinase inhibitor or to down-regulation of the receptors. *Genes Dev* **20**, 1496-1510 (2006).

189. Regales, L*., et al.* Development of new mouse lung tumor models expressing EGFR T790M mutants associated with clinical resistance to kinase inhibitors. *PloS one* **2**, e810 (2007).
190. Davies, H*., et al.* Mutations of the BRAF gene in human cancer. *Nature* **417**, 949-954 (2002).
191. Zebisch, A. & Troppmair, J. Back to the roots: the remarkable RAF oncogene story. *Cellular and molecular life sciences : CMLS* **63**, 1314-1330 (2006).
192. Gerber, D.E. & Minna, J.D. ALK inhibition for non-small cell lung cancer: from discovery to therapy in record time. *Cancer Cell* **18**, 548-551 (2010).
193. Dankort, D*., et al.* A new mouse model to explore the initiation, progression, and therapy of BRAFV600E-induced lung tumors. *Genes Dev* **21**, 379-384 (2007).
194. Soda, M*., et al.* A mouse model for EML4-ALK-positive lung cancer. *Proc Natl Acad Sci U S A* **105**, 19893-19897 (2008).
195. Haura, E.B., Zheng, Z., Song, L., Cantor, A. & Bepler, G. Activated epidermal growth factor receptor-Stat-3 signaling promotes tumor survival in vivo in non-small cell lung cancer. *Clin Cancer Res* **11**, 8288-8294 (2005).
196. Li, D*., et al.* Bronchial and peripheral murine lung carcinomas induced by T790M-L858R mutant EGFR respond to HKI-272 and rapamycin combination therapy. *Cancer Cell* **12**, 81-93 (2007).
197. Liang, W*., et al.* Network meta-analysis of erlotinib, gefitinib, afatinib and icotinib in patients with advanced non-small-cell lung cancer harboring EGFR mutations. *PloS one* **9**, e85245 (2014).
198. Jenkins, B.J., Roberts, A.W., Najdovska, M., Grail, D. & Ernst, M. The threshold of gp130-dependent STAT3 signaling is critical for normal regulation of hematopoiesis. *Blood* **105**, 3512-3520 (2005).
199. Jenkins, B.J*., et al.* Imbalanced gp130-dependent signaling in macrophages alters macrophage colony-stimulating factor responsiveness via regulation of c-fms expression. *Mol Cell Biol* **24**, 1453-1463 (2004).
200. Ruwanpura, S.M*., et al.* Interleukin-6 promotes pulmonary emphysema associated with apoptosis in mice. *Am J Respir Cell Mol Biol* **45**, 720-730 (2011).
201. Lowry, O.H., Rosebrough, N.J., Farr, A.L. & Randall, R.J. Protein measurement with the Folin phenol reagent. *J Biol Chem* **193**, 265-275 (1951).
202. Roberts, P.J. & Stinchcombe, T.E. KRAS mutation: should we test for it, and does it matter? *Journal of clinical oncology : official journal of the American Society of Clinical Oncology* **31**, 1112-1121 (2013).
203. Brambilla, E., Travis, W.D., Colby, T.V., Corrin, B. & Shimosato, Y. The new World Health Organization classification of lung tumours. *Eur Respir J* **18**, 1059-1068 (2001).
204. Ji, B*., et al.* Robust acinar cell transgene expression of CreErT via BAC recombineering. *Genesis* **46**, 390-395 (2008).
205. Blasco, R.B*., et al.* c-Raf, but not B-Raf, is essential for development of K-Ras oncogene-driven non-small cell lung carcinoma. *Cancer Cell* **19**, 652-663 (2011).
206. Karreth, F.A., Frese, K.K., DeNicola, G.M., Baccarini, M. & Tuveson, D.A. C-Raf is required for the initiation of lung cancer by K-Ras(G12D). *Cancer discovery* **1**, 128-136 (2011).
207. Kissil, J.L*., et al.* Requirement for Rac1 in a K-ras induced lung cancer in the mouse. *Cancer Res* **67**, 8089-8094 (2007).
208. Grabner, B*., et al.* Disruption of STAT3 signalling promotes KRAS-induced lung tumorigenesis. *Nature communications* **6**, 6285 (2015).
209. Jerome Marson, V*., et al.* Expression of TTF-1 and cytokeratins in primary and secondary epithelial lung tumours: correlation with histological type and grade. *Histopathology* **45**, 125-134 (2004).
210. Coussens, L.M. & Werb, Z. Inflammation and cancer. *Nature* **420**, 860-867 (2002).
211. Bromberg, J. & Wang, T.C. Inflammation and cancer: IL-6 and STAT3 complete the link. *Cancer Cell* **15**, 79-80 (2009).

212. Sansone, P. & Bromberg, J. Environment, inflammation, and cancer. *Current opinion in genetics & development* **21**, 80-85 (2011).
213. Houghton, A.M. Mechanistic links between COPD and lung cancer. *Nature reviews. Cancer* **13**, 233-245 (2013).
214. Nowell, M.A*., et al.* Therapeutic targeting of IL-6 trans signaling counteracts STAT3 control of experimental inflammatory arthritis. *J Immunol* **182**, 613-622 (2009).
215. Woo, C.C., Kumar, A.P., Sethi, G. & Tan, K.H. Thymoquinone: potential cure for inflammatory disorders and cancer. *Biochemical pharmacology* **83**, 443-451 (2012).
216. Anderson, G.P. COPD, asthma and C-reactive protein. *Eur Respir J* **27**, 874-876 (2006).
217. Ruwanpura, S.M*., et al.* Deregulated Stat3 signaling dissociates pulmonary inflammation from emphysema in gp130 mutant mice. *Am J Physiol Lung Cell Mol Physiol* **302**, L627-639 (2012).
218. Okada, F*., et al.* Impact of oncogenes in tumor angiogenesis: mutant K-ras up-regulation of vascular endothelial growth factor/vascular permeability factor is necessary, but not sufficient for tumorigenicity of human colorectal carcinoma cells. *Proc Natl Acad Sci U S A* **95**, 3609-3614 (1998).
219. Sparmann, A. & Bar-Sagi, D. Ras-induced interleukin-8 expression plays a critical role in tumor growth and angiogenesis. *Cancer Cell* **6**, 447-458 (2004).
220. Gaglio, D*., et al.* Oncogenic K-Ras decouples glucose and glutamine metabolism to support cancer cell growth. *Molecular systems biology* **7**, 523 (2011).
221. Gao, S.P*., et al.* Mutations in the EGFR kinase domain mediate STAT3 activation via IL-6 production in human lung adenocarcinomas. *J Clin Invest* **117**, 3846-3856 (2007).
222. Ruwanpura, S.M*., et al.* IL-6/Stat3-driven pulmonary inflammation, but not emphysema, is dependent on interleukin-17A in mice. *Respirology* **19**, 419-427 (2014).
223. Bihl, M*., et al.* Proliferation of human non-small-cell lung cancer cell lines: role of interleukin-6. *Am J Respir Cell Mol Biol* **19**, 606-612 (1998).
224. Naugler, W.E. & Karin, M. The wolf in sheep's clothing: the role of interleukin-6 in immunity, inflammation and cancer. *Trends Mol Med* **14**, 109-119 (2008).
225. (!!! INVALID CITATION !!!).
226. Shaw, A.T., Kirsch, D.G. & Jacks, T. Future of early detection of lung cancer: the role of mouse models. *Clin Cancer Res* **11**, 4999s-5003s (2005).
227. Herzog, C.R., Noh, S., Lantry, L.E., Guan, K.L. & You, M. Cdkn2a encodes functional variation of p16INK4a but not p19ARF, which confers selection in mouse lung tumorigenesis. *Molecular carcinogenesis* **25**, 92-98 (1999).
228. Malkinson, A.M*., et al.* Experimental evidence from an animal model of adenocarcinoma that chronic inflammation enhances lung cancer risk. *Chest* **117**, 228S (2000).
229. Barron, C.C., Moore, J., Tsakiridis, T., Pickering, G. & Tsiani, E. Inhibition of human lung cancer cell proliferation and survival by wine. *Cancer cell international* **14**, 6 (2014).
230. McKeown, D.J., Brown, D.J., Kelly, A., Wallace, A.M. & McMillan, D.C. The relationship between circulating concentrations of C-reactive protein, inflammatory cytokines and cytokine receptors in patients with non-small-cell lung cancer. *British journal of cancer* **91**, 1993-1995 (2004).
231. Tas, F*., et al.* Serum levels of leptin and proinflammatory cytokines in advanced-stage non-small cell lung cancer. *Medical oncology* **22**, 353-358 (2005).
232. Gomes, M*., et al.* IL-6 polymorphism in non-small cell lung cancer: a prognostic value? *Tumour biology : the journal of the International Society for Oncodevelopmental Biology and Medicine* **36**, 3679-3684 (2015).
233. Yang, L*., et al.* Nkx2-1: a novel tumor biomarker of lung cancer. *Journal of Zhejiang University. Science. B* **13**, 855-866 (2012).

234. Gabay, C.*, et al.* Tocilizumab monotherapy versus adalimumab monotherapy for treatment of rheumatoid arthritis (ADACTA): a randomised, double-blind, controlled phase 4 trial. *Lancet* **381**, 1541-1550 (2013).
235. Garbers, C.*, et al.* Plasticity and cross-talk of interleukin 6-type cytokines. *Cytokine & growth factor reviews* **23**, 85-97 (2012).
236. Schaper, F. & Rose-John, S. Interleukin-6: Biology, signaling and strategies of blockade. *Cytokine & growth factor reviews* (2015).
237. Mullberg, J.*, et al.* The soluble interleukin-6 receptor is generated by shedding. *European journal of immunology* **23**, 473-480 (1993).
238. Ratschiller, D.*, et al.* Cyclin D1 overexpression in bronchial epithelia of patients with lung cancer is associated with smoking and predicts survival. *Journal of clinical oncology : official journal of the American Society of Clinical Oncology* **21**, 2085-2093 (2003).
239. Gao, J.*, et al.* MUC1 is a downstream target of STAT3 and regulates lung cancer cell survival and invasion. *Int J Oncol* **35**, 337-345 (2009).
240. Song, L., Turkson, J., Karras, J.G., Jove, R. & Haura, E.B. Activation of Stat3 by receptor tyrosine kinases and cytokines regulates survival in human non-small cell carcinoma cells. *Oncogene* **22**, 4150-4165 (2003).
241. Yeh, H.H.*, et al.* Ha-ras oncogene-induced Stat3 phosphorylation enhances oncogenicity of the cell. *DNA and cell biology* **28**, 131-139 (2009).
242. Seki, Y.*, et al.* STAT3 and MAPK in human lung cancer tissues and suppression of oncogenic growth by JAB and dominant negative STAT3. *Int J Oncol* **24**, 931-934 (2004).
243. Jenkins, B.J.*, et al.* Pathologic consequences of STAT3 hyperactivation by IL-6 and IL-11 during hematopoiesis and lymphopoiesis. *Blood* **109**, 2380-2388 (2007).
244. Tye, H.*, et al.* STAT3-driven upregulation of TLR2 promotes gastric tumorigenesis independent of tumor inflammation. *Cancer Cell* **22**, 466-478 (2012).
245. Zhu, Z.*, et al.* Inhibition of KRAS-driven tumorigenicity by interruption of an autocrine cytokine circuit. *Cancer discovery* **4**, 452-465 (2014).
246. Dowlati, A., Levitan, N. & Remick, S.C. Evaluation of interleukin-6 in bronchoalveolar lavage fluid and serum of patients with lung cancer. *The Journal of laboratory and clinical medicine* **134**, 405-409 (1999).
247. Enewold, L.*, et al.* Serum concentrations of cytokines and lung cancer survival in African Americans and Caucasians. *Cancer Epidemiol Biomarkers Prev* **18**, 215-222 (2009).
248. Yoon, Y.K.*, et al.* KRAS mutant lung cancer cells are differentially responsive to MEK inhibitor due to AKT or STAT3 activation: implication for combinatorial approach. *Molecular carcinogenesis* **49**, 353-362 (2010).
249. Sunaga, N.*, et al.* Oncogenic KRAS-induced interleukin-8 overexpression promotes cell growth and migration and contributes to aggressive phenotypes of non-small cell lung cancer. *International journal of cancer* **130**, 1733-1744 (2012).
250. Giard, D.J.*, et al.* In vitro cultivation of human tumors: establishment of cell lines derived from a series of solid tumors. *Journal of the National Cancer Institute* **51**, 1417-1423 (1973).
251. Lieber, M., Smith, B., Szakal, A., Nelson-Rees, W. & Todaro, G. A continuous tumor-cell line from a human lung carcinoma with properties of type II alveolar epithelial cells. *International journal of cancer* **17**, 62-70 (1976).
252. Guo, J.*, et al.* IKBKE is induced by STAT3 and tobacco carcinogen and determines chemosensitivity in non-small cell lung cancer. *Oncogene* **32**, 151-159 (2013).
253. Hodge, D.R., Hurt, E.M. & Farrar, W.L. The role of IL-6 and STAT3 in inflammation and cancer. *European journal of cancer* **41**, 2502-2512 (2005).
254. Chung, K.F. Cytokines in chronic obstructive pulmonary disease. *Eur Respir J Suppl* **34**, 50s-59s (2001).
255. Schafer, Z.T. & Brugge, J.S. IL-6 involvement in epithelial cancers. *J Clin Invest* **117**, 3660-3663 (2007).

256. Guo, W*., et al.* Water-soluble andrographolide sulfonate exerts anti-sepsis action in mice through down-regulating p38 MAPK, STAT3 and NF-kappaB pathways. *International immunopharmacology* **14**, 613-619 (2012).
257. Achcar Rde, O., Cagle, P.T. & Jagirdar, J. Expression of activated and latent signal transducer and activator of transcription 3 in 303 non-small cell lung carcinomas and 44 malignant mesotheliomas: possible role for chemotherapeutic intervention. *Arch Pathol Lab Med* **131**, 1350-1360 (2007).
258. Rossi, J.F., Lu, Z.Y., Jourdan, M. & Klein, B. Interleukin-6 as a therapeutic target. *Clin Cancer Res* **21**, 1248-1257 (2015).
259. Barnes, P.J., Shapiro, S.D. & Pauwels, R.A. Chronic obstructive pulmonary disease: molecular and cellular mechanisms. *Eur Respir J* **22**, 672-688 (2003).
260. Ruwanpura, S.M*., et al.* Interleukin-6 promotes Pulmonary Emphysema Associated with Apoptosis in Mice. *Am J Respir Cell Mol Biol* (2011).
261. Mantovani, A. Chemokines in neoplastic progression. *Seminars in cancer biology* **14**, 147-148 (2004).
262. Mantovani, A*., et al.* The chemokine system in diverse forms of macrophage activation and polarization. *Trends in immunology* **25**, 677-686 (2004).
263. Atreya, R*., et al.* Blockade of interleukin 6 trans signaling suppresses T-cell resistance against apoptosis in chronic intestinal inflammation: evidence in crohn disease and experimental colitis in vivo. *Nat Med* **6**, 583-588 (2000).
264. Ancrile, B., Lim, K.H. & Counter, C.M. Oncogenic Ras-induced secretion of IL6 is required for tumorigenesis. *Genes Dev* **21**, 1714-1719 (2007).
265. Jemal, A*., et al.* Cancer statistics, 2009. *CA: a cancer journal for clinicians* **59**, 225-249 (2009).

Appendix I
Buffers and Solutions

Tail buffer
0.05M Tris-HCL base (Sigma), 0.025M Ethylenediaminetetraacetic acid (EDTA, Sigma), 0.05M Sodium chloride (NaCl, Panreac), 0.005% Sodium Dodecyl Sulphate (SDS, Merck)

T.E. buffer
10mM Tris-HCL base (Sigma), 1mM EDTA (Sigma), adjusted to pH 8.0

2% Agarose gel
2% (w/v) Agarose (Promega) & make up with TAE buffer (1X)

TAE buffer (1X)
40mM Tris-HCL base (Sigma), 11.4% (v/v) Glacial acetic acid (Sigma), 20% (v/v) 0.5M EDTA (Sigma), in DepC

Acid Alcohol
5% (v/v) Hydrochloric acid (HCL, Sigma), 70% (v/v) ethanol

Scott's tap water
240mM sodium bicarbonate, 11mM magnesium sulphate, in 1000ml tap water

Citrate buffer
01.2mM citric acid, 10mM trisodium citrate, in 500ml dH_2O, adjust pH to 6.0

0.01M Phosphate buffered saline (PBS, pH 7.4)
0.8% (w/v) Sodium chloride (Panreac), 0.14% (w/v) Sodium phosphate Dibasic orthophosphate (Amersco), 0.02% (w/v) Potassium chloride (Amersco), 0.02% (w/v) Potassium Dihydrogen orthophosphate (BDH) & $MQ.H_2O$ (Millipore) & then adjust pH to 7.4 with Hydrochloric acid (Merck)

PBS + Tween 20 (PBS/T)
0.05%(v/v) Tween-20 (Croda International, Snaith, East Yorkshire UK) in 0.01M PBS

75% ethanol/Diethylpyrocarbonate water
75% (v/v) ethanol, in Diethylpyrocarbonate (DepC) water

Diethyl pyrocarbonate (DepC) water
0.1% (v/v) DepC solution (Thermo Fisher), in $MQ.H_2O$

DNase incubation mix
12.5% (v/v) DNase I stock solution (Qiagen) to 87.5% (v/v) Buffer RDD (Qiagen)

Protein lysis buffer (2X)
100mM NaCL (Panreak), 100mmol Tris-HCL (pH 7.5, Merck), 2% (v/v) Glycerol (Amersco), 2% (v/v) Triton X-100 (BDH), 0.2% (v/v) Sodium Dodecyl Sulphate (Merck), 4mmol EDTA (Amresco) & MQ.H_2O

Protein lysis buffer (1X)
100µl of Sodium Fluoride (NaF, Sigma), 40µl of Sodium Vanadate (NaV, Sigma), 100µl of Protease Inhibitor (PI, Roach) & make up to 1ml with Protein lysis buffer (2X)

Lower gel Buffer (4X) (pH 8.8)
1.5M Tris-HCL base, 0. 4% (v/v) Sodium Dodecyl sulphate & MQ.H_2O

Upper gel buffer (4X) (pH 6.8)
500mM Tris-HCL base, 0.004% (v/v) Sodium Dodecyl sulphate & MQ.H_2O

10% SDS-PAGE gel (Resolving gel)
10% (v/v) Acrylamide/Bis (Bio-Rad), 26% (v/v) Lower gel buffer, 40% (v/v) MQ.H_2O, 0.001% (v/v) Ammonium Persulfate (Bio-Rad) & 0.0004% (v/v) TEMED (Bio-Rad)

5% SDS-PAGE gel (Stacking gel)
5% (v/v) Acrylamide/Bis (Bio-Rad), 16% (v/v) Upper gel buffer, 25% (v/v) MQ H_2O, 0.02% (v/v) Ammonium Persulfate & 0.0008% (v/v) TEMED

10% APS
10% (w/v) Ammonium Persulfate (APS, Bio-Rad) & MQ.H_2O

SDS-PAGE running buffer (10X)
250mM Tris-HCL base, 1.94mol Glycine (Amresco), 35mM Sodium Dodecyl Sulphate & MQ.H_2O

2 x Sample buffer
30% (v/v) Glycerol, 4.6% (w/v) Sodium Dodecyl sulphate, 25% (v/v) Upper gel buffer (4X), add bromophenol blue till deep blue & 5% (v/v) β-Mercaptoethanol (Sigma)

Transfer buffer (10X) (pH 8.3)
250mmol Tris-HCl base, 1.94mol Glycine & MQ.H_2O

Transfer buffer (1X) (pH 8.3)
10% (v/v) Transfer buffer (10X), 20% (v/v) Methanol (Merck) & MQ.H_2O

Membrane stripping buffer
2% (v/v) Sodium Dodecyl sulphate, 60mmol Tris-HCL base & 6.9% (v/v) β-Mercaptoethanol

Coating buffer (IL-6)
0.1M Sodium Carbonate, 7.13g $NaHCO_3$, 1.59g Na_2CO_3, in MQ.H_2O, pH 9.5

Coating buffer (sIL-6r and sgp130)
1% (v/v) Bovine Serum Albumin, in Phosphate buffered saline

***Bovine* Serum Albumin (BSA)**
10mg/ml *Bovine* Serum Albumin (Sigma) & MQ.H_2O

Working detection solution (IL-6)
50% detection antibody & 50%Streptavidin-HRP

Stop wash buffer
2N Sulfuric acid (H_2SO_4, Sigma)

Appendix II
Primer sequences and PCR protocols

Gene	Primer 1	Primer 2	Primer 3
Gp130	ctgaatgaactgcaggacga	caagtgttctcaaggtccgagtccac	tgaagccactcgtctttagc
Kras	gtcgacaagctcatgcggg	cgcagactgtagagcagcg	ccatggcttgagtaagtctgc
Stat3	agcagctgacaacgctggctgagaagct	ttgctgctctcgctgaagcgcagtagg	atcgccttctatcgccttcttgacgag
Il-6	ttctcatttccacgattttccccc	ttccatccagttgccttcttg	gaccgcttcctggtgctttac

Genes	Gp130			Kras		
Steps	**Temp**	**Time**	**cycles**	**Temp**	**Time**	**cycles**
1. Initiation/Melting	94	10	1	94	3	1
2. Denaturing	94	1	35	94	0.5	35
3. Annealing	60	1	35	69	1	35
4. Elongation	72	1	35	72	1	35
5. Strand completion	72	10	1	72	2	1
6. Finish	20	∞	n/a	20	∞	n/a

Genes	Stat3			Il-6		
Steps	**Temp**	**Time**	**cycles**	**Temp**	**Time**	**cycles**
1. Initiation/Melting	94	2	1	94	4	1
2. Denaturing	94	0.5	40	94	1	35
3. Annealing	65	1	40	60	1	35
4. Elongation	72	1	40	72	1	35
5. Strand completion	72	5	1	72	10	1
6. Finish	20	∞	n/a	20	∞	n/a

Name	Primer Forward	Primer Reverse
Mouse primers		
18S	cggctaccacatccaaggaa	gctggaattaccgcggct
IL-6	atggatgctaccaaactggat	tgaaggactctggctttgtct
IL-6r	aagcagcaggcaatgttacc	cataaatagtccccagtgtcg
Socs3	gcgggcacctttcttatcc	tccccgactgggtcttgac
Human Primers		
18S	cggctaccacatccaaggaa	gctggaattaccgcggct
IL-6	ctccaggagcccagctctga	cccagggagaaggcaactg
IL-6r	aaagctgggcaggttggtg	agcttgtgcagaggtgttgag
Socs3	ggccactctttcagcatctc	atcgtactggtccaggaactc
Tace	gaagtgccaaggaggcgatta	cgggcactcactgctattacc

Appendix III
LEICA ASP300 Ethanol Processing Program

Station	Reagent	4.5 hrs	6 hrs
1	70% Ethanol	0:05	0:15
2	90% Ethanol	0:05	0:15
3	Absolute Ethanol	0:05	0:15
4	Absolute Ethanol	0:20	0:15
5	Absolute Ethanol	0:20	0:30
6	Absolute Ethanol	0:45	0:45
7	Xylene	0:05	0:20
8	Xylene	0:10	0:20
9	Xylene	0:45	0:45
10	Paraffin	0:15	0:30
11	Paraffin	0:20	0:30
12	Paraffin	0:40	0:45

Note:
Pressure valves = On
Temperature Stations 1-10 = 40°C
Temperature Stations 11-12 = 62°C

Appendix IV
Primary antibody concentration

Primary antibody	Concentration	Company	Secondary antibody	kDa
phospho(Y705)-Stat3	1:1000	Santa Cruz (Santa Cruz, USA)	Anti-rabbit	80
Total Stat3	1:1000	Translabs (Franklin lakes, USA)	Anti-rabbit	86
sIL-6r	1:1000	R&D systems (Minneapolis, USA)	Anti-rabbit	80
Actin	1:500	Santa Cruz	Anti-mouse	44